

VYSOKÉ UČENÍ TECHNICKÉ V BRNĚ

BRNO UNIVERSITY OF TECHNOLOGY



FAKULTA STROJNÍHO INŽENÝRSTVÍ

ÚSTAV AUTOMOBILNÍHO A DOPRAVNÍHO  
INŽENÝRSTVÍ

FACULTY OF MECHANICAL ENGINEERING

INSTITUTE OF AUTOMOTIVE ENGINEERING

# CFD SIMULATION OF EXHAUST GASES FLOW THROUGH THE WASTEGATE OF PETROL ENGINES TURBOCHARGER

CFD SIMULACE PROUDĚNÍ VÝFUKOVÝCH PLYNŮ PŘEPOUŠTĚCÍM VENTILEM  
TURBODMYCHADLA PRO ZÁŽEHOVÉ MOTORY

DIPLOMOVÁ PRÁCE  
MASTER'S THESIS

AUTOR PRÁCE  
AUTHOR

Bc. ANDREJ TRŠKA

VEDOUCÍ PRÁCE  
SUPERVISOR

Ing. JAN VANČURA

BRNO 2012

Vysoké učení technické v Brně, Fakulta strojního inženýrství

Ústav automobilního a dopravního inženýrství

Akademický rok: 2011/2012

## ZADÁNÍ DIPLOMOVÉ PRÁCE

student(ka): Bc. Andrej Trška

který/která studuje v **magisterském navazujícím studijním programu**

obor: **Automobilní a dopravní inženýrství (2301T038)**

Ředitel ústavu Vám v souladu se zákonem č.111/1998 o vysokých školách a se Studijním a zkušebním řádem VUT v Brně určuje následující téma diplomové práce:

### **CFD simulace proudění výfukových plynů přepouštěcím ventilem turbodmychadla pro zážehové motory**

v anglickém jazyce:

### **CFD simulation of exhaust gases flow through the wastegate of petrol engines turbocharger**

Stručná charakteristika problematiky úkolu:

S využitím počítačové simulace sestavte výpočtový model proudění přepouštěcím ventilem "wastegate" turbodmychadla pro zážehové motory, proveďte výpočet a navrhnete možné změny konstrukce za účelem lepšího rozložení teplot na výstupu z turbinové skříně pro rovnoměrnější zahřátí katalyzátoru.

Cíle diplomové práce:

- 1) Proveďte rešerši současného stavu konstrukce turbodmychadel spalovacích motorů, jejich regulace a konstrukčního provedení regulačních mechanismů.
- 2) Vytvořte výpočetní model sestavy turbinové skříně s přepouštěcím ventilem současného designu.
- 3) Proveďte simulaci proudění pro zadaný pracovní režim turbodmychadla a určete průběh teplot na výstupu z turbinové skříně při různých otevřeních ventilu.
- 4) Zhodnoťte získané výsledky a navrhnete konstrukční změny mechanismu pro dosažení lepšího rozložení teplot na výstupu z turbinové skříně / vstupu do katalyzátoru.

Seznam odborné literatury:

Hofmann, Karel: Turbodmychadla, vozidlové turbíny a ventilátory: Přepřehování spalovacích motorů

Vedoucí diplomové práce: Ing. Jan Vančura

Termín odevzdání diplomové práce je stanoven časovým plánem akademického roku 2011/2012.

V Brně, dne 24.11.2010

L.S.

---

prof. Ing. Václav Pištěk, DrSc.  
Ředitel ústavu

---

prof. RNDr. Miroslav Doupovec, CSc., dr. h. c.  
Děkan fakulty



## **ABSTRACT**

This thesis deals with turbochargers and CFD simulation of wastegated turbocharger for petrol engine applications. The aim is to give a general overview on turbocharging and design fundamentals. It describes the procedure of building a 3-dimensional virtual model of turbine housing assembly, extracting fluid volume, mesh and setup of computer CFD calculation, which is evaluated in the end. The result serves to propose different design of turbine housing in order to improve exhaust gases heat distribution at outlet and shorten catalytic converter light-off time.

## **KEYWORDS**

Turbocharger, wastegate, catalytic converter, petrol engine, CFD

## **ABSTRAKT**

Tato diplomová práce se zabývá turbodmychadly a CFD simulací turbodmychadla s integrovaným přepouštěcím ventilem pro benzínový motor. Cílem je poskytnout všeobecný přehled o přeplnování a konstrukci turbodmychadel. Práce popisuje proces tvorby 3-rozměrného virtuálního modelu sestavy turbínové skříně, extrakci negativního objemu plynů, tvorbu meshe a nastavení počítačové CFD simulace, která je v závěru práce vyhodnocena. Výsledky simulace slouží pro návrh odlišného provedení turbínové skříně za účelem zlepšení rozložení teplot výfukových plynů na výstupu a zkrácení aktivační doby výfukového katalyzátoru.

## **KLÍČOVÁ SLOVA**

Turbodmychadlo, přepouštěcí ventil, katalyzátor, benzínový motor, CFD



## **BIBLIOGRAPHIC CITATION**

TRŠKA, A. *CFD simulace proudění výfukových plynů přepouštěcím ventilem turbodmychadla pro zážehové motory*. Brno: Vysoké učení technické v Brně, Fakulta strojního inženýrství, 2012. 115 s. Vedoucí diplomové práce Ing. Jan Vančura.



## STATEMENT OF AFFIRMATION

Herewith I affirm the thesis is work of my own.

It has been created with guidance of Ing. Petr Čížek, PhD (Gasoline Product Engineering Leader at Honeywell Turbo Technologies in Brno) and Ing. Jan Vančura (Institute of Automotive Engineering at Brno University of Technology).

All the cited sources of literature are perceptibly marked and listed at the end of this document.

Brno, 5<sup>th</sup> of May, 2012

.....  
Andrej Trška



## ACKNOWLEDGEMENTS

I would like to express my grateful thankfulness to Ing. Petr Čížek, PhD, my mentor at Honeywell Turbo Technologies, for very valuable support whenever I needed the guidance in the world of turbomachinery. Words of thank you are also aimed to Ing. Milan Nejedlý, PhD for his attitude and friendly advices, to all my colleagues in Honeywell and to Ing. Jan Vančura, my supervisor at Institute of Automotive Engineering.

I would also like to take this opportunity to thank my family for all the support during my studies, for never-ending discussions about my future and for everything they are doing for me. Without you, I would not be writing these words today. You have created a place where I can always come back, take a rest and energy for everything I am doing.

This thesis is dedicated to Mirka.

Mirka, thank you for all the love you are giving me, believing in me and supporting me. You have made it possible to combine work and studies and at the same time to enjoy the life with you. Thank you for always being here.

Thank you!

Brno, May 2012

*Andrej Trška*



# CONTENTS

Prologue .....	17
1 Introduction.....	18
2 Basics .....	21
2.1 Engine power.....	21
2.2 Brake mean effective pressure BMEP .....	22
2.3 Intake air density .....	23
2.4 Volumetric efficiency.....	24
3 Working principal .....	25
4 Turbocharger design .....	26
4.1 Compressor assembly.....	27
4.2 Compressor wheel .....	27
4.3 Bearing assembly .....	28
4.4 Turbine assembly .....	29
4.5 Turbine wheel.....	31
4.6 Constant-Pressure Turbocharging .....	33
4.7 Pulse Turbocharging .....	33
5 Turbocharger Control.....	34
5.1 Variable Nozzle Turbine – VNT.....	34
5.2 Wastegate .....	36
5.3 Two-Stage Turbocharging.....	38
5.4 Hybrid Turbo.....	39
6 Working conditions.....	40
7 Catalytic Converter .....	42
8 Adiabatic expansion.....	46
9 Computational Fluid Dynamics – CFD .....	48
10 Current Design 1 .....	49
10.1 Turbine Housing.....	50
10.1.1 Radial passage.....	51
10.1.2 Gas Passage (volute) .....	52
10.1.3 Core.....	53
10.1.4 Casting .....	55
10.1.5 Machining .....	56
10.2 Turbine Wheel.....	57
10.3 Arm & Valve Assembly.....	59
10.4 Turbine Housing Assembly.....	59
10.5 Fluid Volume.....	61
11 CFD calculation of current design 1 .....	63
11.1 Mesh.....	64
11.1.1 Volute.....	65
11.1.2 Turbine Wheel .....	65
11.1.3 Discharge .....	67
11.1.4 Extension.....	68
11.1.5 Mesh statistics summary .....	68
11.2 Pre-Processing .....	69



11.2.1	Boundary Conditions .....	70
11.2.2	Interfaces .....	71
11.2.3	Walls .....	72
11.2.4	Porous domain .....	73
11.2.5	Output Control .....	75
11.3	Solver .....	76
11.4	Post-Processing .....	77
11.5	Results .....	78
11.5.1	Closed Wastegate Position .....	79
11.5.2	5 deg open .....	82
11.5.3	15 deg open .....	83
11.5.4	30 deg open .....	84
11.5.5	50 deg open .....	85
11.5.6	80 deg open .....	86
11.5.7	Summary of current design calculation .....	87
12	Design 2 (reversed bushing) .....	89
12.1	Results .....	90
13	Design 3 (horizontal bushing axis) .....	93
13.1	Results .....	95
14	Design 4 (duct outlet leaned out) .....	97
14.1	Results .....	98
15	Design 5 (butterfly valve) .....	100
15.1	Results .....	101
16	Results Summary & Conclusion .....	105
17	Bibliography .....	110
18	Nomenclature .....	113
19	Supplement .....	115



## PROLOGUE

The subject of this thesis has arisen from a need to understand and affect behavior of exhaust gases passing from turbine housing with wastegate mechanism into the catalytic converter. Regular temperature distribution of exhaust gases over the area of turbine housing outlet can positively influence catalytic converter efficiency and reduce light-off time after the start-up of an engine.

The thesis is created at Honeywell Turbo Technology Research and Development centre based in Brno, Czech Republic at a Gasoline Product Engineering team.

At the beginning, it explains the need to be concerned with these kinds of design and simulation problems which are resulting from continuous improvements being done by world automotive leaders, consumer demand, government regulations and driving the technology forward to an environmentally friendly future.

The first part gives an overview on turbocharging, basic engine theory and turbocharging fundamentals. It also describes the common design of compressor, turbine and central housing assemblies. The thesis also deals with various turbocharger control mechanisms, working conditions, exhaust gas after treatment system and thermodynamics fundamentals used in turbocharger's industry. Moreover, it treats with fluid dynamics fundamentals and its implementation in contemporary computer simulation methods (CFD- computational fluid dynamics).

The second part describes processes that product, design and simulation engineers have to cope with everyday. Procedures are described systematically from the first design idea, building a 3D virtual model, putting the assembly parts all together and extracting the fluid volume out of an assembly all done in CATIA V5. Subsequently importing the geometry into the ANSYS 13.0 CFX environment, considering simplifications, separate domains definition, mesh, setup and finally running a computer calculations. Results from this calculations serves for better understanding of what is happening inside the turbine housing, exact definition of velocity, pressure, temperature and other important values used in fluid dynamics, which are only hardly or impossible to measure on gas-stand or on-engine tests. Based on this, other turbine housing designs are introduced and calculated in order to confirm or disprove the expectations of better temperature distribution. Impact on performance is evaluated as well.



# 1 INTRODUCTION

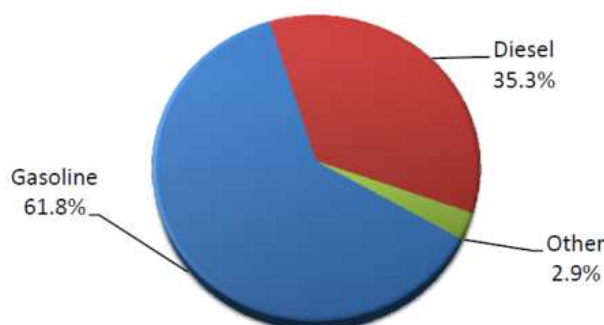
References: [1], [2], [3], [4], [5]

Development in automotive industry is very dynamic these days. Automobile manufacturers have to face strict commitments to the government and to its customers. The European Automobile Manufacturers Association has made an obligation to reduce the average carbon dioxide emissions in new vehicles to 140g/km by the year 2008. This corresponds to fuel consumption of 6.0 l/100 km for gasoline passenger cars and of 5.3 l/100 km for diesel passenger cars. Furthermore, examinations are currently being performed to see if an EU threshold of 120 g/km is achievable by the year 2012.

Table 1 Euro emission standards [1]

EURO EMISSION STANDARD	YEAR	CO	HC	HC+NOx	NOx	PM	PN
		[g/km]					[#/km]
Euro 1	1992	2.72	-	0.97	-	-	-
Euro 2	1996	2.2	-	0.5	-	-	-
Euro 3	2000	2.30	0.20	-	0.15	-	-
Euro 4	2005	1.0	0.10	-	0.08	-	-
Euro 5	2009	1.0	0.10	-	0.06	0.005	-
Euro 6	2014	1.0	0.10	-	0.06	0.005	$6.0 \times 10^{11}$

This means the automakers competition for developing more economical and environmentally friendly cars is driven not only by a consumer demand but also by government regulations. Many technical problems have to be faced to achieve these high goals. A slight increase in percentage of diesel passenger cars we have seen last years in Europe has definitely a positive effect on the CO<sub>2</sub> emissions, but this alone will not lead us to the goal. We have to concentrate on a development of the most commonly used drive unit, the gasoline engine, with market share of 62% in Europe and more than 95% in the USA, in order to increase efficiency and lower the emissions.



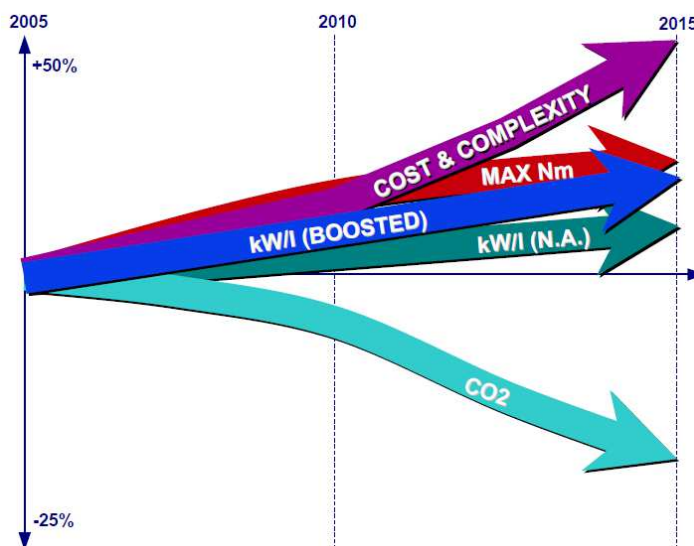
Graph 1 Gasoline engine market in Europe in 2009[1]

The most promising way to reduce fuel consumption is downsizing of gasoline engines. This means the large displacement of naturally aspirated engine is replaced by a turbocharged engine with small displacement and fewer cylinders. These smaller engines also have higher efficiency due to lower friction and lower mass. Reduction in consumption of up to 20% can be achieved this way.



Engines with three or four cylinders and displacements between 0.6 and 2.0 liters are being discussed currently. The output density can vary between 60kW/l and 100kW/l. All of these engines will be boosted by a gasoline turbocharger.

On Graph 2, we can see the prediction of gasoline engines development in coming years by Ricardo. Downsizing trend is obvious and makes difference in a turbocharger matching and design.



Graph 2 Gasoline engine development prediction [2]

New generation of gasoline turbochargers is therefore a commitment to the future. It will have to fulfill even higher demands of a higher temperature and pressure conditions. The pressure will increase and the airflow rate range will expand as well as a temperature will rise by about 50 to 100°C. The thermal inertia and the surface area of the turbine housing has to be as small as possible in order to keep emissions and vehicle mass low.

A very good example of development trends nowadays is a winner of International Engine of the Year Awards in 2011 the BMW gasoline 1.6-litre turbo engine used in BMW 116i/118i models and Mini Cooper models. It is a straight inline four-cylinder engine, with is known by its codename "Prince engine". It was launched in 2011 as a continuous BMW's effort of building efficient engines (EfficientDynamics). It is a replacement for naturally aspirated BMW N43 four-cylinder engine.

Prince engine is turbocharged by a TwinScroll turbocharger with wastegate, direct injected with variable valve timing system. This results in a power of 135kW, torque of 380Nm with declared combined fuel consumption of 5.8l/100km and CO2 emissions 130g/km.

Another representative of downsizing trends is FORD's 1.6 liter EcoBoost GTDi (gasoline turbocharged direct injected) engine with four cylinders, mono scroll wastegated turbocharger and roughly the same power output parameters. It was officially announced in 2009 at Frankfurt Motor Show. It is used on wide range of vehicles for example Ford Fusion, Focus, Mondeo, S-Max, C-Max, and Volvo S60.



*Figure 1 FORDS's GDTi 1.6 liter engine [4]*

As we can see on pictures of the small-downsized engines, the three-way catalytic converter is often mounted directly behind the turbocharger into a place where exhaust gases temperature is optimal for chemical reaction processes inside (reduction of nitrogen oxides NO<sub>x</sub> and oxidation of carbon monoxide CO & hydrocarbons HC). Another reason for this is also space restrictions under the bonnet. Therefore, turbine housing outlet shape with wastegate plays a vital role in turbo – catalyst interaction, which is a subject of this thesis.



*Figure 2 BMW's N20 four-cylinder engine with TwinScroll turbocharger [5]*



## 2 BASICS

### 2.1 ENGINE POWER

References: [6], [7], [8], [9]

The output power of an engine is dependent on engine swept volume, rotational speed of a crankshaft and the mean effective pressure as we can see in Formula 1. Increase of swept volume by means of increasing cylinder volume or adding additional cylinders results in building a bigger and heavier engine. Increasing engine speed does not increase the power per cycle, but increases the rate at which power is produced as the number of cycles per period increase. On the other hand, all engine components are subject of a greater wear. Therefore, engine speed increase is used in motorsport for a sport cars and motorcycles where a long technical life is not needed. For common applications in passenger and commercial vehicles sector, the best way of building a powerful engine with relatively low mass is increasing its BMEP (brake mean effective pressure) which is done by forcing more air into the combustion chamber by a turbocharger. Nowadays almost every diesel engine and around 20% of petrol engines are turbocharged.

Engine power [8]:

$$P = BMEP \cdot V \cdot i \cdot \frac{n}{\tau} \quad [W] \quad (1)$$

where:

BMEP	[Pa]	- brake mean effective pressure applied to piston
V	[m <sup>3</sup> ]	- volume of one cylinder
n	[s <sup>-1</sup> ]	- engine rotational speed
i	[-]	- number of cylinders
τ	[-]	- cycle coefficient, τ = 2 for four stroke engine; τ = 1 for two stroke engine

All naturally aspirated Otto and Diesel cycle engines rely on the downward stroke of a piston to create a low-pressure area (less than atmospheric pressure) above the piston in order to draw air through the intake system. With the rare exception of tuned-induction systems with resonance intake manifold, most engines cannot inhale their full displacement of atmospheric-density air. The measure of this loss or inefficiency in four-stroke engines is called volumetric efficiency. Power loss is often compounded by the loss of density seen with elevated altitudes. Thus, a natural use of the turbocharger is with aircraft engines. As an aircraft climbs to higher altitudes, the pressure of the surrounding air quickly falls off.

The objective of a turbocharger is to improve engine's volumetric efficiency by increasing the intake density. The compressor draws in ambient air and compresses it before it enters into the intake manifold. This results in a greater mass of air entering the cylinders on each intake stroke. The power needed to spin the centrifugal compressor is derived from high pressure and temperature of the engine's exhaust gases. A turbocharger may also be used to increase fuel efficiency, by recovering waste energy in the exhaust and feeding it back into the engine intake. By using this otherwise wasted energy to increase the mass of air, it becomes easier to ensure that all fuel is burned before being vented at the start of the exhaust stage.



## 2.2 BRAKE MEAN EFFECTIVE PRESSURE BMEP

References: [8], [11]

Brake mean effective pressure BMEP is usually measured on dynamometer. It is used to describe the engine capacity to do work independently of displacement volume.

Brake mean effective pressure [8]:

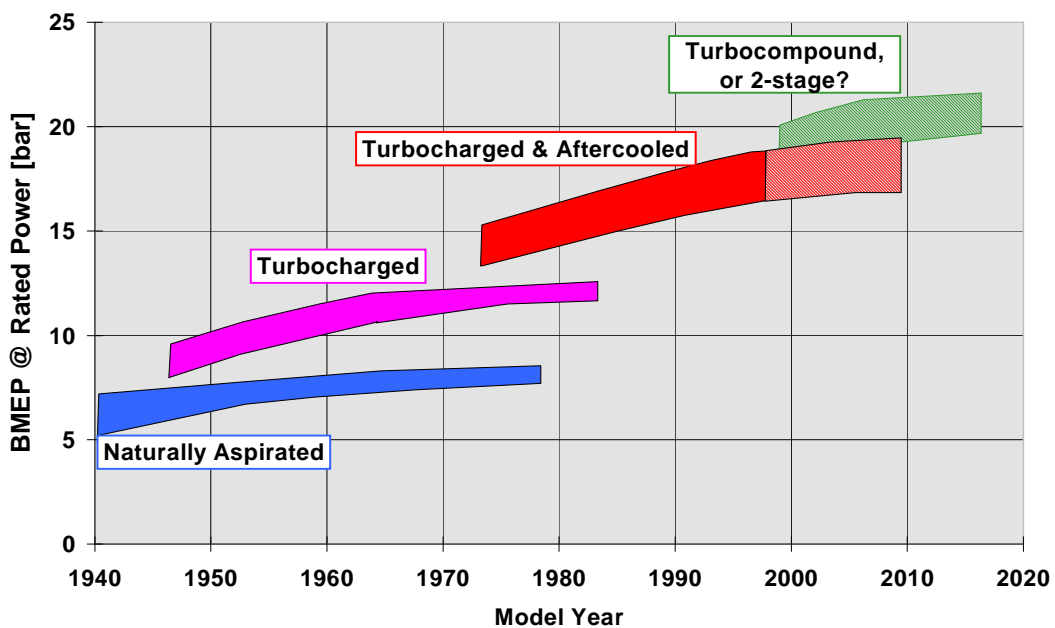
$$BMEP = \frac{H_C}{AFR \cdot \lambda} \rho \eta_f \eta_i \eta_m \quad [\text{Pa}] \quad (2)$$

where:

$H_C$	[J.kg <sup>-1</sup> ]	- heat of combustion
$AFR_{stoich}$	[-]	- air - fuel ratio
$\lambda$	[-]	- lambda
$\rho$	[kg.m <sup>-3</sup> ]	- intake air density
$\eta_v$	[-]	- volumetric efficiency
$\eta_i$	[-]	- indicated efficiency
$\eta_m$	[-]	- mechanical efficiency

The lambda is calculated as a ratio of actual AFR and  $AFR_{stoich}$ . Lambda of 1.0 is at stoichiometry, rich mixtures are less than 1.0, and lean mixtures are greater than 1.0. Typical  $AFR_{stoich}$  for a gasoline mixture is 14.7:1.

Graph 3 shows how BMEP has been changing throughout the internal combustion engine history. We can see enormous rise in an engine power, which is proportional to BMEP. Turbocharging has a great positive impact on engine output power. Moreover, with a use of an intercooler, which increases the intake air density further, the BMEP is even higher.



Graph 3 BMEP since 1940 [10]



### 2.3 INTAKE AIR DENSITY

References: [8], [10]

Intake air density can be increased by increasing air intake pressure or lowering intake air temperature. This simple principal is obvious from the Formula 3. In contemporary engines, both of these principals are used simultaneously. The air is pressurized by a turbocharger and then cooled down in an intercooler. This is done in order to be closer to efficiency of Carnot cycle, thus engine overall efficiency is higher.

Air density [8]:

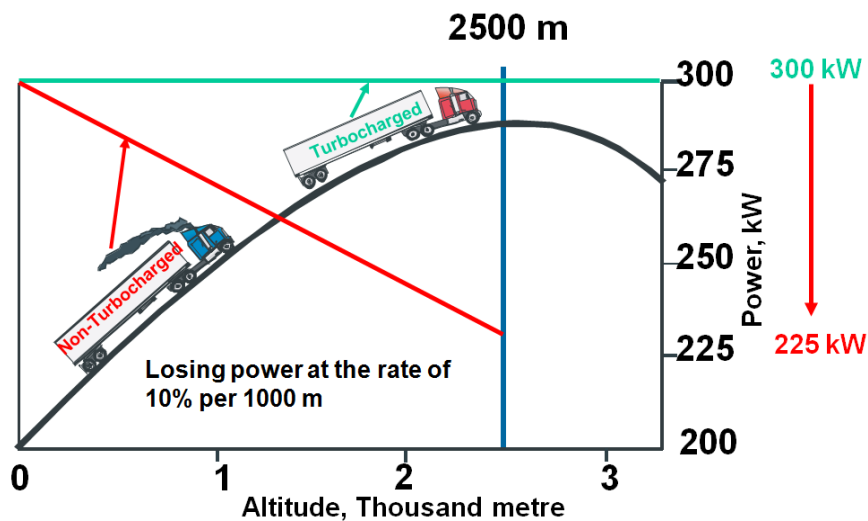
$$\rho = \frac{p}{r.T} \quad [\text{kg.m}^{-3}] \tag{3}$$

where:

- p [Pa] - boost intake air pressure
- r [J.kg<sup>-1</sup>.K<sup>-1</sup>] - specific gas constant, for dry air r = 287.058 J.kg<sup>-1</sup>.K<sup>-1</sup>
- T [K] - intake air temperature

Air density decreases with increased altitude and so does the air pressure. It also changes with variances in temperature or humidity. At sea level and 15°C, the air density is approximately 1.225kg.m<sup>-3</sup>.

On the Graph 4, we can see the difference between naturally aspirated and turbocharged engine. The engine output power is dependent on air density and intake pressure, which decreases with altitude in naturally aspirated engines but in general retains power with use of the turbocharger.



Graph 4 Power loss due to higher altitude [10]



## 2.4 VOLUMETRIC EFFICIENCY

References: [8], [12]

Volumetric efficiency  $\eta_v$  (Formula 4) is given as a ratio of actual mass of air-fuel mixture trapped inside the cylinder at the end of induction stroke and theoretical mass  $m_t$ , which would be obtained in a case of ideal naturally aspirated induction.

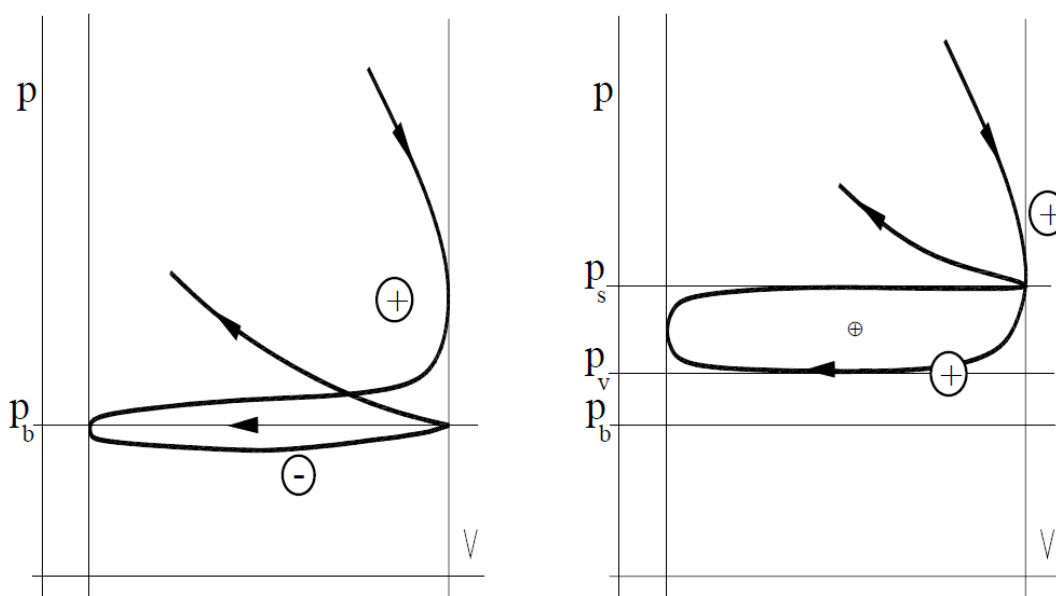
Volumetric efficiency [8]:

$$\eta_v = \frac{m}{m_t} = \frac{m}{V \cdot \rho} \quad [-] \quad (4)$$

where:

$m$	[kg]	- mass of air-fuel mixture at the end of induction stroke
$m_t$	[kg]	- theoretical air-fuel mixture mass at ideal induction state
$V$	[m <sup>3</sup> ]	- cylinder volume
$\rho$	[kg.m <sup>-3</sup> ]	- intake air density

Volumetric efficiency can be improved in a number of ways. For example, the size and a number of intake valves, the resonance systems, variable valve timing and most notably by so called forced induction such as supercharging or turbocharging. Real-cycle p-V diagram of turbocharged internal combustion engine (Graph 5- right) is different in an area of exhaust and induction stroke, which represents engine breathing. Pressure of gasses at exhaust stroke ( $p_v$ ) is lower than intake air pressure ( $p_s$ ). For this reason, the area defined by exhaust and induction curves in a diagram is positive. Volumetric efficiency of naturally aspirated engine is lower than 100% whereas turbocharged engines can reach volumetric efficiency even higher than 100% by means of pressurized air (above ambient-barometric). This is the main difference between naturally aspirated and turbocharged engine cycles.



Graph 5 p-V diagram of naturally aspirated (left) and turbocharged engine (right) [12]



### 3 WORKING PRINCIPAL

References: [10], [13]

As a forced induction system, a turbo is nothing more than an air pump that is driven by the exhaust gasses of a car engine. It consists of a compressor wheel and a turbine wheel that are connected by a common shaft. Turbocharger is in fact a turbine driven supercharger, which is powered by waste exhaust gasses. A compressor wheel compresses ambient air and forces it into the engine cylinder thus increasing air pressure and density. The pressurized air is then cooled in intercooler (charge air cooler) furthermore increasing air density. The more air means more fuel that can be burned. This results in production of higher engine output power. As a compressor wheel is mounted on a common turbine-compressor shaft, it rotates at the same rotational speed as a turbine wheel.

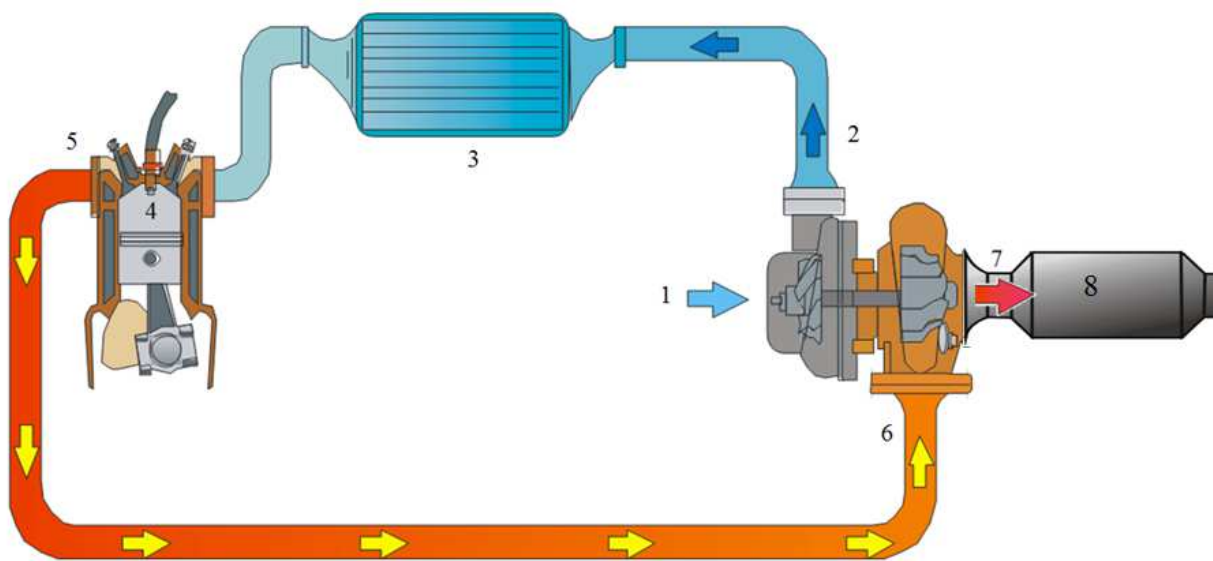


Figure 3 Scheme of turbocharged engine [10]

Working principal is obvious on Figure 3. An ambient air is after passing through air particulate filter sucked into compressor housing [1]. Rotating compressor wheel compresses it to higher pressure, which is also accompanied by a rise of a temperature. The pressurized air then flows out of a compressor discharge [2] into an intercooler [3], which cools compressed air down and increases its density even further. This high-density air then passes through intake manifold and intake valve into the engine cylinder [4]. Air is mixed with certain amount of fuel, ignited and burned thus creating power stroke. Burned gases then flows out of an engine at exhaust stroke through exhaust valve [5] into the turbine housing inlet [6]. The turbine creates backpressure to the engine, which means engine exhaust pressure is higher than atmospheric pressure. At these very hostile conditions of high pressure and high temperature, it flows through turbine housing volute causing turbine wheel to rotate. The exhaust gasses losses a fraction of its energy inside turbine housing, which is transformed into kinetic energy of a turbine and provides power necessary to drive compressor. After this, gasses flow out of turbine housing discharge [7] into the exhaust pipeline or in some cases directly into the catalytic converter [8], where so called after treatment is employed. The emissions are reduced and the noise is muffled in an exhaust silencer further downstream.



## 4 TURBOCHARGER DESIGN

References: [10]

The turbocharger is composed of three major assemblies. Those are compressor assembly [1], bearing assembly [2] and turbine assembly [3]. Each of these assemblies is specific and has to undergo different thermal and mechanical loads. Every single component is optimized for best performance, thermal resistance, high cycle fatigue and low price.

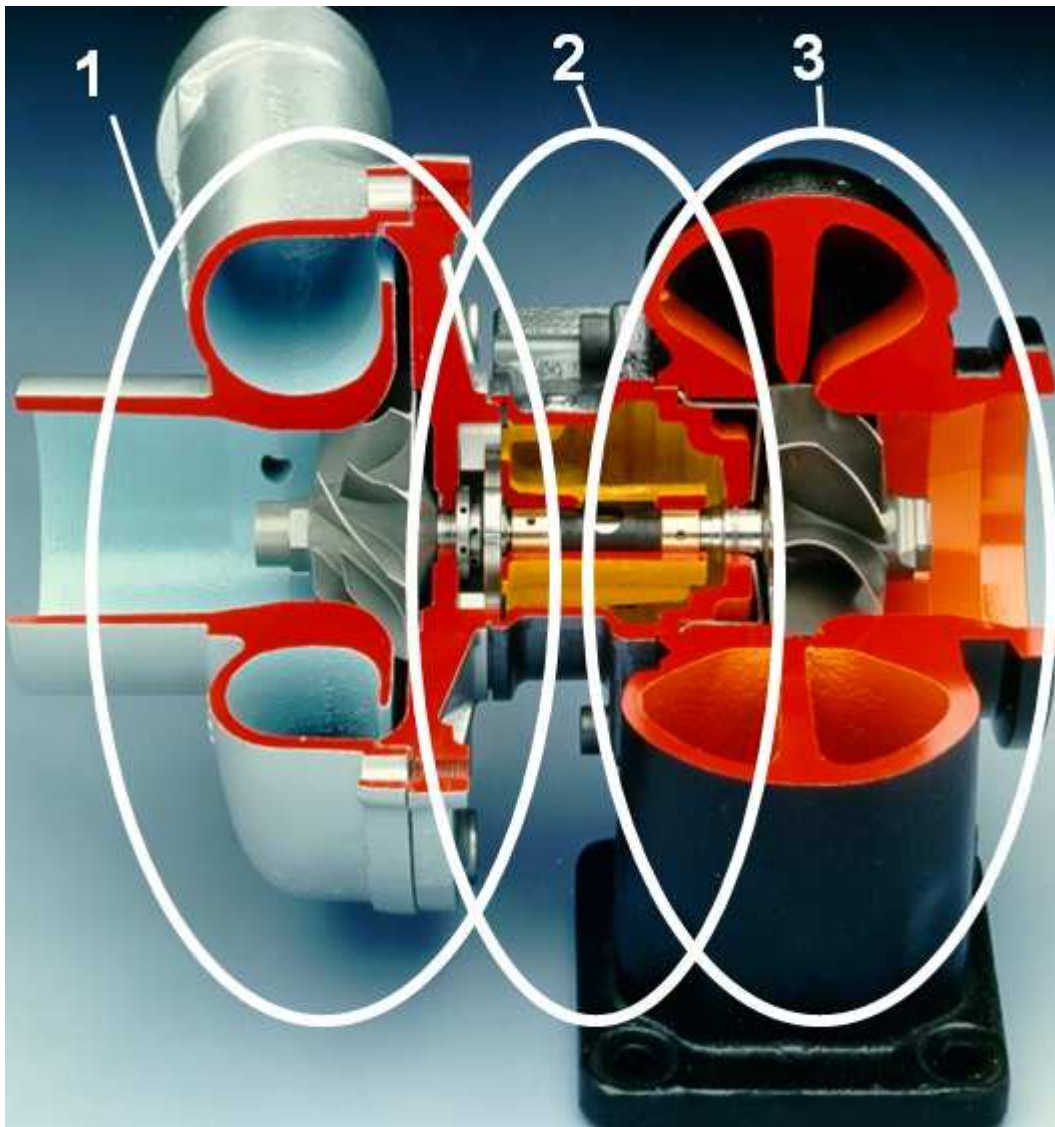


*Figure 4 Turbocharger design [10]*



## 4.1 COMPRESSOR ASSEMBLY

References: [10]

Compressor assembly is composed of compressor housing, compressor wheel and other complementary components such as speed or pressure sensors. In addition, an actuator, which operates wastegate valve, is usually mounted directly on compressor housing integrated bracket.

Objective of compressor housing assembly is described on section view through compressor housing at Figure 5. The ambient air is sucked inside the compressor housing [1] due to a slight under pressure, it is speeded up by rotating compressor wheel [2] and then passes through the diffuser [3], which slows air down converting kinetic energy to static pressure. Then the air flows into the housing spiral volute [4], which collects pressurized air and directs it through housing outlet into the engine intake manifold.

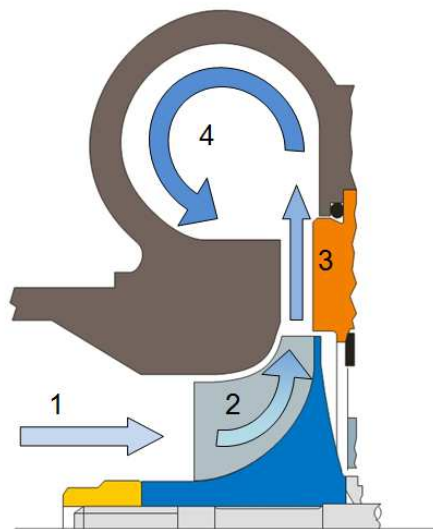


Figure 5 Section view of compressor housing [10]

Because pressurized air has temperature of approximately  $180^{\circ}\text{C}$ , the compressor housing is subject to higher temperature and vibration load. A very good material for these conditions is aluminum alloy, which have sufficient temperature and strength capability. It has very low density around  $1/3$  compared to steel, therefore weight saving is obtained.

## 4.2 COMPRESSOR WHEEL

A compressor is defined as a mechanical device in which energy is continuously transferred to a compressible fluid by means of a shaft driven impeller or wheel.

Compressor wheel has to withstand conditions of approximately  $180^{\circ}\text{C}$  and high vibrations. It is usually made of aluminium alloy with heat treatment consisting of solution treatment and artificial ageing. It can be casted or fully-machined depending on production quantity and accuracy of dimensions.

Challenges for the compressor wheel design are greater flow range, higher efficiency and higher pressure-ratio with keeping minimum size and mass.



### 4.3 BEARING ASSEMBLY

References: [10], [14], [15]

Bearing assembly is placed between compressor and turbine assembly (sometimes also collectively called as ending assemblies). Its role is to hold shaft, connecting turbine wheel and compressor wheel, in place, to provide sufficient lubrication and cooling and prevent wheel contact with housing. It has to provide stiffness and damping to control rotor motion. The stability of shaft motion without any unbalanced forces is a key.

The greatest temperature gradient in the turbocharger arises between the turbine housing and the bearing housing. That is why an optimum connection of the two housings is so important to the service life of the turbocharger.

Central housing is made of grey iron by casting with separate oil and water cores. Liquid grey irons are very fluid-like, therefore thin wall section of small housing with oil and water passages can be casted very easily.

The journal and thrust bearings are placed inside central housing. These are made of copper alloy and provide certain level of self-lubrication. Bearings are hydro-dynamically lubricated. The rotation of a shaft drags viscous oil into the gap between shaft and bearing, creating pressurized oil film.



*Figure 6 Thrust (left) and journal (right) bearings [14]*

Some turbochargers use ball bearings. It has been developed by Honeywell motorsport department for several racing series. It has 15% faster response to throttle change, which translates in better car drivability and acceleration. The ball bearing design reduces the amount of oil required to provide adequate lubrication. This reduces the chance for seal leakage.

Central housing is sealed to prevent oil passing into the end housing (thus increasing emissions) and to minimize the quantity of gas entering the centre housing. It is very important to find a balance between pressures in end housings and pressure in oil core.

Because of high exhaust gasses temperature, the central housing has to be cooled by oil and for gasoline applications furthermore by coolant from engine cooling system.



## 4.4 TURBINE ASSEMBLY

References: [10], [15], [16], [17]

Turbine assembly is composed of turbine housing, turbine wheel and depending on type of turbo regulation of wastegate (WG) components or VNT (variable nozzle turbocharger) components. Turbine assembly is exposed to high exhaust gasses temperatures up to 1050°C for gasoline applications, pressure impulses, engine vibrations and high oxidation reactions caused by exhaust gasses.

The turbine assembly is vital part of turbocharger as it extracts energy from exhaust gasses and transforms it into the kinetic energy of turbine wheel.

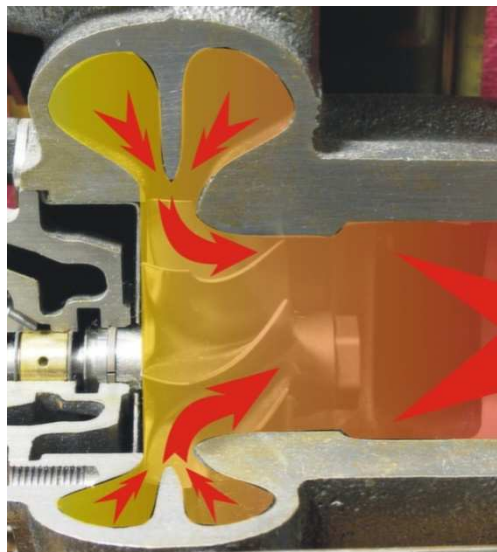


Figure 7 Exhaust gases flow through turbine assembly [16]

Turbine housing has design of spiral volute (similar to snail shell shape), which accelerates gas and directs it to the turbine wheel. Its radial sections are aerodynamically optimized to minimize hydraulic losses. The gas then flows through turbine wheel channels, where it hands over its energy to turbine wheel. This happens in a fraction of second and in thermo mechanics terms can be reproduced as adiabatic expansion without heat transfer.

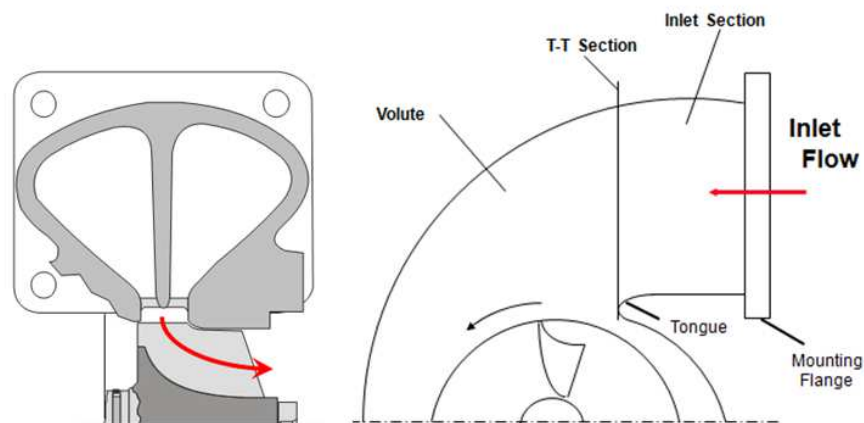
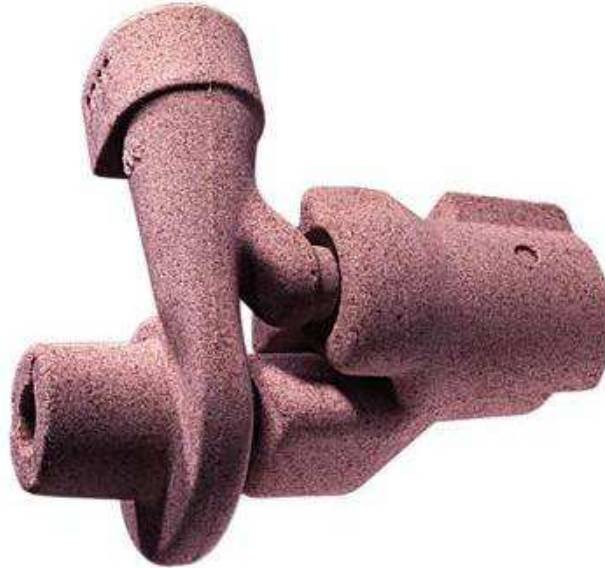


Figure 8 Turbine housing nomenclature [10]



Housing can be divided by a barrier in a volute. This design is called twin-scroll turbocharger and is used to prevent exhaust gas pulses from the engine cylinders to interfere with each other and to use its pulse energy to drive the wheel. As a result, the turbine inlet passage has better pressure distribution and more efficient gas delivery to the turbine wheel.

Turbine housing is usually made of ductile iron or stainless steel by green sand casting. It has to withstand high thermal fatigue stresses due to temperature change, variable section thickness and physical property interactions (expansion coefficient & thermal conductivity).



*Figure 9 Turbine housing core [17]*

Thin walls are desired to significantly reduce the weight of the turbine housing and simultaneously reduce the thermal inertia of the turbine housing. This leads to faster activation of the catalytic converter during the cold-start phase of the engine, which in turn could significantly improve the emission levels of the vehicle.



*Figure 10 Turbine housing casting [17]*



## 4.5 TURBINE WHEEL

References: [18], [19]

Turbine wheel is a mechanical device in which energy is continuously extracted from a working fluid by means of a shaft-mounted, bladed wheel.

The most suitable type of turbine wheel for passenger vehicle turbocharger is a radial wheel because of its compact design and strength, good efficiency for small size turbines and high expansion ratios. Mixed-flow wheel has similar efficiency as a radial wheel and has higher flow capacity. For this reason, it is used mainly in commercial vehicles. Axial wheels are used for large sized turbochargers, with low expansion ratio in motorsport projects thanks to its very low moment of inertia.

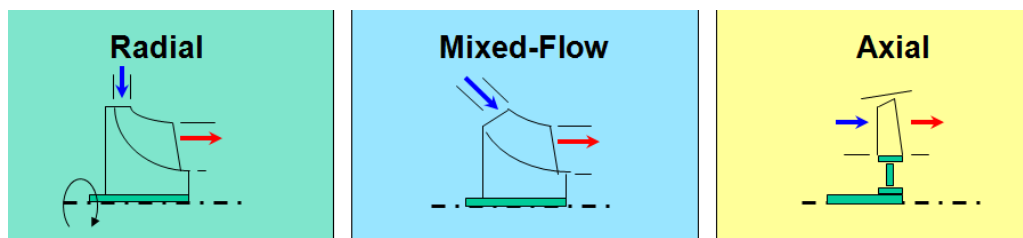


Figure 11 Turbine wheel types [18]

Typical turbine wheel shares approximately 70% of rotating masses moment of inertia, which is also very important measure of turbocharger performance. The objective in turbine wheel design is to minimize inertia for improved turbocharger response in transient states. For this reason scalloped backdisc wheels, reduced wheel diameter, minimal hub radius, reduced wheel axial length and lower density materials (e.g. ceramics and TiAl) are being developed. This is big challenge for the development because 1% loss in turbo efficiency negates response benefit of 10% reduction in rotor inertia.

A turbine wheel operates in a terribly hostile environment. The turbine is driven by exhaust gasses that can exceed 1050°C and are very corrosive. Although there is expansion across the turbine nozzle, therefore some cooling of the gasses, the temperature at the tips of the turbine rotor can approach exhaust gas temperatures. In addition, the rotor system operates up to 280,000 RPM. That imposes huge tensile loads from the centrifugal forces, as well as bending and vibratory loads.

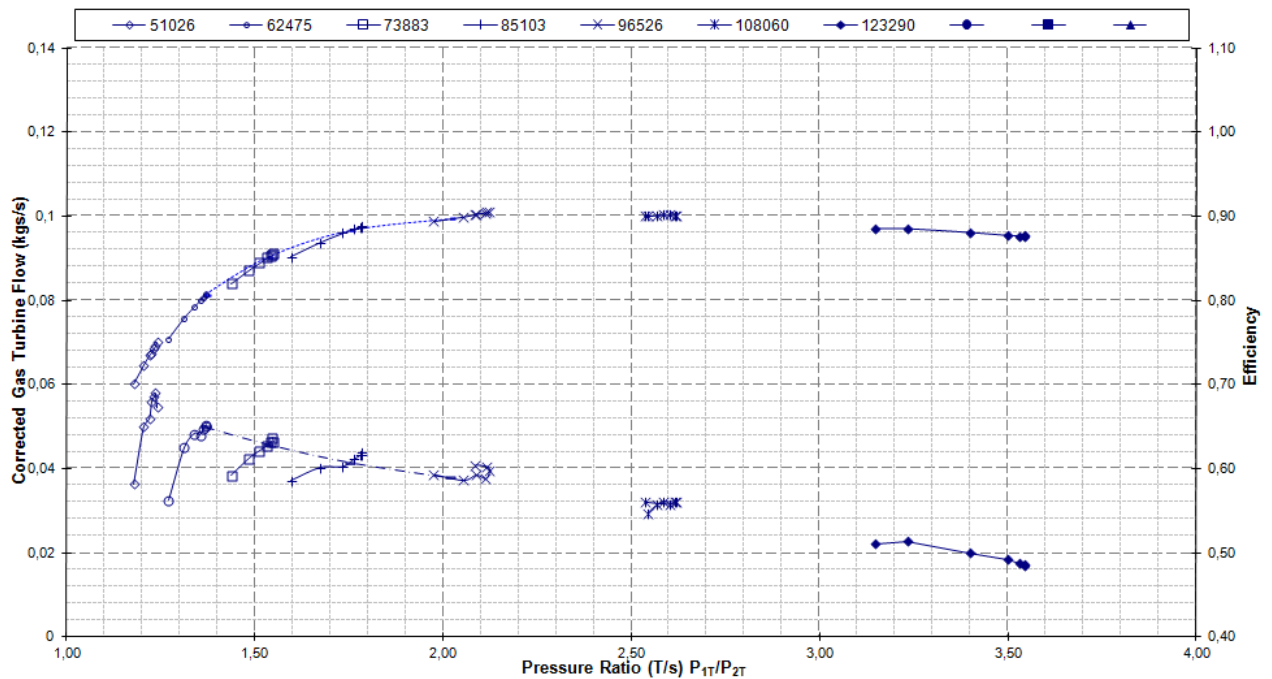


Figure 12 Turbine wheel [19]



Turbine wheels are made of Nickel base super alloys, which exhibit high strength, moderate ductility and excellent oxidation resistance over a very wide temperature range. The cost of turbine wheels is high due to the expensive metallic additions in the alloys (such as chrome, aluminium and molybdenum), and the need to process the materials under vacuum conditions to prevent the loss of the vital strengthening elements.

Laboratory measurement of turbine wheels on gas-stand provide turbine aerodynamic map (Graph 6), which shows relation between pressure ratio (inlet pressure  $P_{1T}$  to outlet pressure  $P_{2T}$ ) mass flow and turbine efficiency. Based on this graph we can predict turbine operation in a real on-engine environment.



Graph 6 Turbine aerodynamic map [18]



## 4.6 CONSTANT-PRESSURE TURBOCHARGING

References: [20]

In constant pressure turbocharging system, the exhaust gasses flows through large manifold to reduce the magnitude of pulsations before it is delivered to the turbine. The turbine wheel extracts energy mostly from potential and thermal energy of exhaust gasses. The efficiency of energy conversions within the turbine is significantly higher than that of pulse turbocharging, but on the other hand the gas losses much of its kinetic energy as it leaves exhaust ports. Moreover, unless the large manifold is thermally insulated, the heat losses from the gas may be considerable. There are several other disadvantages of constant-pressure turbocharging, for example poor response to the sudden load changes. This is because of length of time needed to reduce or increase the pressure inside large manifold volume. For this reason it is used for large and stationary engines (marine engines for example) where sudden loads changes are not present. This system uses so-called “mono-scroll” turbine housing with undivided volute.

## 4.7 PULSE TURBOCHARGING

References: [19], [20]

The principal disadvantage of pulse turbocharging is because of pulsating flow from individual cylinders into the turbine. The efficiency is lower than that of the constant-pressure system. However, in multi-cylinder engines, this disadvantage can be largely obviated by appropriate exhaust manifold design, which is “twin-scroll” turbine housing with divided volute. To take maximum advantage of pulse energy, the turbocharger should be sited as close as possible to the engine exhaust ports, so that the volumes of the passages from the valve ports to the turbocharger are small. This helps to ensure rapid turbocharger response in transient conditions.

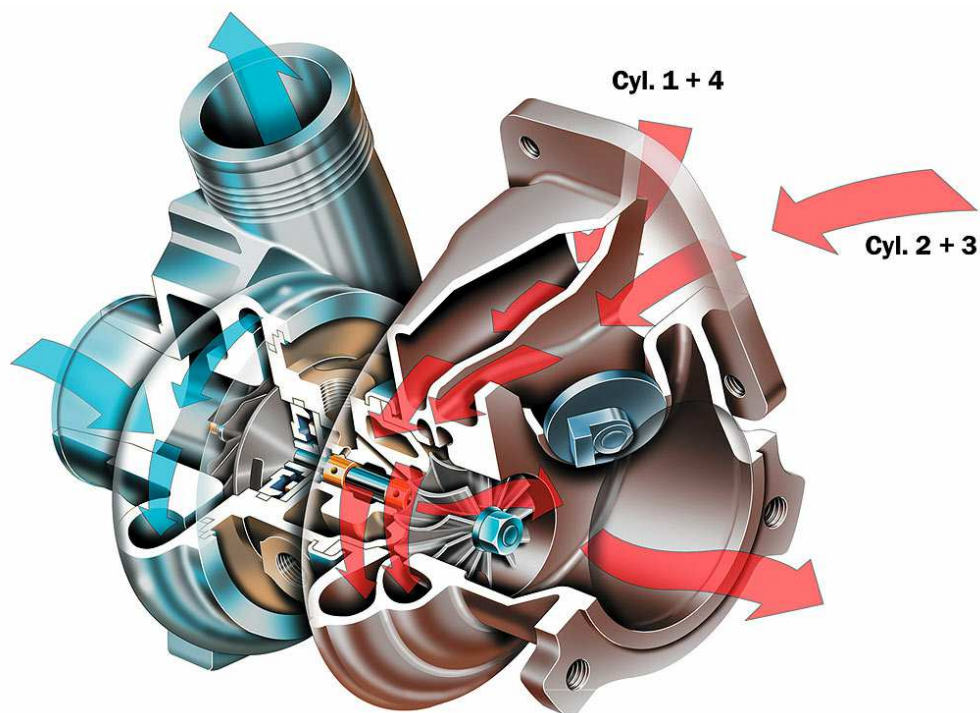


Figure 13 Twin-Scroll turbocharger [19]



## 5 TURBOCHARGER CONTROL

References: [10]

Internal combustion engines work at different operating conditions. Especially engines for road vehicles are typical with rapid speed changes and loads making the engine very complex device that has to be efficient over the whole working range and in transient states.

To get an ideal boost pressure coming from the compressor for different engine conditions the turbocharger needs to be controlled by airflow regulation before it enters the turbine wheel. This is very important especially at low engine speeds to provide more turbine power and boost pressure and at high engine speeds, where airflow is very high, to avoid turbocharger over-speed and over-boost.

This can be done in several ways:

- Variable Nozzle Turbocharger (VNT), used mostly for diesel applications
- bypassing exhaust gasses through wastegate (WG) channel mostly used for gasoline applications
- two-stage turbocharging

There are some other rarely used types of turbocharger regulation systems, for example changing the width of turbine stator (slide-vane concept- one piece VNT) or turning directional flap, both used to change inlet cross-sectional area of turbine housing.

Turbocharger without regulation system is called free-floating turbocharger. Its maximum rotational speed is determined by wheel size solely.

### 5.1 VARIABLE NOZZLE TURBINE – VNT

References: [10], [19], [21], [22]

The goal of a VNT turbocharger is to expand the usable flow range while maintaining a high level of efficiency. VNT mechanism regulates exhaust gasses inflow angle and inflow speed by guide vanes located upstream the turbine wheel.

VNT turbocharger works by adjusting the gas throat section at the inlet of the turbine wheel in order to optimize turbine power with required flow velocity.

At low engine speed and small gas flow, the turbocharger reduces the throat section by closing the vanes (lowering inter-vane distance) increasing exhaust gas velocity entering the turbine wheel and thus increasing turbine power and boost pressure. At full engine speed and high gas flow, the VNT increases the throat section by opening the vanes (increasing inter-vane distance) and reduces gas velocity entering turbine wheel to avoid turbocharger over-speed and over-boost.



The throat section modulation can be controlled directly by the compressor pressure using pressure actuator, or by engine management system using a vacuum actuator, rotary or linear electric actuator.

VNT mechanism is also used as an exhaust brake in commercial vehicles. In addition to high temperatures and vibrations, this creates high mechanical strength demands on VNT components.



*Figure 14 Open VNT mechanism [21]*

VNT mechanism is composed of movable vanes that are placed circumferentially around turbine wheel axis in between two ring plates. These rings are separated by several spacers that secure rings mutual position and provide vane axial clearance to keep vanes turning freely after whole assembly is heated up to the temperatures of exhaust gas. Vanes are welded together with arms, which fit into the unison ring slots. Unison ring is operated by a main arm, which is connected directly to external mechanism of actuator rod or lever. Whole mechanism has to be designed carefully to keep it operating at high exhaust gas temperatures, high vibrations and pressures. Kinematics simulations and fluid mechanics calculations are common case when it comes to VNT load studies and its development. Vane profile is optimized by CFD calculation methods to reduce backpressure and increase turbine efficiency. This way for example, new-cambered vanes are being developed nowadays.

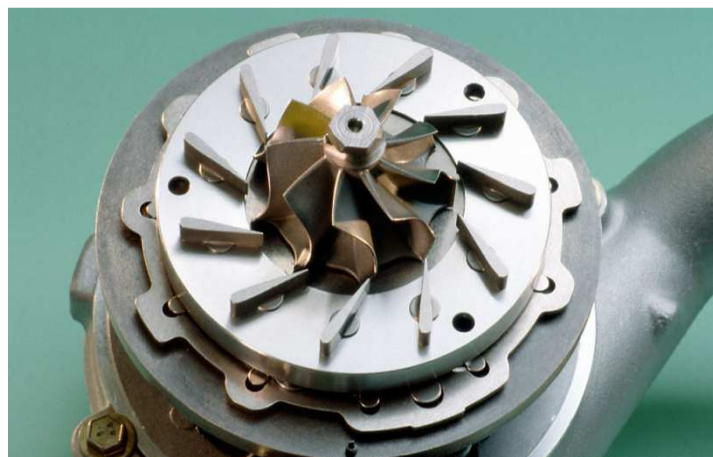


*Figure 15 VNT cartridge and turbine wheel [19]*

## 5.2 WASTEGATE

References: [10], [20], [23]

Wastegate (or turbine bypass) is a valve, which allows some of the exhaust gasses to bypass the turbine wheel and thus regulates its rotational speed. Wastegated turbocharger allows a use of smaller turbine wheel and smaller A/R turbine housing to cover low engine speeds, resulting in less turbo lag time. At high engine speed, a valve opens and preserves turbocharger to over-speed.

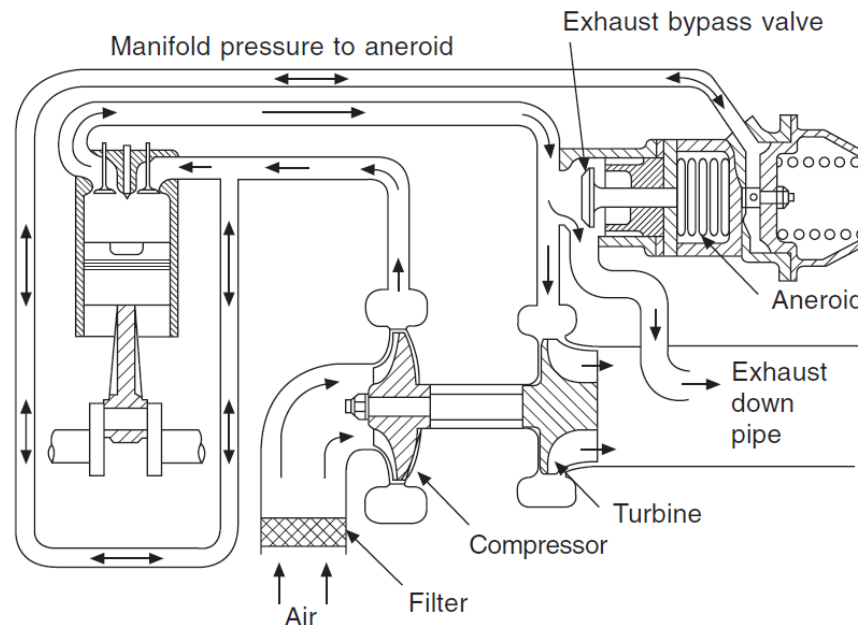


Figure 16 Wastegate turbocharger coupling with engine [20]

By bypassing excess exhaust gasses, the energy is also being bypassed. This reduces the power driving the turbine wheel to match the power required for a given boost level.

When a valve is opened, exhaust gasses (flowing into the turbine housing out of an engine) are divided. A fraction of gasses flows through the turbine wheel, where it loses some of its energy (which is extracted by turbine wheel) and the rest is bypassed through the wastegate duct. This proportion is determined by valve opening, housing and duct design and wastegate diameter. All of this has to be considered very carefully to keep turbocharger running in optimal working conditions.

The valve is controlled by pneumatic actuator directly by compressor boost pressure or by vacuum actuator controlled by ECU.

There are two types of wastegates. Internal wastegate (Figure 17) is built directly into the turbine housing. The wastegate duct in this case has to be placed before (upstream) the turbine housing T-T section so it does not influence exhaust gasses flow inside a spiral volute.

The external wastegate is added to the exhaust plumbing on the exhaust manifold or header. The advantage of external wastegate is that the bypassed flow can be reintroduced into the exhaust stream further downstream of the turbine. This tends to improve the turbine's performance. In racing applications wastegated exhaust flow can be vented directly to atmosphere to prevent turbulence in turbine housing exhaust flow and reduce backpressure in the exhaust system.



Figure 17 Internal wastegate [23]

As a wastegate is operating in very hostile conditions of temperatures up to 1050°C in petrol engines, the valve has to be robust and withstand high thermal and mechanical loads. For this reason, a simple swing valve type is used for wastegates nowadays.

Wastegate components are made of austenitic stainless steels or Inconel (austenitic nickel-chromium-based super alloy). These materials are suitable for high temperature applications.

The main in-service problem with the arm and bushing is galling and sticking as a result of actuator spring loads, temperatures and vibrations.

The wastegate external mechanism is simple. The actuator rod is connected to crank which is welded together with arm. The arm is turning around bushing axis placed inside turbine housing wall.

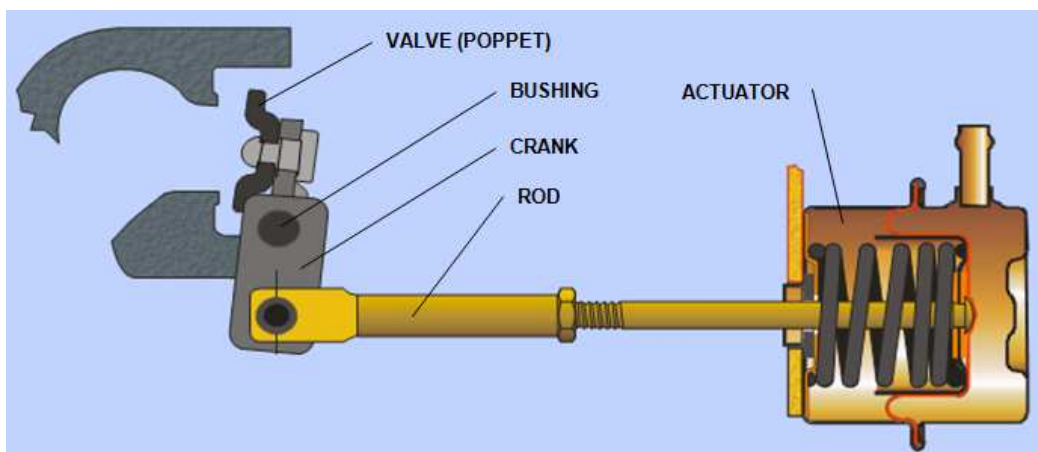


Figure 18 Wastegate controlled by pneumatic actuator [23]



### 5.3 TWO-STAGE TURBOCHARGING

References: [24], [25]

The engine with two-stage turbocharging system is equipped with two turbochargers that work side-by-side in parallel or serial system. This helps to keep boost pressure optimal for wide range of engine speeds and loads and further increase engine performance and efficiency. As a result, this reduces fuel consumption and satisfies power requirements for passenger cars and commercial vehicles. Very good turbocharging control can be obtained this way.

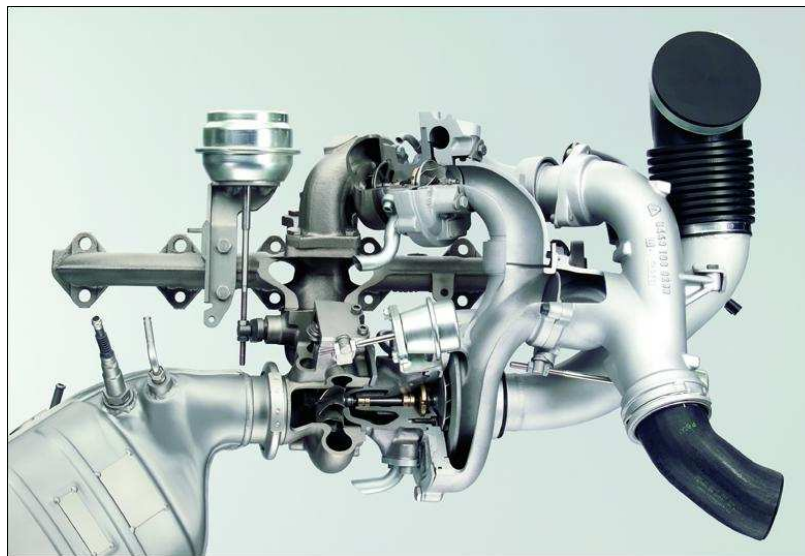


Figure 19 BMW's Twin-Turbo system [24]

At low engine speeds, i.e. when the exhaust mass flow rate is low, the wastegate remains completely closed and the entire exhaust mass flow is expanded by the HP turbine. This results in a very quick and high boost pressure rise. As the engine speed increases, the job of expansion is continuously shifted to the LP turbine by increasing the cross-sectional area of the wastegate accordingly. The system can be regulated via pneumatic actuators that control the bypass and wastegate valve.

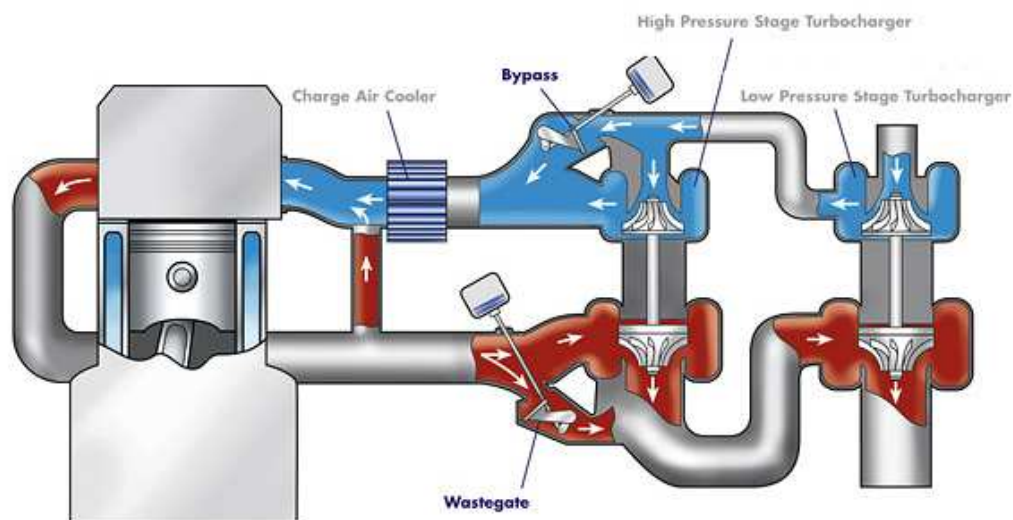


Figure 20 Scheme of two-stage turbocharging [25]



## 5.4 HYBRID TURBO

References: [26], [27]

A hybrid turbocharger is an electric turbocharger without mechanical link between turbine and compressor wheel. The turbine wheel is connected to the electrical motor with permanent magnets. When energy generated by turbine wheel is higher than is required by compressor, the electrical motor works as a generator and charges the storage device (battery). This energy can be later used to drive the compressor to cover power demand at rapid engine acceleration.

This design has many benefits. Those are easier packaging by enabling the turbine and compressor to be placed in separate parts of the engine, ECU controlled boost levels that enable more predictive control of boost pressure, lower moment of inertia of compressor wheel and much quicker response to rapid throttle changes in transient states.

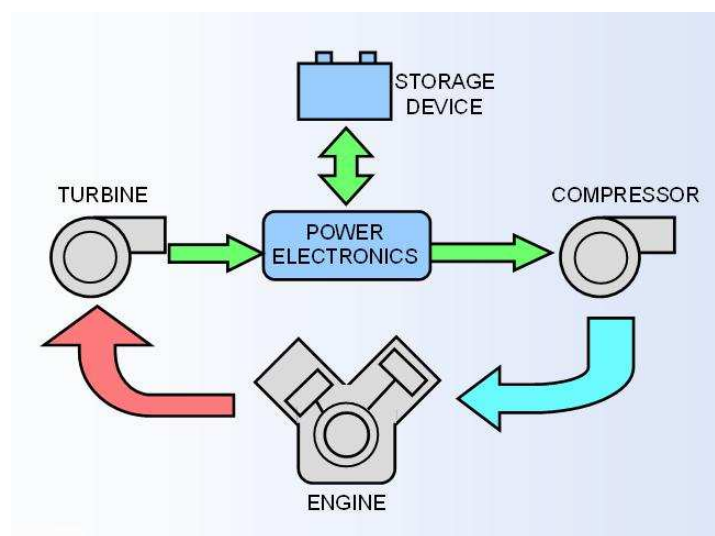


Figure 21 Scheme of hybrid turbocharging system [26]

This technology is very promising way of forced induction system in the future, and gives many advantages when talking about turbo lag and its regulation.

It is currently being developed under several market codenames by Aeristech as a Hybrid turbo, BorgWarner as eBooster and Honeywell as an electrically assisted turbocharger.



Figure 22 Electrically driven compressor EDC [27]





Because of expansion processes and different expansion ratio in diesel and petrol engines, the temperature of exhaust gasses differs. **Diesel** produces exhaust gasses with temperature up to **830°C**. In contrast, the temperature of turbocharged **petrol** engine can rise up to **1050°C**. Exhaust gasses with this temperature flows out of an engine, through exhaust manifold directly into the turbine housing inlet. Turbocharger is placed as close to engine exhaust ports as possible to take advantage of exhaust gasses high energy.

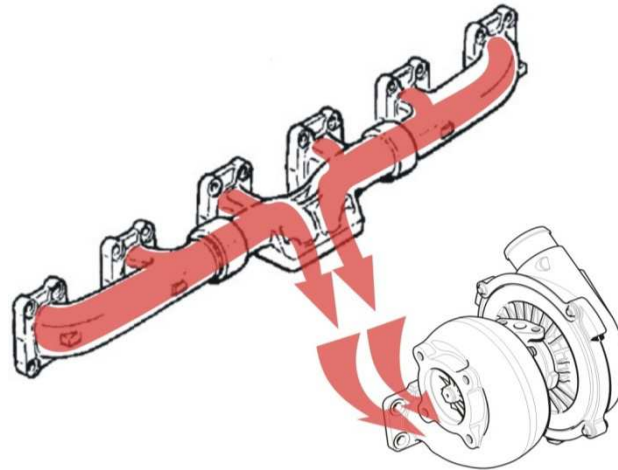


Figure 23 Exhaust manifold and turbocharger [16]

However, not only the higher exhaust gasses temperature put higher demands on gasoline turbocharger. It is also the fact that a petrol engine rotational speed varies much more (wider speed range) than a diesel engine (which also runs at lower rotational speeds). This creates many transient states where turbo-lag is very important. In addition petrol engine uses throttle butterfly valve in intake manifold to control mass of air entering the cylinders. When a throttle is closed suddenly, a backpressure occurs in compressor outlet (engine intake) tract, which can result in compressor wheel surge or even its damage.

All of these are reasons why gasoline turbocharger nowadays uses wastegate regulation with very simple swing type valve. The VNT mechanism is usually very weak to withstand conditions of petrol engine. However, there are some representatives of VNT turbocharger for gasoline applications. These use very expensive materials, have limited life, and therefore are suitable for motorsport and racing applications only.



Figure 24 Gasoline turbocharger environment at full load [16]

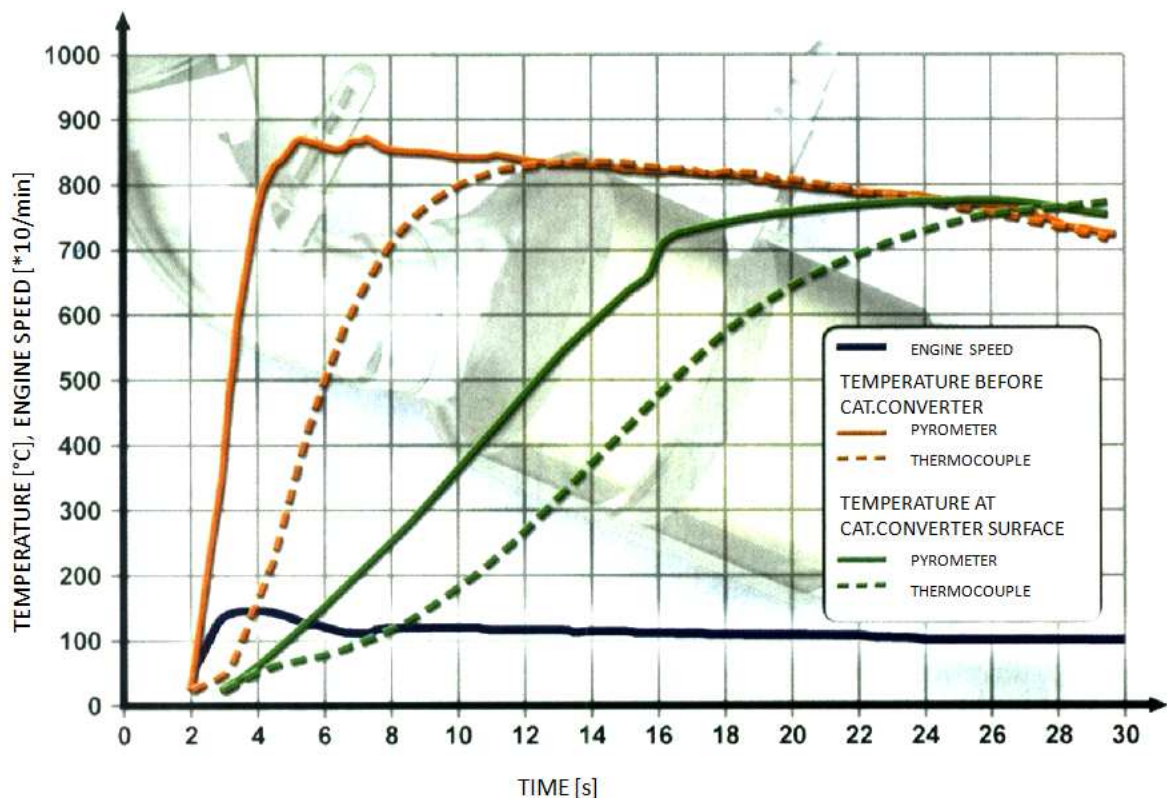
## 7 CATALYTIC CONVERTER

References: [31], [32], [33], [34], [35], [36], [37]

Exhaust gas emitted from vehicles contains many components that contribute to air pollution, namely carbon monoxide (CO), hydrocarbons (HC) and nitrogen oxides (NO<sub>x</sub>).

For this reason catalytic converter, which reduces these pollutant emissions, is a common device installed into an exhaust tract of every single vehicle nowadays.

Recent studies has shown that currently used three way catalytic converters used in vehicles are able to reduce the CO, HC and NO<sub>x</sub> emissions by about 95%. However, the operating conditions of the catalytic converters vary extremely with the driving mode of the vehicle, its size, type, location in exhaust after treatment system and time elapsed since engine start.



Graph 8 Temperature of exhaust gas and catalytic converter surface after engine cold start [31]

For emission control of petrol engines, the three-way catalytic converter is used. Its name comes from three chemical reactions taking place within its honeycomb structure. These are reduction of NO<sub>x</sub>, oxidation of CO and oxidation of unburned HC, which can be described by following chemical equations [33]:

Oxidation of carbon monoxide to carbon dioxide:  $2\text{CO} + \text{O}_2 \rightarrow 2\text{CO}_2$

Oxidation of HC to carbon dioxide and water:  $\text{C}_x\text{H}_{2x+2} + [(3x+1)/2]\text{O}_2 \rightarrow x\text{CO}_2 + (x+1)\text{H}_2\text{O}$

Reduction of nitrogen oxides to nitrogen and oxygen:  $\text{NO}_x \rightarrow x\text{O}_2 + \text{N}_2$



In regard to the catalyst type, the two most common types are used. The ceramic and metallic substrates.

In automotive applications ceramics monoliths are made of synthetic cordierite, that is highly resistant to fracture due to thermal shock, is resistant to oxidation and has high melting temperatures around 1450°C.

Metallic monoliths are used where even higher temperatures are experienced. It is made of metals such as Fecralloy (73% Fe, 20% Cr, 5%Al plus small amounts of Ni and Si) with melting temperature up to 1500°C.

Metallic monoliths provide higher geometric surface area while offering lower back pressure. Furthermore, metallic monoliths are being used in close coupled applications due to their higher thermal conductivity that guarantees more uniform temperature distribution between monolith channels as compared to that of ceramic monoliths.

Metallic substrates allow its utilization closer to the engine, which is essential to improved conversions during cold start conditions.

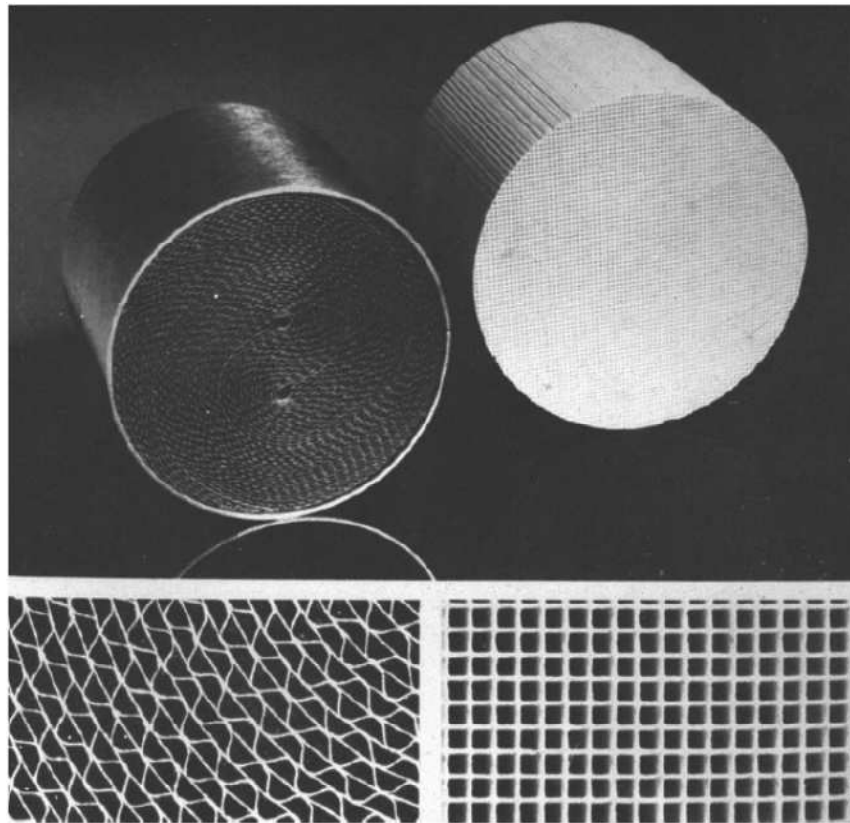


*Figure 25 Metallic (left) and ceramic (right) monoliths [20]*

The honeycomb material is a unitary structure with uniform-sized and parallel channels. Therefore, it creates a backpressure to the engine exhaust and restricts the gasses flow inside the structure. The magnitude of pressure drop within catalytic converter depends on channel design, cell density (cpsi=number of cells per square inch) and boundary layer surface roughness. Furthermore, entrance effects such as flow maldistribution and sudden contraction when flow enters the monolith occurs due to the inlet porous boundary layer. This contributes to the overall pressure drop as well.



To simulate the exhaust gas flow within the catalytic converter in a CFD calculation method, the porous media is defined with a streamwise directional loss coefficient. This allows to substitute honeycomb structure with virtual porous domain without modeling detailed catalyst channel design, details of the flow around obstacles and simulation without chemical reactions.

Directional source of resistance (permeability) is defined by quadratic resistance coefficient  $K_Q$  [ $\text{m.kg}^{-4}$ ] which can be calculated using Formula 5.

Pressure gradient in streamwise direction [35]:

$$\frac{\partial p}{\partial x} = -K_Q U_x^2 \quad (5)$$

where:

$\frac{\partial p}{\partial x}$       [ $\text{Pa.m}^{-1}$ ]      - pressure drop gradient in streamwise direction

$K_Q$       [ $\text{m.kg}^{-4}$ ]      - quadratic resistance coefficient

$U_x$       [ $\text{m.s}^{-1}$ ]      - average velocity in streamwise direction

This means that to determine the directional loss coefficient  $K_Q$ , we need to know the pressures before and after the catalytic converter, its length and average gas velocity entering the porous domain.

As monolith has a parallel channels, the flow is inhibited in transverse directions, so the gas does not flow in between the channels. The flow is straightened and velocity has only streamwise direction components.

To achieve this in CFD simulation software, the transverse coefficients are taken to be specified as a factor times the streamwise coefficient. The transverse multiplier is typically taken to be around 10-100.

This theory of porous media definition in CFD software is later used in flow simulations and exact quadratic resistance coefficient calculation for a given engine.

Truth to be said in the end of this chapter, catalytic converter efficiency can be improved especially in cold start conditions in number of ways. One of them is regular temperature distribution over the catalyst inlet surface.

This is very important particularly when catalytic converter is placed right behind turbocharger outlet, which is a very common layout in current turbocharged petrol engines.

Light-off time can be reduced by exhaust gasses bypassing in cold start conditions, thus allowing the hot gas to flow directly onto the catalyst inlet surface. The wastegate valve would be opened in this case for a certain period after engine start until the catalytic converter reaches operating temperature.

Unfortunately, current turbocharger discharge design uses swing valve regulation (typical wastegate), which directs gasses along the discharge wall which results in uneven temperature distribution (when bypassing). The aim of this thesis is to create new wastegate design and simulate the flow in different valve positions, in order to improve temperature distribution.



The evidence of effort to achieve regular temperature distribution over the catalytic converter inlet surface area could be the diverter for catalytic converter patented in 2004. Its role is to evenly distribute exhaust gasses passing from a small diameter upstream exhaust gas pipe section into a much larger diameter catalytic converter assembly. The diverter includes a diverter element and mounting brackets. The diverter element has a central hole and has conical walls. The large conical angle of the diverter effectively directs exhaust gases to the periphery of the large diameter catalytic converter, while the holes in the conical diverter walls allow sufficient exhaust gases to reach the radially intermediate portion of the catalyst.

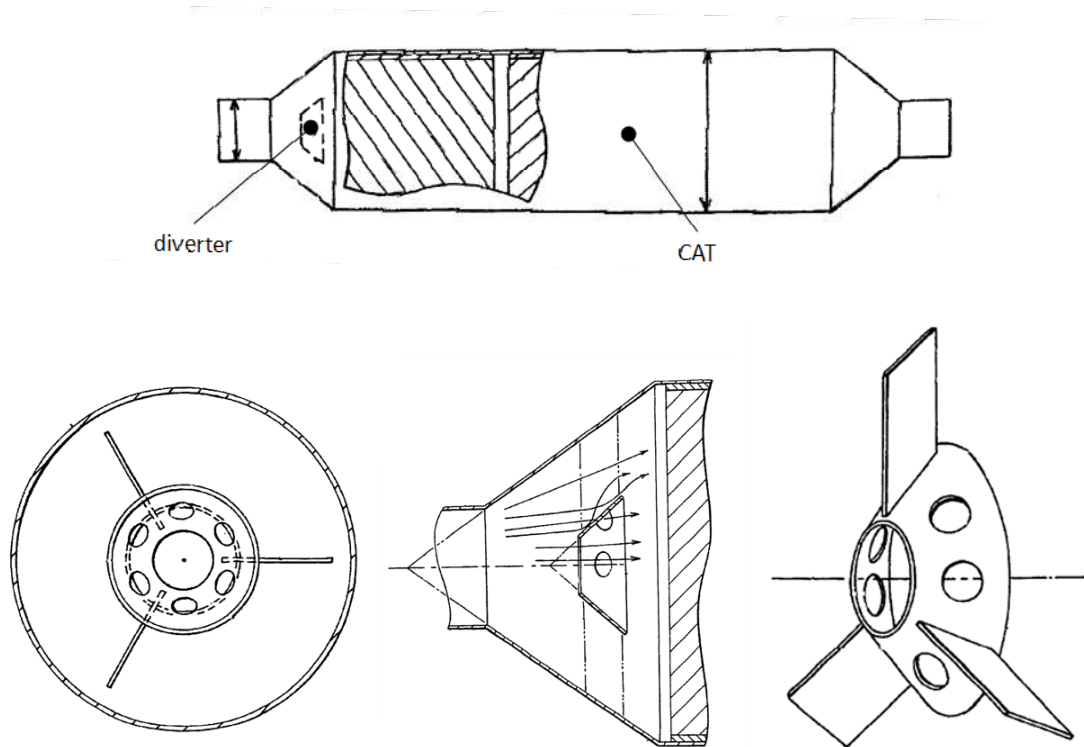


Figure 26 Catalytic converter with diverter element [37]



## 8 ADIABATIC EXPANSION

References: [18], [38]

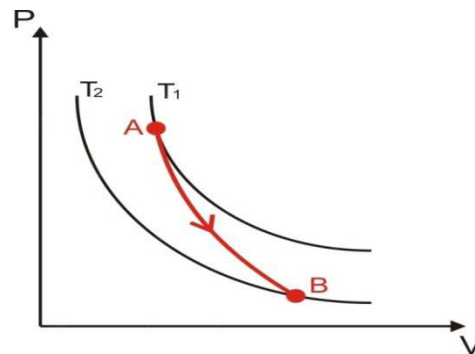
Processes taking place inside turbine housing can be interpreted as an adiabatic expansion process in open thermodynamic system without heat exchange to turbine surroundings, with some measure of simplification. This simplification can be used in a case, when the system is thermally insulated or the process happens in a very short time. These conditions are met in case of turbine housing and flow character inside turbine passages.

The adiabatic process shown at p-v diagram (Graph 9) is described by following equations [38]:

$$pv^\kappa = \text{constant} \quad (6)$$

$$\frac{T_2}{T_1} = \left(\frac{p_2}{p_1}\right)^{\frac{\kappa-1}{\kappa}} \quad (7)$$

The energy of gasses, flowing inside the turbine housing, is derived from its pressure and temperature. This energy is than transformed to mechanical work of turbine wheel where it losses portion of its energy. The pressure downstream of turbine wheel decreases and the temperature goes down as well. This is represented as an adiabatic expansion process, in which the heat transfer from working fluid is zero ( $dQ=0$ ).

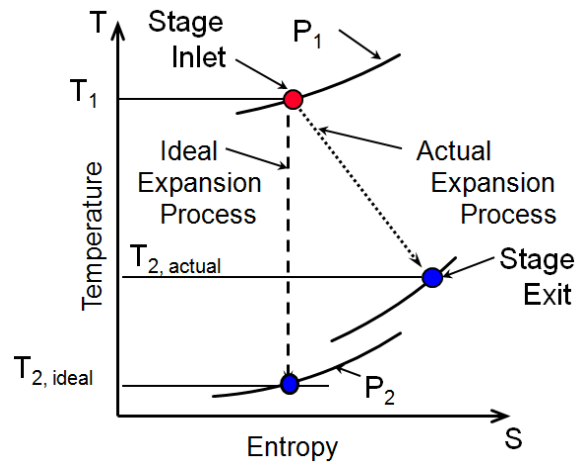


Graph 9 Adiabatic expansion in p-V diagram [18]

The measure of energy transformation quality is thermal efficiency. In turbo machinery branch the expansion process efficiency is judged by a comparative isentropic process, which represents the most-ideal process without frictional losses. The isentropic efficiency is therefore a measure of volute, wheel and other fluid channels design quality. It is calculated as a ratio of actual technical work done and ideal comparative isentropic work, which would be gained with the same pressure values without aerodynamic losses (shown in Formula below).

Isentropic efficiency of energy conversion [38]:

$$\eta_{iz}^T = \frac{a_t}{a_{t, ideal}} = \frac{c_p dT}{c_p dT_{ideal}} = \frac{T_1 - T_2}{T_1 - T_{2,ideal}} = \frac{T_1 - T_2}{T_1 - T_1 \left(\frac{p_2}{p_1}\right)^{\frac{\kappa-1}{\kappa}}} = \frac{1 - \frac{T_2}{T_1}}{1 - \left(\frac{p_2}{p_1}\right)^{\frac{\kappa-1}{\kappa}}} \quad (8)$$



Graph 10 Adiabatic expansion in T-s diagram [18]

The power of turbine wheel is transferred to the compressor wheel by means of a common shaft but a fraction of the turbine power is lost due to friction losses in the journal and thrust bearings and oil seals. The ratio of the power delivered to the compressor to the power produced by the turbine wheel is defined as the mechanical efficiency  $\eta_{\text{mechanical}}$ , of the bearing system and seals as shown by

Formula below. Mechanical efficiency depends on the size of the turbocharger and the turbo speed. Typical values are ranging from 90 to 98%.

In turbine design, knowing the mechanical efficiency is important because of the need to determine how much power the turbine must produce to both drive the compressor and to overcome the losses in the bearings and seals. Empirical correlations are used to estimate mechanical efficiency.

Mechanical efficiency can be also measured as ratio of compressor power output to turbine power input.

Mechanical efficiency [18]:

$$\eta_{\text{mechanical}} = \frac{\text{Power}_{\text{compressor}}}{\text{Power}_{\text{turbine}}} \tag{9}$$

The actual (total) efficiency is therefore even lower than isentropic efficiency of turbine. It includes mechanical efficiency  $\eta_{\text{mechanical}}$  (losses in bearing and sealing system).

Total efficiency [18]:

$$\eta_T^T = \eta_{iz}^T \cdot \eta_{\text{mechanical}} \tag{10}$$



## 9 COMPUTATIONAL FLUID DYNAMICS – CFD

References: [39], [40], [41]

CFD Computational Fluid Dynamics is branch of fluid mechanics that uses numerical methods and algorithms to analyze problems with fluid flow, interaction liquids and gases with surfaces defined by boundary conditions. The three basic principals are used in CFD calculations. Those are the conservation of mass, momentum and energy transcribed to partial differential equations of Navier-Stokes and Euler.

CFD allows to predict, with confidence, the impact of fluid behavior in various applications such as an aerodynamic of cars, planes, flow inside internal combustion engine cylinder, turbines, exhaust manifolds and windmills. It is also capable to simulate combustion processes, radiation, heat transfer, different gas flow mixing processes and others.

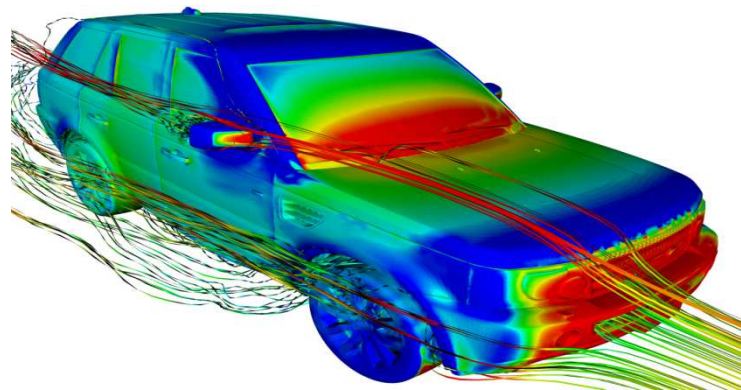


Figure 27 CFD simulation of airflow around car [41]

To simulate a fluid flow the fluid volume geometry has to be extracted from a computer model (sometimes also referred as a negative volume). This volume occupied by the fluid is divided into discrete cells (the mesh). The fluid volume can be divided into separate domains in which different mesh can be defined. These domains are than put together in pre-processor by an interface definition. The boundary conditions are than defined such as inlet, outlet, boundary walls, rotational domains and interfaces. Than a simulation is prepared for run, where fluid dynamics equations are solved for every single discrete cell (element) of fluid volume and a number of variables is calculated such as a pressure, density, temperature, velocity, Mach number, energy and lots of others. Finally, a post-processor is used for the analysis and visualization of resulting solution. For example, the pressures can be integrated over the defined area to get a force or momentum applied to the surface of interest. The velocity field, temperature distribution or a streamlines can be visualized on every single element of virtual model.



Graph 11 CFD flowchart

Nowadays software such as ANSYS CFX, ANSYS FLUENT, CCM+, EXA Power FLOW, FloEFD and others are used to solve fluid dynamics technical and experimental problems.



## 10 CURRENT DESIGN 1

This chapter describes the process of building a 3D virtual model of turbine housing assembly components, all of which are needed for drawing creation, casting shape manufacture, machining operations in production but in the terms of this thesis especially for running a CFD simulation (described in following chapters).

The investigated design is based on the Honeywell gasoline turbine housing MGT 15, which is because of its shape and size suitable for gasoline engines with volume around 1.6÷1.8 liters. It has an undivided mono-scroll volute (without barrier) with wastegate channel. The wastegate is operated by swing type valve using vacuum actuator controlled per compressor boost pressure.

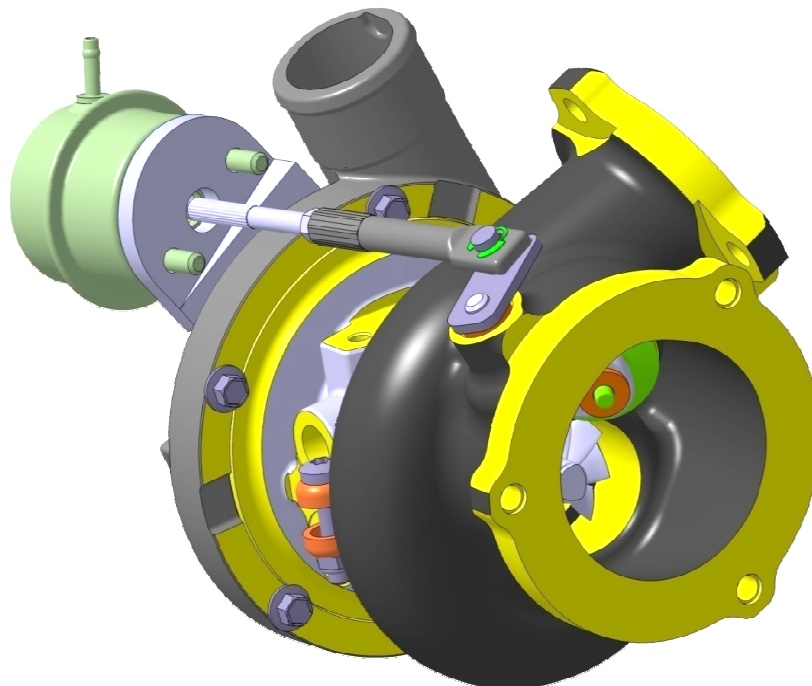


*Figure 28 Honeywell's MGT 15 gasoline turbocharger*

The following passages clarify systematically the method of 3D models creation in CATIA V5 the PART DESIGN and GENERATIVE SHAPE DESIGN (GSD).

It starts with definition of snail-shape volute passage and inlet passage, which forms gas passage and are the base model of turbine housing. It represents negative (fluid) volume, in which exhaust gasses are flowing through. Then the wastegate duct design and discharge design are created, which are put together with whole gas passage to form one compact core. This core model is used in a foundry in order to create pressurized sand core, which is placed inside the mould when the iron is casted.

The casting model is created later, based on the core model, where the walls thickness plays vital role. This casting is machined afterwards to complete the final form of turbine housing and meet required tolerances.

The turbine wheel nomenclature, arm & valve assembly and turbine housing assembly are also described in the following chapters.

## 10.1 TURBINE HOUSING

Figure 29 shows an axial view, looking into the outlet of turbine housing. Starting at the inlet, the initial portion of the housing flow passage is named the ‘inlet section’, which is the flow passage between the mounting flange and plane called the T-T section. The T-T section is a plane, which separates the inlet section from the volute (radial passage).

The volute is a spiral flow path, which surrounds the wheel, gradually decreasing in cross-sectional area. At the tail end of the volute where the outer surface intersects with the lower wall of the inlet section is the tongue.

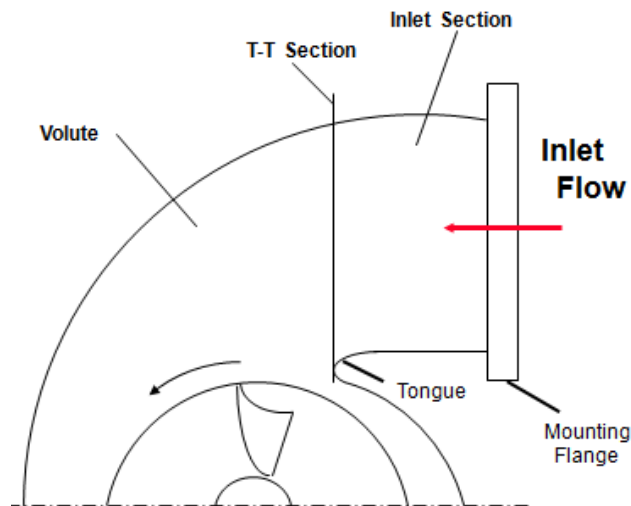


Figure 29 Nomenclature of turbine housing in axial view [10]

The T-T section area “A” and the radius to the dynamic center “R” gives housing A/R. This is very important parameter of housing, as it determines the flow character inside spiral volute.

The larger A/R [inch] provides slower response in low engine speeds, but on the other hand, it is capable to transmit high mass flow at high engine speeds (or big engines with large volume). It gives a presumption of low turbo rotational speed and boost level. The turbine housing with smaller A/R gives quicker response in low engine speeds but creates significant backpressure at high mass flows (high engine speeds or high engine volumes). It gives higher turbo speed and boost level.

Therefore, the A/R parameter is significant measure of turbine housing and has to be determined for every single engine. It is common to offer a range of A/R’s for a given turbine to provide flexibility in satisfying different engine matching requirements.

The challenge in the aerodynamic design of a turbine is to observe how design changes affect efficiency or pressure loss through the various sections of the stage and then select the combination of features that gives the best over-all performance.



### 10.1.1 RADIAL PASSAGE

Firstly, the **T-T section** has to be defined. The T-T section area and its radius to the dynamic center of the T-T section are sketched on YZ plane of Cartesian coordinate system (Figure 30-left). The Y-axis is the axis of rotation of turbine wheel.

Turbine housing created for the purposes of this thesis has  $A/R=0.69$  inch.

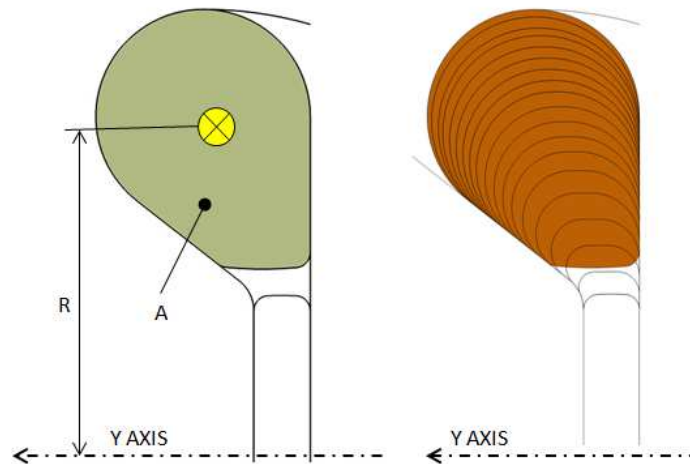


Figure 30 T-T section (left) and radial sections (right)

Afterwards 18 different radial sections are sketched on the same YZ plane (Figure 30- right). These sections represent the decrease in radial cross-sectional area. It is aerodynamically optimized in order to get same exhaust gas speed entering the wheel around the cylindrical surface called the inducer. The smallest of all sections is called the **A-A section**.

Each of these sections is rotationally offset by 20 degrees from the previous one around the Y-axis (Figure 31- left). Then a smooth curves, called the streamlines, interconnecting individual sections and locally perpendicular to the surfaces are created using SPLINE function.

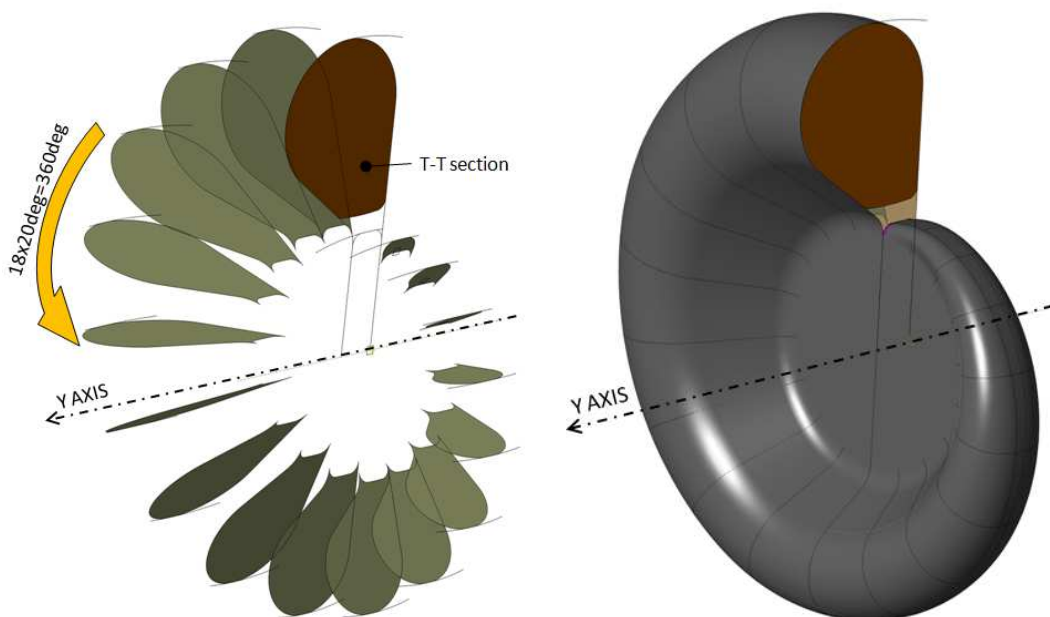


Figure 31 Radial sections (left) and closed surface of radial section (right)



The geometry can be now closed by surfaces defined with individual radial sections and streamlines. To do this LOFT surface command is used. The sections and guides are properly selected and the tangent continuity of required surface is defined. After this, the surface is generated separately for the range of 0-180° and 180-360° (Figure 31- right).

Subsequently, the tongue area is defined in order to close radial passage by surfaces. Certain minimal distance has to be kept so the tongue withstands the thermal and mechanical loads. The tongue surfaces are created from splines that has to be locally perpendicular to the T-T and A-A sections. Finally, the surfaces are joined together and closed into one solid body (Figure 32- left) to form radial passage.

### 10.1.2 GAS PASSAGE (VOLUTE)

The gas passage (Figure 32- right) is composed of **radial passage** and **inlet section**. Inlet section interconnects the inlet surface and T-T section. The inlet position and streamlines are defined for this reason. The inlet section is often changed in order to fit the turbocharger into the customer engine layout. The radial section always remains the same for a given turbocharger size.

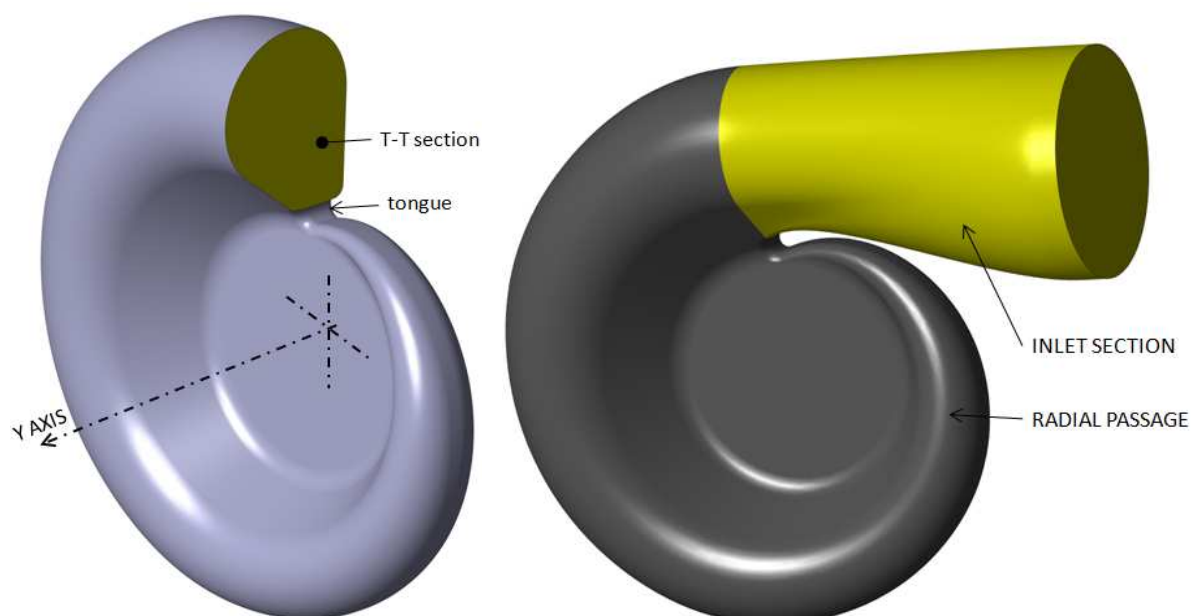


Figure 32 Radial section (left) and gas passage (right)

The distance between the radial section outer surface and inlet section lower surface must not be too low and has to be increasing from a tongue to the inlet.

This gas passage (volute) will not be changed anymore for any purposes of the thesis. It will remain the same during whole process of building turbine housing, fluid volume extract, mesh and calculation. It will also remain the same in the models of other wastegate designs. It is used as a base model for all other operations, which are described later.



### 10.1.3 CORE

The core design is very complex. It requires multiple bodies' definition and Boolean operations in CATIA V5 to control the shape.

It is composed of the **gas passage, duct** (wastegate channel) and **discharge**.

Firstly, the duct (or the wastegate channel) has to be added to the volute (Figure 33- left). As this is an integrated wastegate type, it has to lie in between the T-T section and inlet surface of volute. It should not be too close to the T-T section so the flow inside the inlet section and turbulences caused by wastegate channel does not influence the flow in radial passage, which would result in lower stage efficiency and increased pressure loss. In addition, the inlet is extended in a negative X-axis direction.

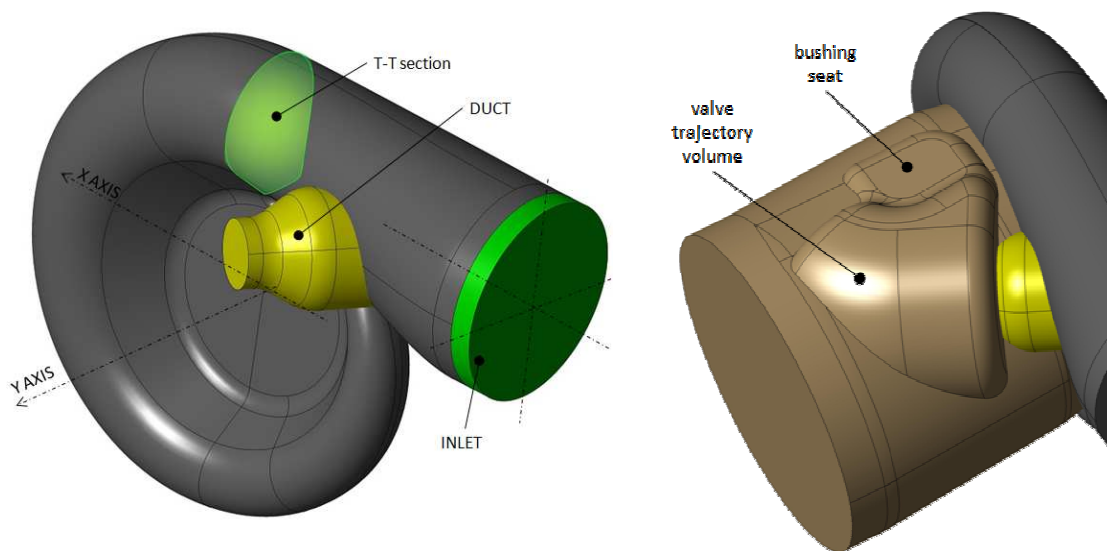


Figure 33 Duct position (left) and base discharge volume (right)

After the wastegate channel is complete, the discharge volume is created. It is the volume, which collects the gas flowing from a turbine wheel and the wastegate channel and directs it to the turbine housing outlet. The bushing seat-pad and valve trajectory volumes are added to the discharge body (Figure 33- right).

The volute surface is offset by distance representing desired housing wall thickness way out and the discharge body is sliced by this surface (Figure 34- left). The groove volume around the wastegate channel is cut off (Figure 34- right) to provide enough space for iron in casting process. Then all sharp edges of discharge body are rounded (Figure 35- left).

Finally the volute, duct and discharge bodies are assembled together to form one part, the core (Figure 36).

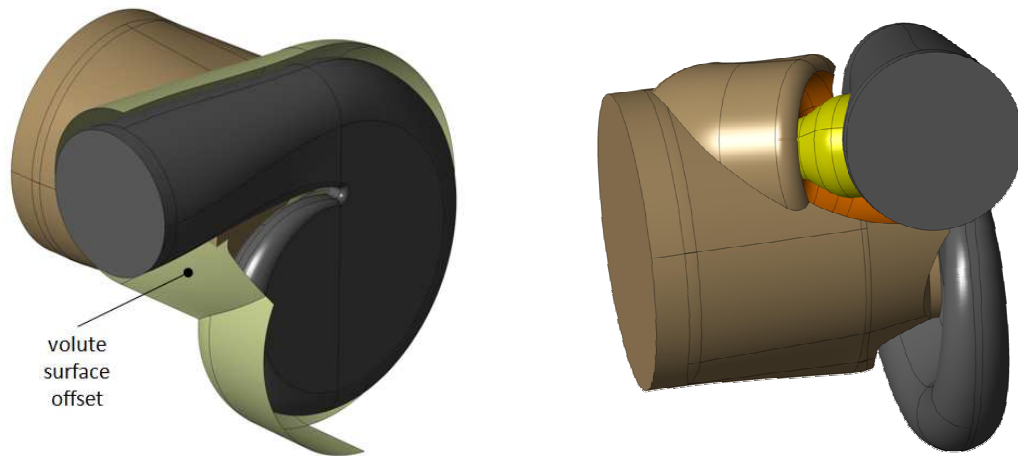


Figure 34 Volute surface offset (left) and groove around wastegate channel (right)

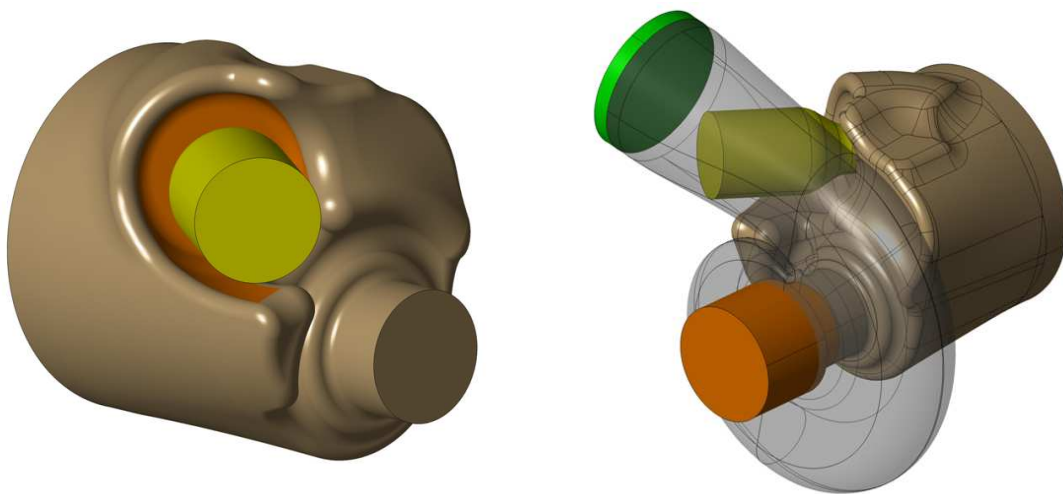


Figure 35 Final discharge volume (left) and its mutual position with volute (right)

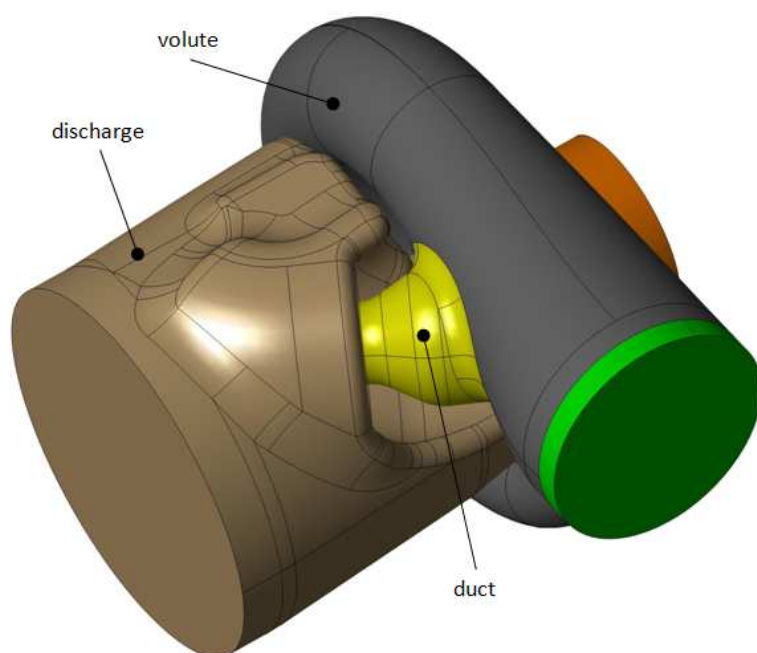


Figure 36 Core model



### 10.1.4 CASTING

The turbine housing casting is created from the core. The aim is to keep **wall thickness** as small as possible to keep thermal inertia low and strong enough to withstand hostile conditions of exhaust gasses. The design has to respect casting principals such as **draft angles** and **corner radiuses**.

Whole core surface is offset by desired wall thickness way out in GSD module (Figure 37- left).

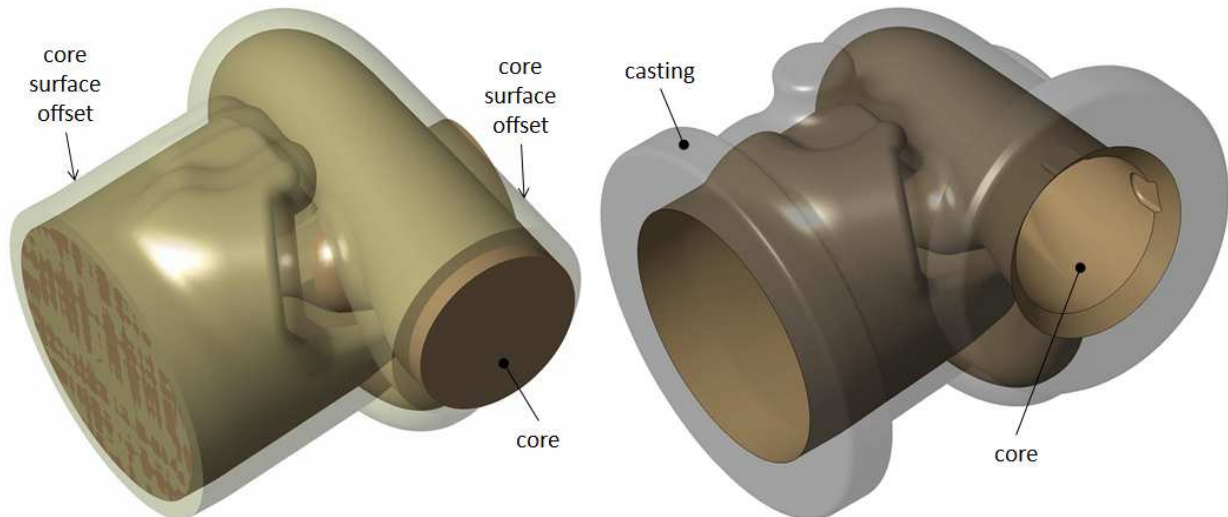


Figure 37 Core surface offset (left) and final transparent casting design (right)

The offset surface is closed into solid body consequently. **Inlet flange**, **outlet flange** and **bushing pad** are added. The core is than removed from the model using Boolean operations thus forms a cavity inside housing body. The casting identification is added to the outer surface of casting body with definition of material, housing A/R and manufacturer name (Figure 38).

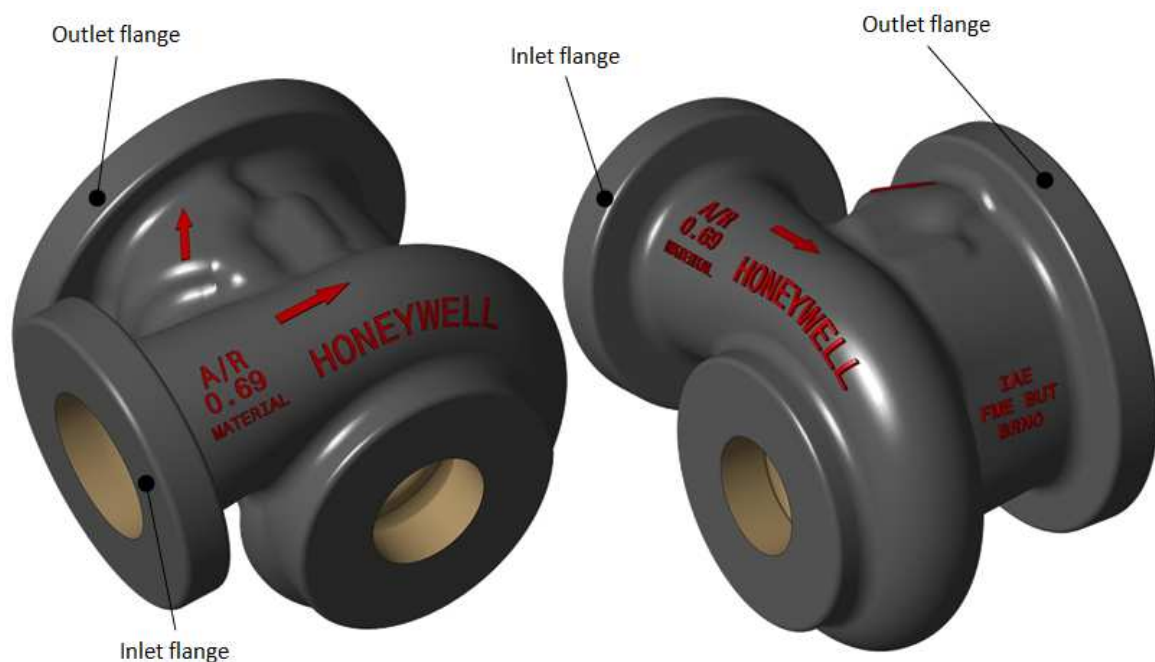


Figure 38 Casting model



Following cutaway views of turbine housing clearly demonstrates the design of inner surfaces derived from the core.

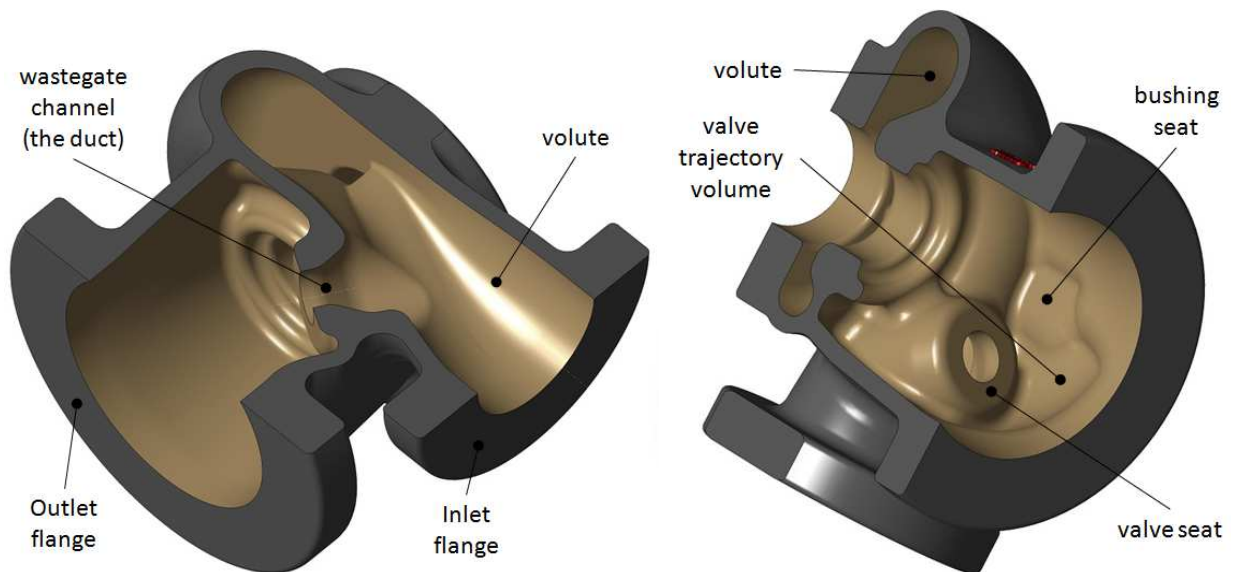


Figure 39 Section view through wastegate channel (left) and turbine wheel axis (Y-axis) (right)

### 10.1.5 MACHINING

Machining is created out of casting by turning on lathe and milling in order to meet fine tolerances and precise shape. The casting virtual model is cut by defined volumes using Boolean operations. The **inlet** and **outlet flanges** are machined and the connecting holes are drilled. Central housing connecting flange and the **shroud contour** of wheel is turned. **Wastegate valve seat** is machined as well and the **channel** is drilled to 25mm in diameter. Finally, the **hole for bushing** is drilled through the housing wall. Machined surfaces are shown in contrast color on following pictures.

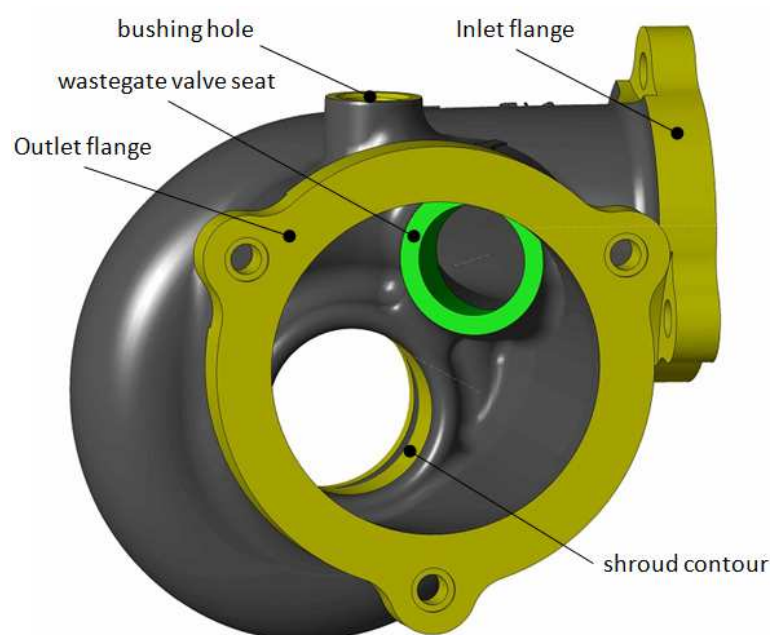


Figure 40 Machined surfaces



Bushing hole axis lies in parallel plane to YZ plane and is perpendicular to housing inlet axis and axis of turbine wheel rotation. Wastegate channel axis lies in a plane parallel to XY plane and it is leaned out by 60 degrees from the inlet axis.

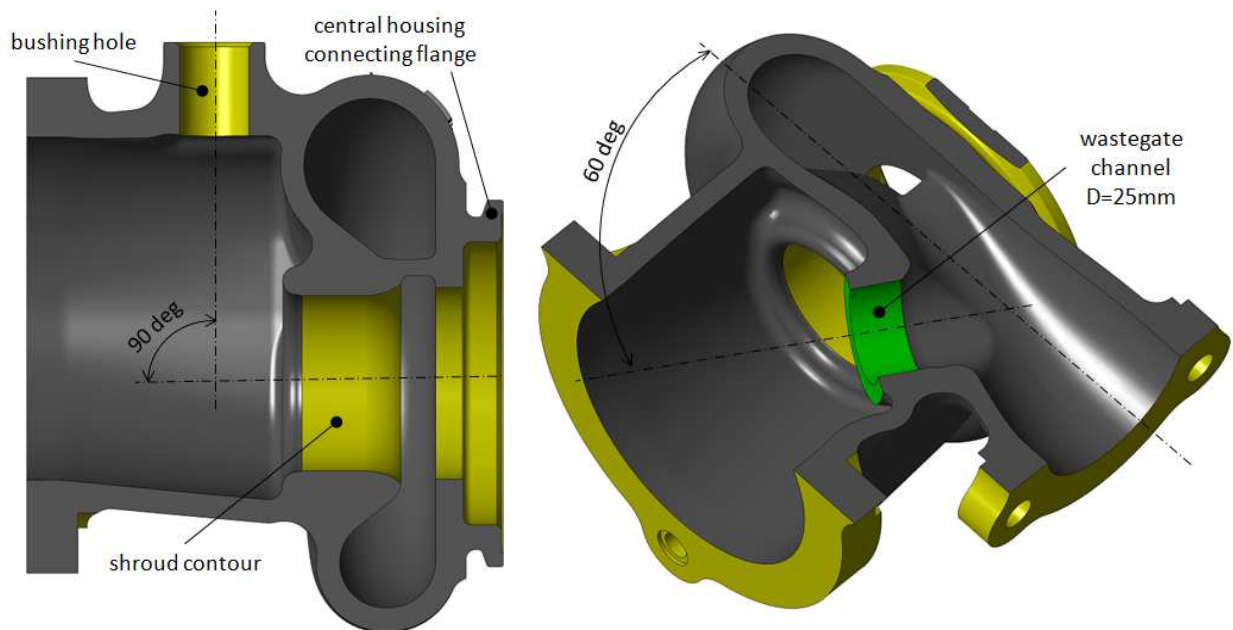


Figure 41 Bushing axis(left) and wastegate channel (right) position

## 10.2 TURBINE WHEEL

The turbine wheel shown in this chapter is used only for nomenclature description and is created in CATIA V5. The wheel used later for mesh and calculation is created individually in ANSYS BladeGen software (a geometry creation tool that is specialized for turbomachinery blades).

The wheel is composed of the base hub and backdisc, which are defined by a contour revolved around axis of wheel rotation. The full backdisc (non-scalloped) design is shown on the Figure 42.

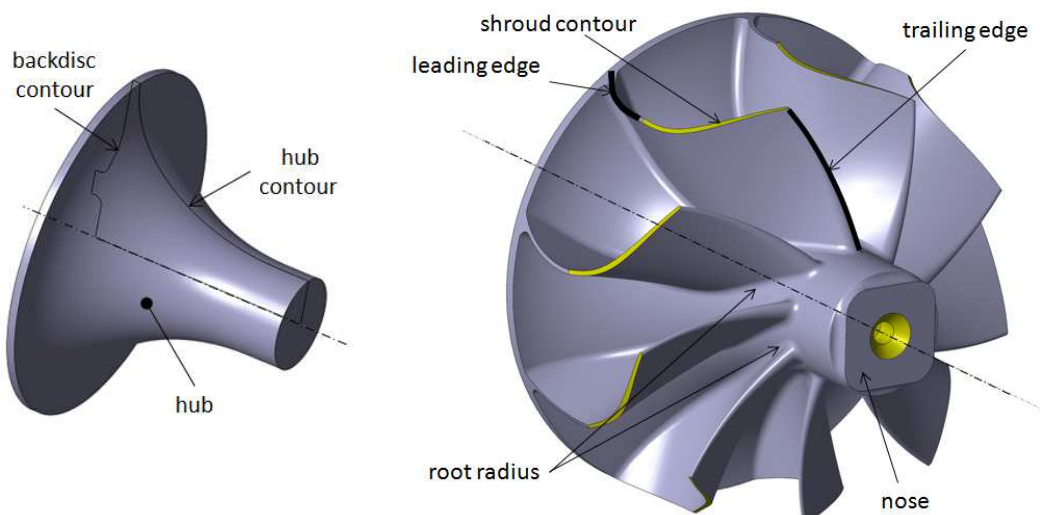


Figure 42 Turbine wheel nomenclature



The blades are located circumferentially around the hub. There are nine same blades on the turbine wheel used in this thesis. Each one of the blades is defined by the **leading edge**, the **trailing edge**, **hub-contour**, **shroud-contour** and blade thickness distribution.

Each blade connects to hub with **root radius** in order to lower stress concentration. Different designs of **nose** are used to differentiate the turbine wheel material. The hole in the turbine wheel nose is drilled for machining purposes.

Shroud contour is parallel to shroud contour of turbine housing. There is certain **axial and radial clearance** between turbine housing and turbine wheel so the wheel can turn freely after assembly, after stretching due to centrifugal forces and expansion due to high operating temperatures.

Very important in turbine wheel design is a **TRIM** parameter:

$$TRIM = \left(\frac{d}{D}\right)^2 \cdot 100 \quad [-] \quad (11)$$

where:

$d$  [mm] - wheel diameter at wheel backdisc  
 $D$  [mm] - exducer diameter

Larger TRIM is suitable for higher flows and gives slower response at low engine RPM while the smaller TRIM is suitable for lower flows and gives quicker response to throttle change.

The TRIM of turbine wheel used in following calculations is 84.

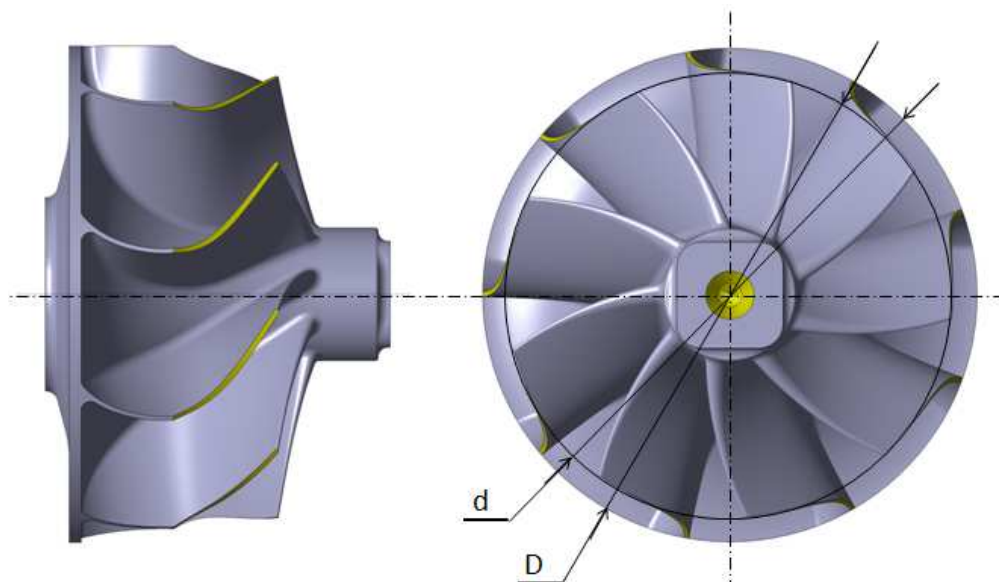


Figure 43 Backdisc diameter  $D$  and exducer diameter  $d$



### 10.3 ARM & VALVE ASSEMBLY

The mechanism is composed of **arm** into which the **valve** (sometimes referred as poppet) is inserted. On the opposite side, it is secured by **washer** and rivet. The bushing is placed into the turbine housing wall and guides the arm in its rotational movement. Contact surfaces of assembly are machined to match each other perfectly and meet strict tolerances.

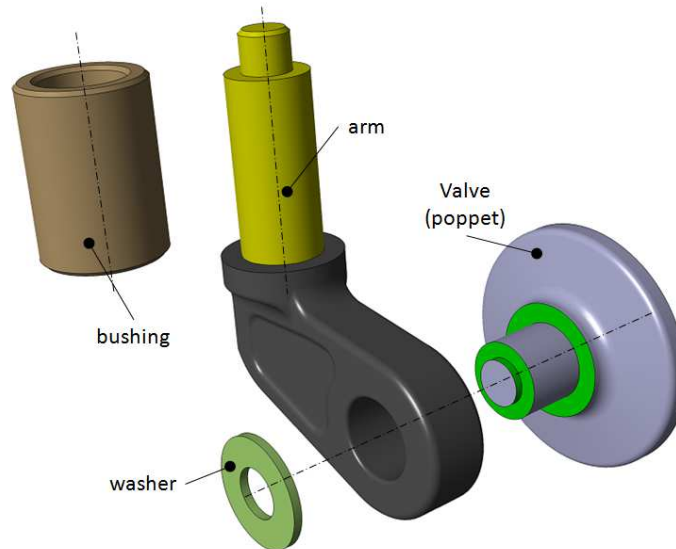


Figure 44 Arm & valve assembly

### 10.4 TURBINE HOUSING ASSEMBLY

Turbine housing assembly is composed of turbine housing, turbine wheel and wastegate components (poppet, arm, bushing and washer). Firstly, the turbine wheel is aligned with turbine housing in virtual model (Figure 45- left).

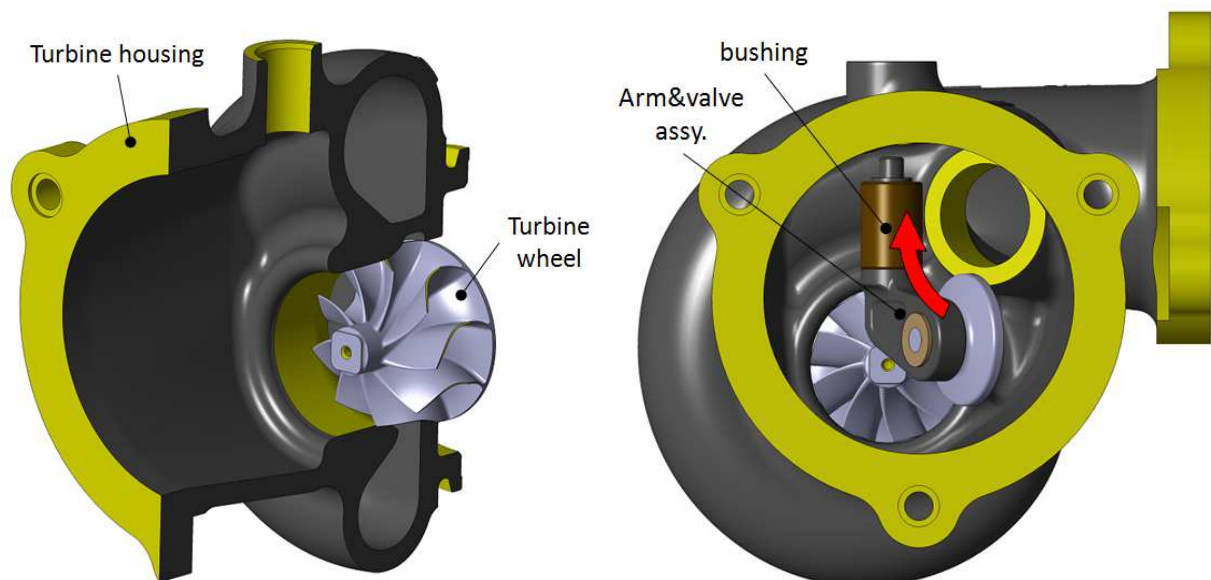


Figure 45 Wheel position (left) and arm & valve montage (right)



Arm and valve with bushing is than placed inside the housing. Notice the turbine housing outlet diameter has to be big enough so the arm & valve assembly could be easily mounted into the position through the outlet opening (Figure 45- right).

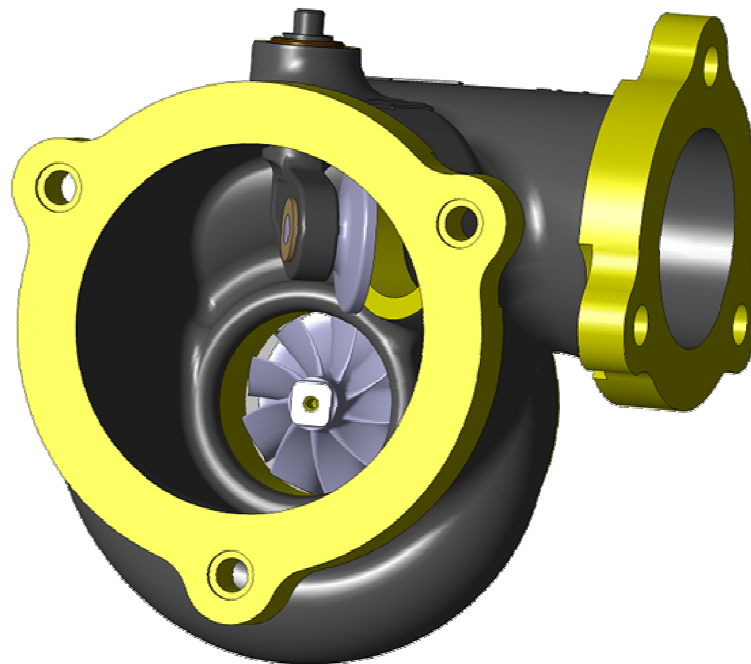


Figure 46 Turbine housing assembly

When the valve is opened, the mass flow of exhaust gasses flowing out of engine is divided into the mass flow passing through turbine wheel and mass flow through wastegate. This proportion will be calculated later for different valve opening angles.

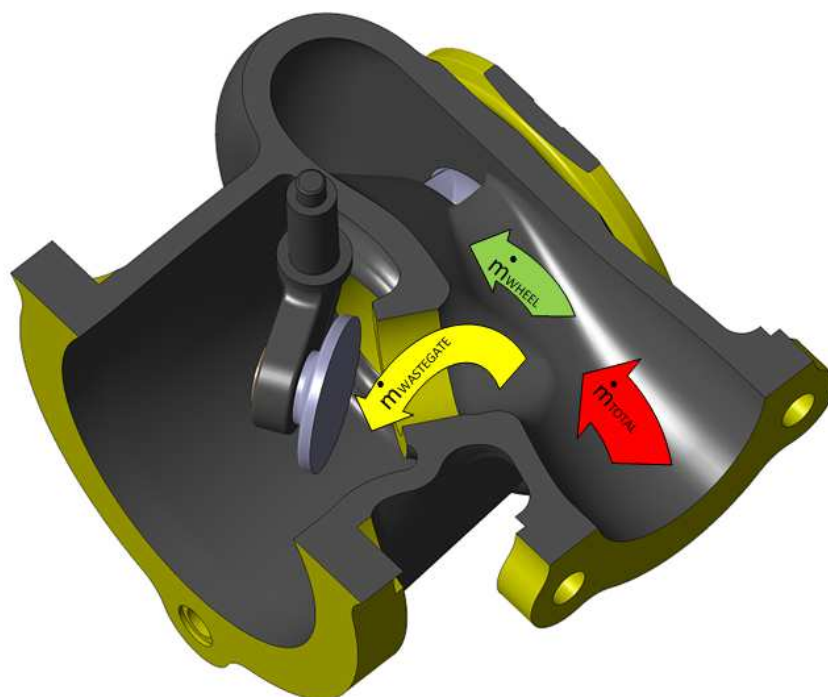


Figure 47 Section view through wastegate channel and awaited flow direction



The virtual model is finalized by adding the catalytic converter to the turbine housing assembly. The catalytic converter used in the thesis has a simplified design and is assembled coaxially with the axis of turbine housing outlet flange. Its inner diameter is 75mm and the length of active monolith honeycomb structure is taken to be 200mm.

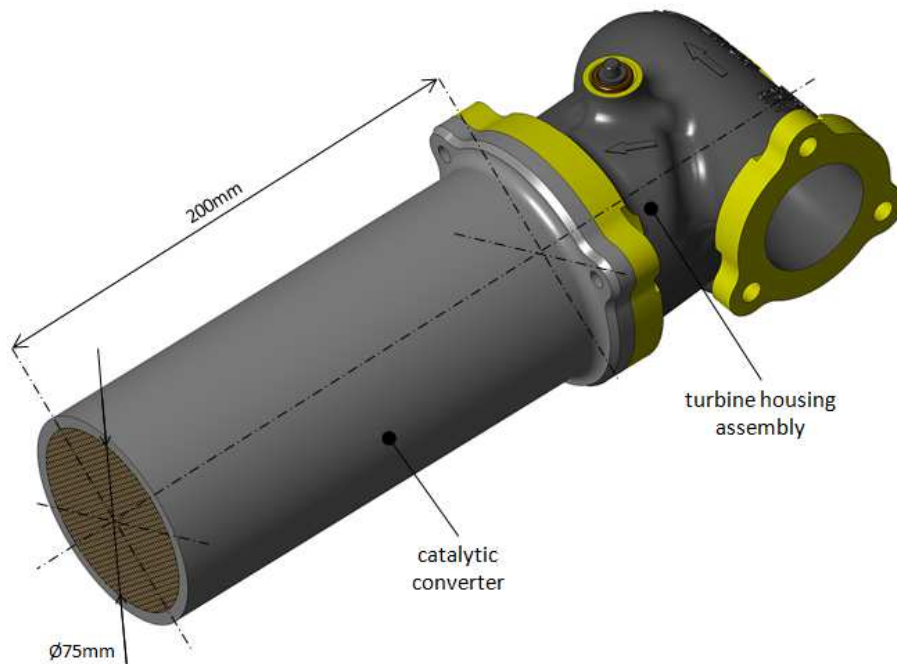


Figure 48 Assembly of turbine housing and catalytic converter

## 10.5 FLUID VOLUME

The fluid volume is extracted from assembly of turbine housing and catalytic converter created in CATIA V5 using FloEFD tool (embedded CFD software for CATIA V5). This fluid volume is then split up into several separate domains, which are then further processed in ANSYS CFX.

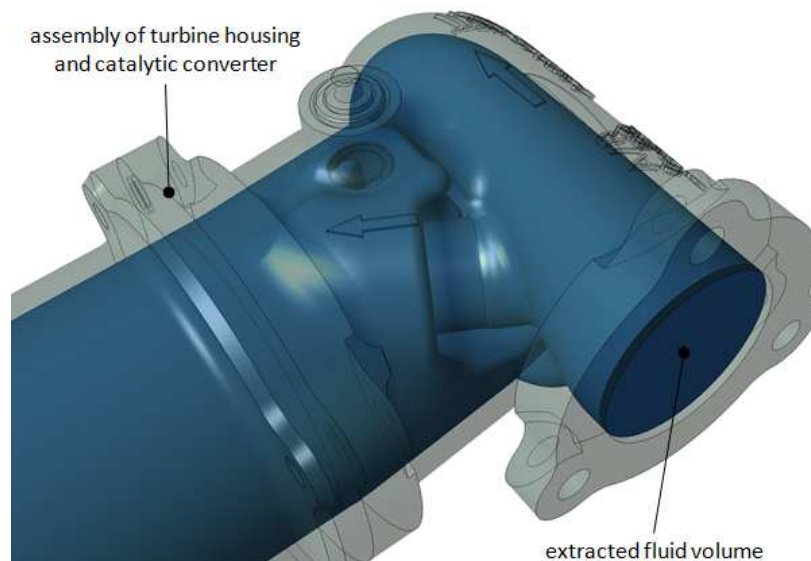


Figure 49 Fluid volume extraction



The fluid volume is extracted by lids creation on every single opening of assembly. Than an inlet and outlet ports are specified and automatic calculation of fluid volume is lunched. This creates one compact part in a separate CATIA window, which can be further processed.

The fluid volume is divided into four separate domains, the **volute**, **wheel segment**, **discharge** and **extension** (catalytic converter) for which different mesh attributes are specified later in ANSYS Mesher.

The wheel segment is created in ANSYS BladeGen tool separately. Extraction of fluid volume around wheel done in FloEFD serves here only to visualize the domains definition.

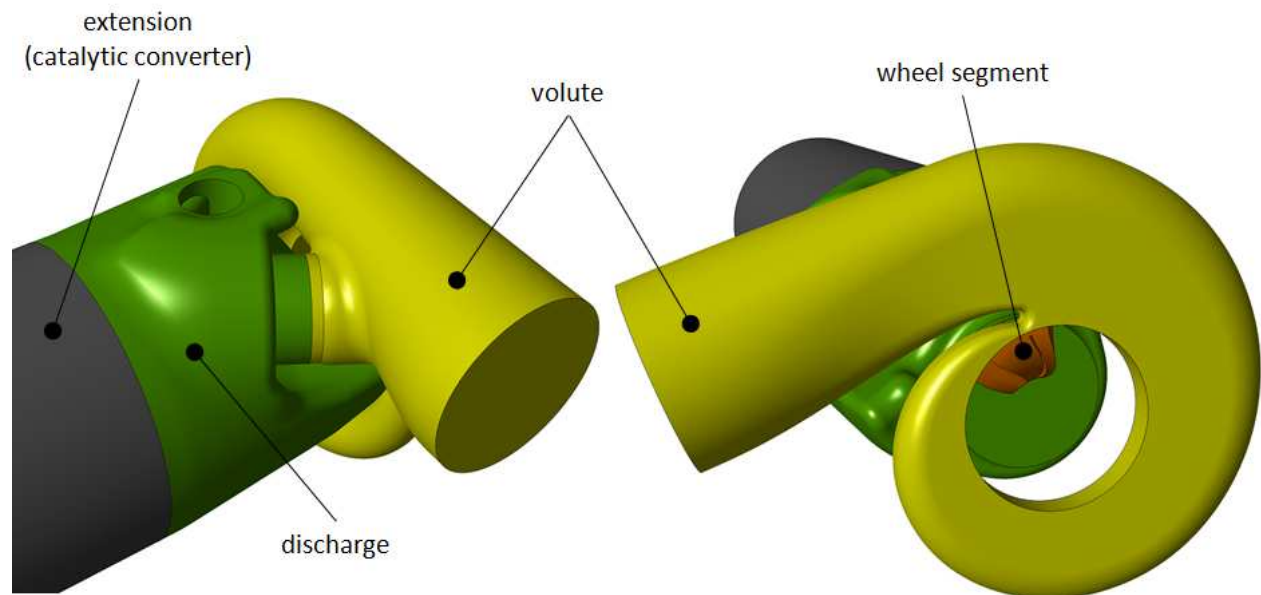


*Figure 50 Fluid volume domains*

Note:

FloEFD software can be used also for CFD calculation. It has very intuitive structure, pre-processing and post-processing is user friendly. It uses automated mash, which simplify the setup process and shorten time required to prepare virtual model for the calculation.

This software has been tested for running a calculation as a part of this thesis but has been abandoned due to instability and unexpected errors, which occurred at higher mesh density. Application of FloEFD tool for certain calculations done at Honeywell Turbo Technology should be considered, but further investigation and results comparison to laboratory tests or other trusted CFD software should to be done before experts rely on the results created by FloEFD.



## 11 CFD CALCULATION OF CURRENT DESIGN 1

Calculation of exhaust gas flow is done in ANSYS 13.0 CFX Workbench platform.

As an input it uses domains of fluid volume (volute, discharge and extension) created in FloEFD tool in CATIA V5, which are imported into the ANSYS DesignModeler environment.

Following Figure 51 shows the flowchart that is created in ANSYS 13.0 Workbench. We can see a mesh definition of volute, wheel, discharge and extension shown on the left side of the flowchart. The mesh is created in ANSYS **Meshing** software. The wheel is created in ANSYS **BladeGen** and is then meshed in ANSYS **TurboGrid**.

The meshes are linked to the setup (pre-processor) of ANSYS **CFX-Pre** module, where all necessary boundary conditions are defined and calculation settings are specified.

The solution follows the setup. The ANSYS **CFX Solver** solves the equations of fluid dynamics with defined boundary conditions. Here the convergence and user defined output control variables have to be monitored in order to supervise equations residuals and calculation accuracy.

Finally, the results obtained from the Solver are post-processed in ANSYS **CFD-Post**, where all necessary information are graphically visualized and quantified.

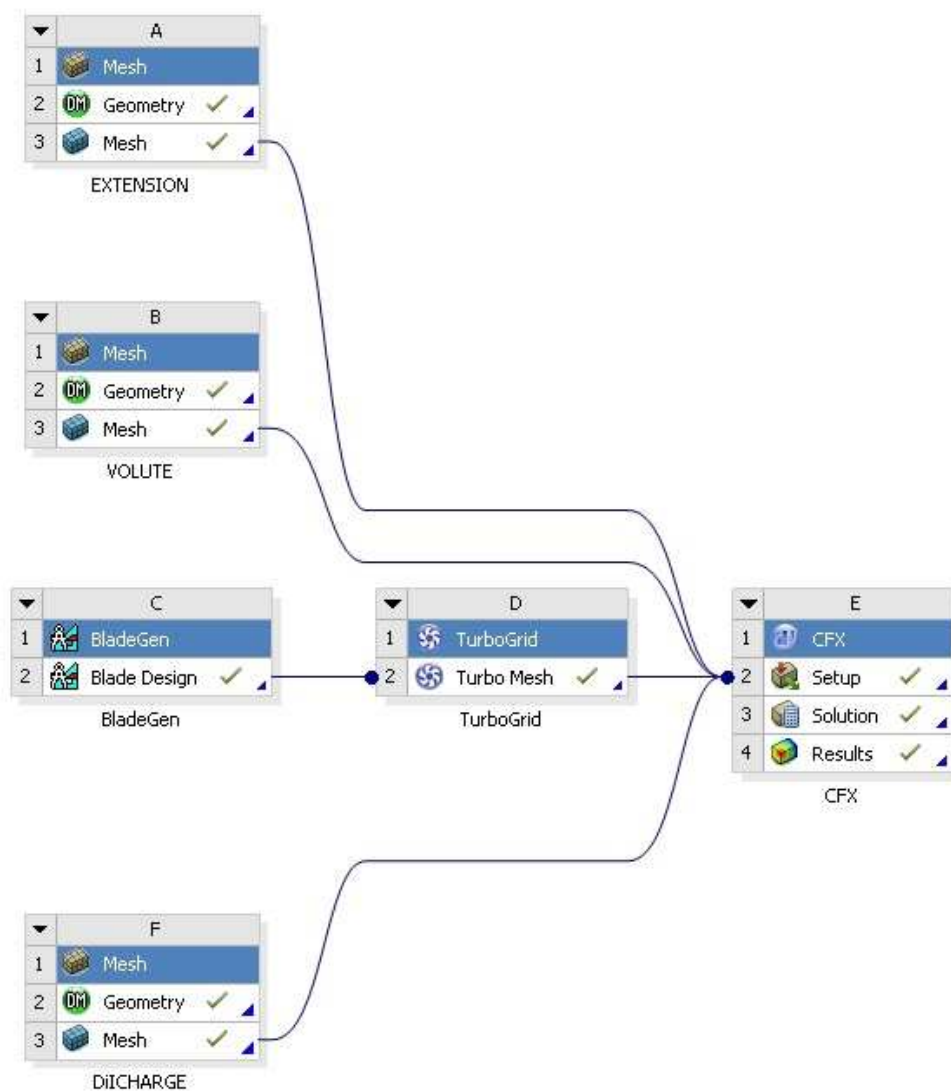


Figure 51 ANSYS 13.0 CFX Workbench flowchart



## 11.1 MESH

The mesh is created in ANSYS Meshing software using special mesh control commands that define the size, shape and other important geometrical characteristics of elements.

Discretization (the mesh) of fluid volume is controlled by these commands and is automatically generated by the software. It uses tetrahedral, prismatic and hexahedral elements shown on Figure 52 below. We can see there are four nodes in tetrahedral element, six nodes in prismatic element and eight nodes in hexahedral element.

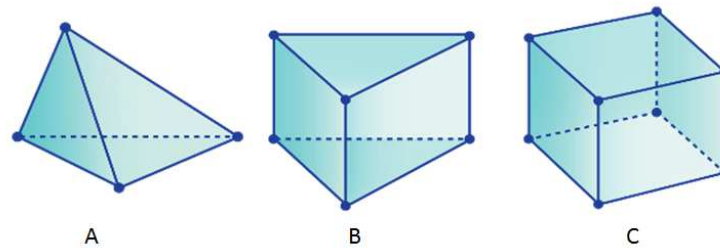


Figure 52 Element types: A-tetrahedral, B-prismatic, C-hexahedral [42]

Usually there is effort to mesh the fluid volumes with hexahedral elements if possible because of its regular shape and high volume occupation. Unfortunately, this is very hard to achieve in complex fluid geometries.

Partial volumes in locations, which are important for the results and are primary investigated are meshed using smaller elements compared to those, which are out of interest. The volumes in which high flow changes are expected are meshed very dense with small elements.

The fluid geometry is simplified a little bit. Small unimportant geometries are suppressed in order to simplify mesh and lower number of elements. Those are mainly small radiuses such as root radius of turbine wheel blades, small radiuses on arm & valve bodies, nose drill on the turbine wheel nose, small pads on turbine housing inlet, which are used as base datums in casting process etc.

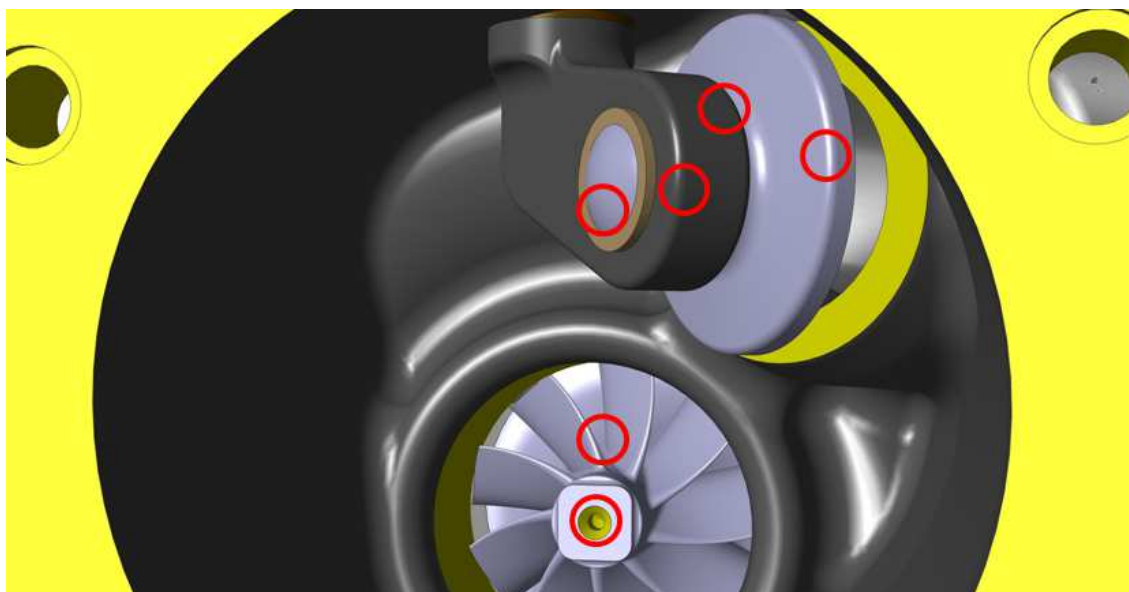


Figure 53 Geometry simplifications



### 11.1.1 VOLUTE

The volute is meshed mostly with tetrahedral elements. There are also prismatic elements defined on the walls of volute by inflation command in order to get very fine mesh around the walls where the velocity gradient in direction perpendicular to wall is high.

The body sizing is defined to be 2mm and the face sizing for walls is 1mm. The inflation defined on the walls has five layers and the first near wall layer is 0.1mm thick.

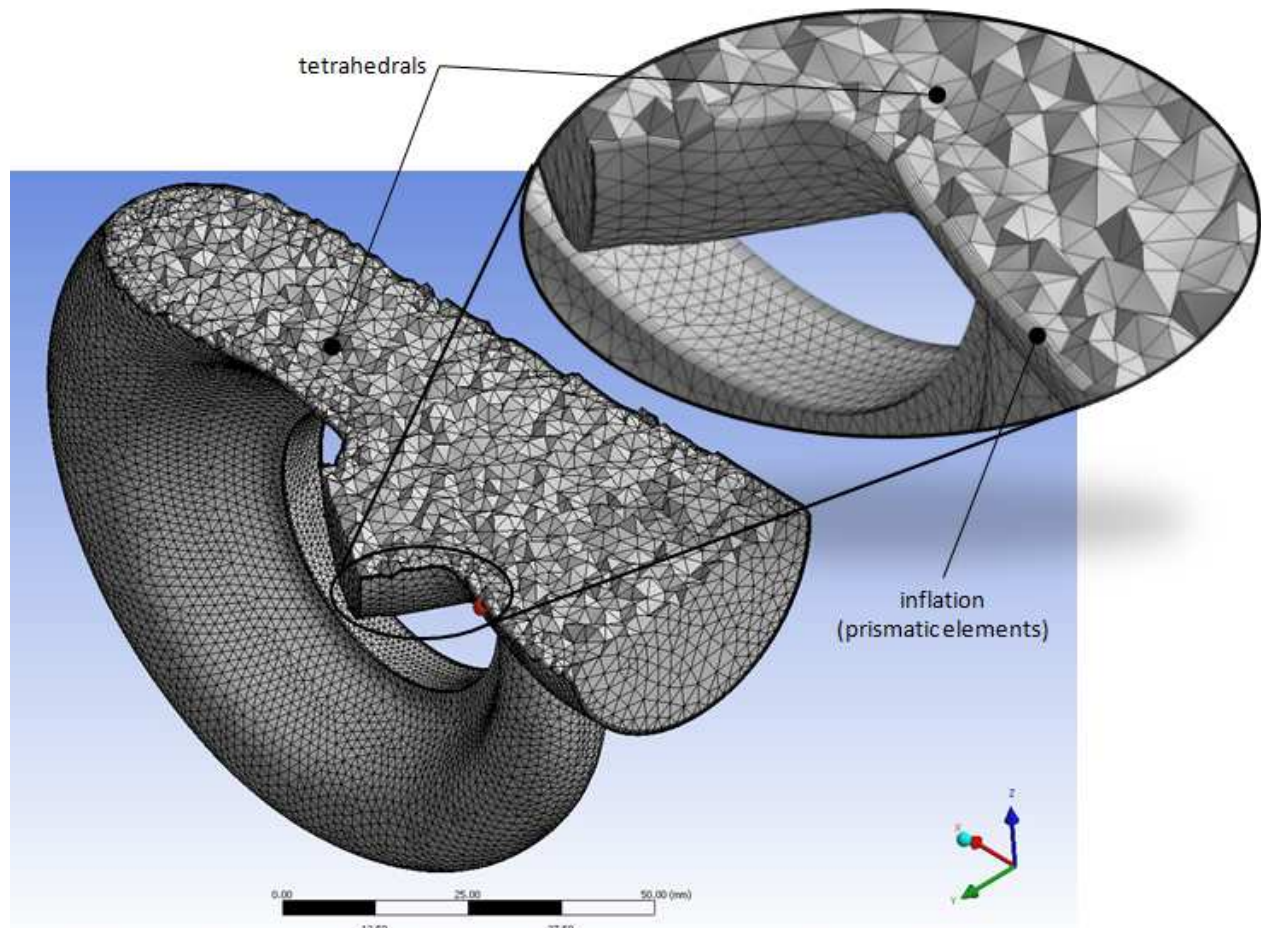


Figure 54 Mesh of volute domain

### 11.1.2 TURBINE WHEEL

Radial inflow turbine wheel is firstly created in ANSYS **BladeGen** software.

Hub profile, shroud contour, leading and trailing edges are defined. Consequentially blade shape is specified. This way, segment around one blade is created. All dimensions set in BladeGen are respecting the size and shape of turbine wheel previously described in design chapter, so the wheel perfectly fits into the turbine housing with shroud contour clearance of 0.3mm.

The wheel segment is than meshed in ANSYS **TurboGrid** module with hexahedral elements and very fine mesh around the wheel surfaces. The wheel segment is copied around axis of rotation for better visualization. Figure 55 shows surface mesh of turbine wheel and the detailed mesh around blade trailing edge.

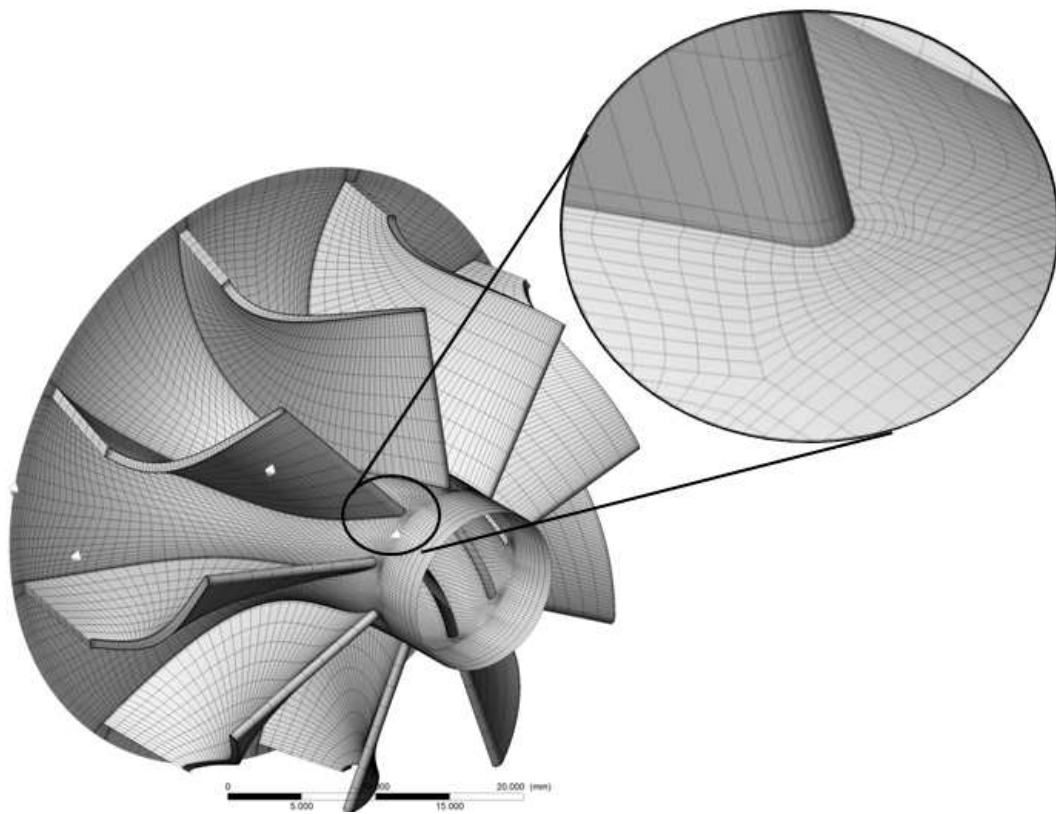


Figure 55 Turbine wheel surface mesh

The mesh is controlled precisely on the wheel surfaces in order to get uniform elements distribution and cube-like shape.

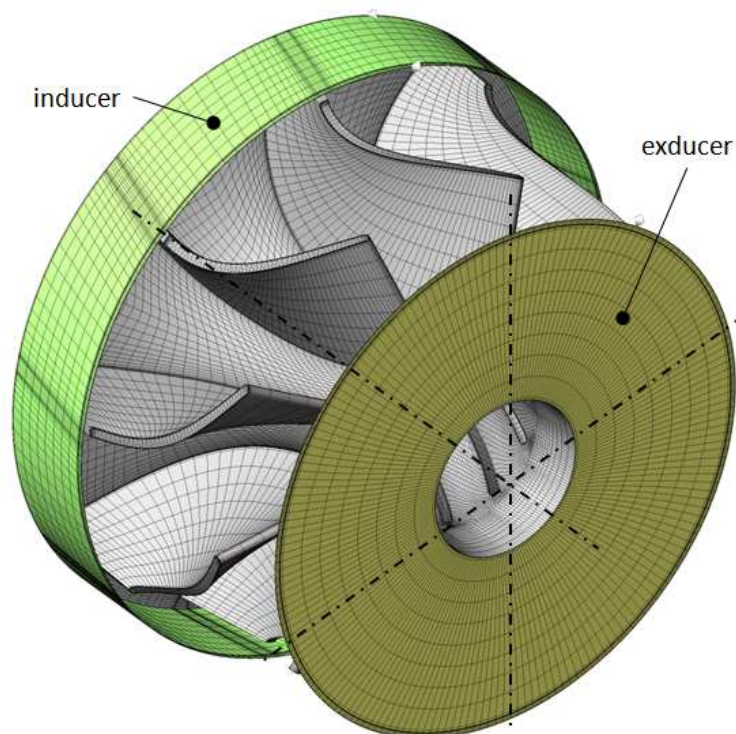


Figure 56 Inducer and exducer of turbine wheel



### 11.1.3 DISCHARGE

Discharge domain is the volume in which the exhaust gas flow is investigated with primary interest. Therefore, it has very dense element definition. The large volumes inside the domain are meshed with hexahedral elements using sweep method. Near-wall elements are prisms defined by inflation function. The rest is meshed with tetrahedral elements. The body sizing is 1.0mm. Face sizing for arm & valve surfaces is 0.3mm and all other faces are meshed with 1mm face sizing. Inflation of five layers with 0.1mm first layer width is defined for all walls.

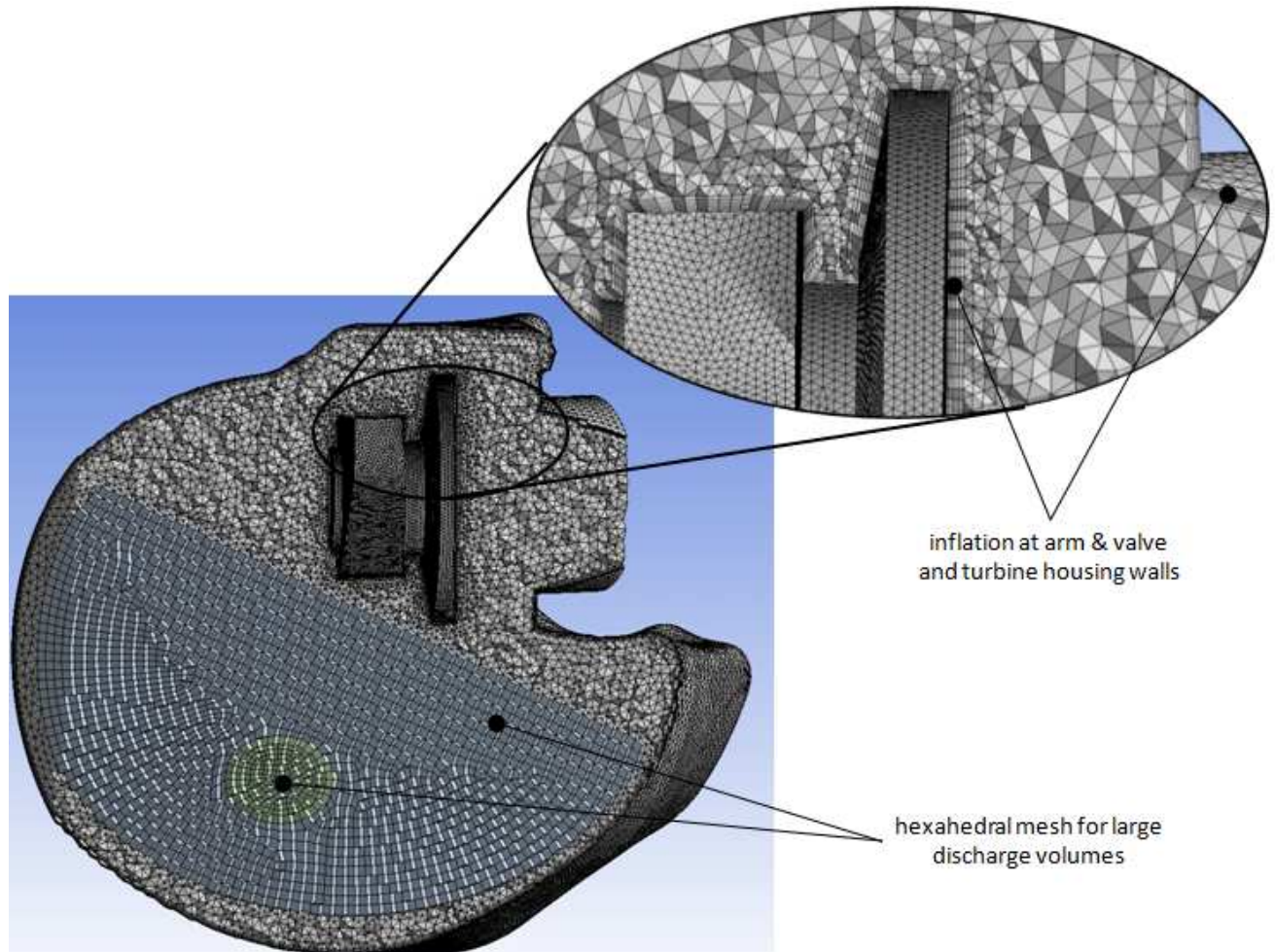


Figure 57 Mesh of discharge domain

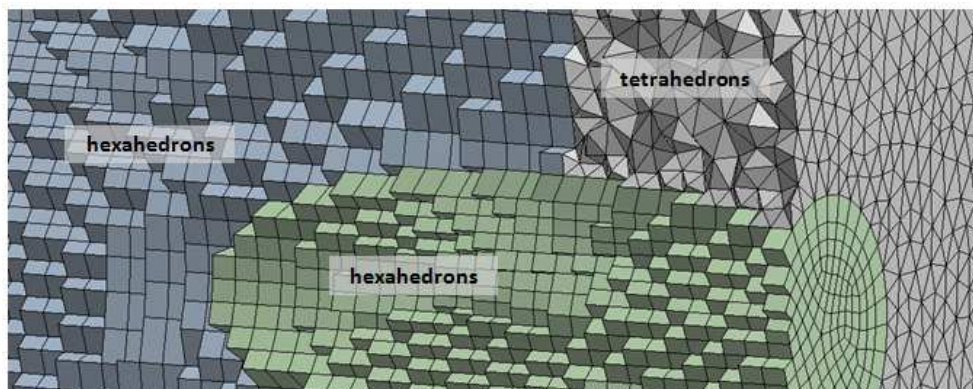


Figure 58 Detail hexahedral and tetrahedral elements used for discharge domain mesh



### 11.1.4 EXTENSION

Extension (catalytic converter) is meshed with hexahedral elements using sweep method. The inflation is defined on the walls. Body sizing and face sizing is 2.0mm.

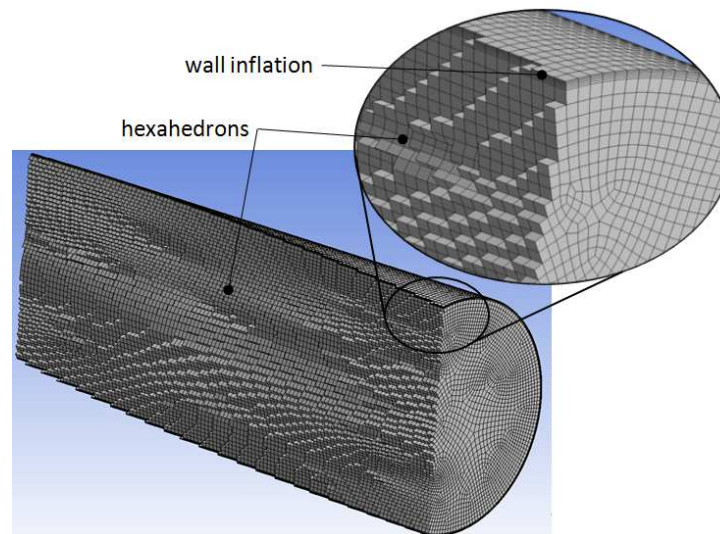


Figure 59 Mesh of extension domain

### 11.1.5 MESH STATISTICS SUMMARY

Following Table 2 summarizes the mesh statistics of individual domains. We can see the highest number of elements is defined for discharge domain, which is the subject of greatest interest. Here the exhaust gas flow is crucial for temperature distribution at turbine housing outlet. The total number of elements is over 2.7 million, for which complicated equations are solved. This indicates the calculation is very demanding. Therefore, it has to run on high-performance computer with multiple cores, high CPU and RAM.

Table 2 Mesh statistics

DOMAIN	element type	# elements	# nodes
VOLUTE	tetrahedral, prismatic	347 258	108 018
TURBINE WHEEL SEGMENT	hexahedral	51 490	58 443
TURBINE WHEEL (9 blades)		463 410	525 987
DISCHARGE	hexahedral, tetrahedral, prismatic	1 380 022	454 508
EXTENSION	hexahedral	542 750	559 370
<b>TOTAL</b>		<b>2 733 440</b>	<b>1 647 883</b>

Note:

The mesh described in this chapter and Table 2 shown above, characterize the current design and wastegate valve opened by 30 degrees. All other opening angles and other designs are meshed in the same manner and the elements number differs slightly.

The greatest difference is in the discharge domain, which is different for other opening angles and in other designs. The volute differs slightly in wastegate channel area in other designs. Wheel and extension domain remains the same.



## 11.2 PRE-PROCESSING

Pre-processing (calculation setup) is done in ANSYS CFX-Pre software. Here all physical characteristic are defined by boundary conditions and definition of fluid properties. Technical assumptions with certain simplifications are made in order to define initial values and clarify analysis.

Analysis is running in **steady state** mode. It uses **SST** (shear stress transport) turbulence model with **first order turbulence numerics**. Convergence is controlled by **maximal number of iterations** set to 1000 and **physical timescale** defined as  $1/\omega$ , where  $\omega$  is angular rotational speed of turbine wheel domain. Heat transfer is set to **total energy**. Convergence criteria is defined by **residual target** set to Root Mean Square  $RMS > 10^{-5}$ .

The fluid is chosen from material library. **Air Ideal Gas** is selected, which has pre-defined physical properties.

The turbine wheel segment is copied around axis of rotation in order to get full nine bladed wheel and positioned, so that any of the blades is not too close to the tongue of the volute.

Domain motion is defined as **stationary** for volute, discharge and extension. The wheel is defined as **rotating domain**, where turbine wheel RPM and axis of rotation are specified.

The volute, wheel and discharge domains use **fluid domain type**, whereas the extension is set to **porous domain** and controlled by **directional loss model**.

Table 3 Setup summary

ANALYSIS TYPE		STEADY STATE
TURBULENCE MODEL		SST - SHEAR STRESS TRANSPORT
TURBULENCE NUMERICS		FIRST ORDER
MAX. # OF ITERATIONS		1000
TIMESCALE		PHYSICAL $1/\omega$
HEAT TRANSFER		TOTAL ENERGY
RESIDUAL TARGET		$RMS > 1e-4$
FLUID		AIR IDEAL GAS
DOMAIN MOTION	VOLUTE, DISCHARGE, EXTENSION	STATIONARY
	TURBINE WHEEL	ROTATING
DOMAIN TYPE	VOLUTE, T. WHEEL, DISCHARGE	FLUID
	EXTENSION	POROUS

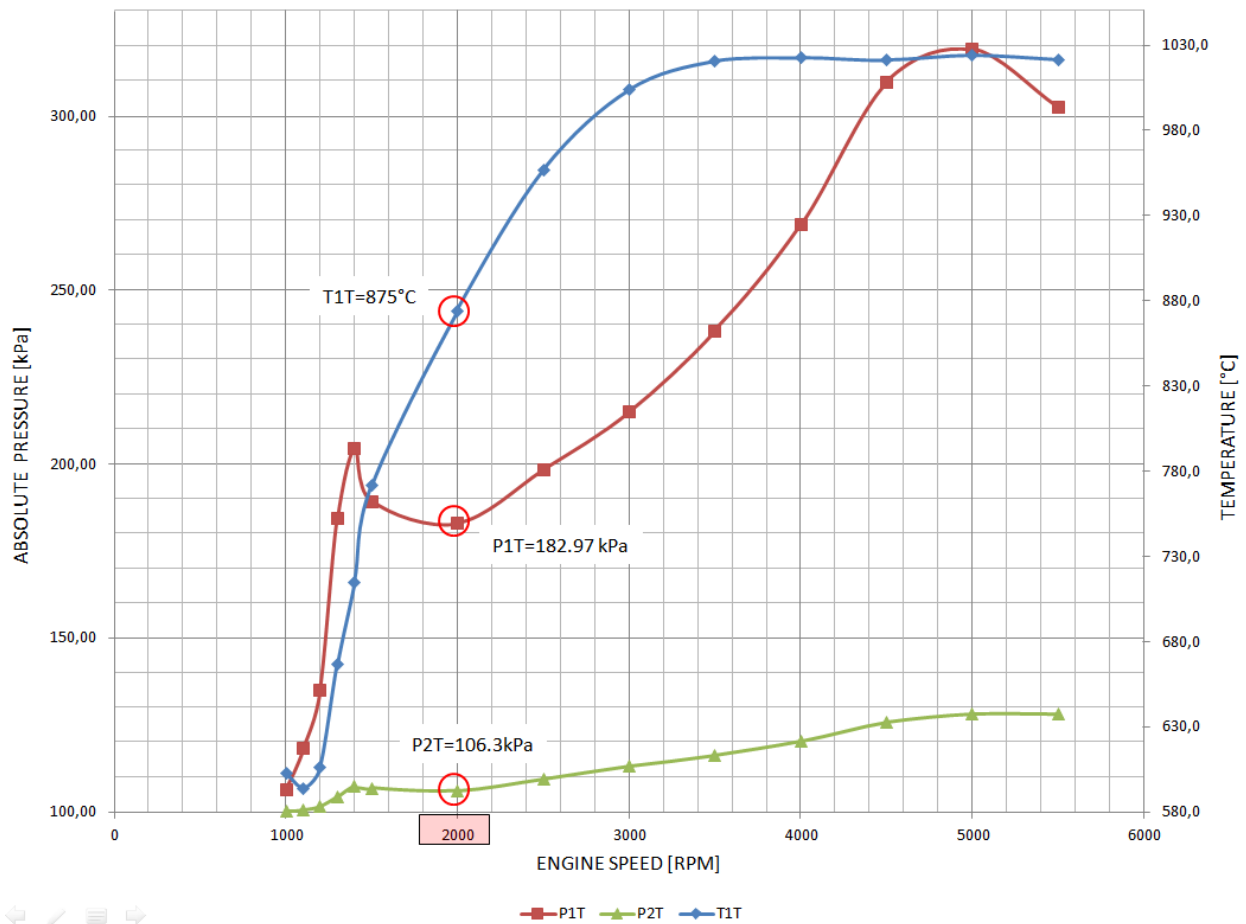
Note:

Analysis settings shown in Table 3 above are recommended for calculation described in this thesis. Although change of some of them could be considered in order to achieve more accurate results and more stable and faster convergence. The calculation setup requires great experiences and expertise. Finding the best way to tune the calculation up is kind of alchemy in certain sense of the word.



## 11.2.1 BOUNDARY CONDITIONS

Boundary conditions are defined in a way to represent situation in engine exhaust shortly after the engine start. The values of **inlet pressure P1T**, **inlet temperature T1T** (exhaust gas temperature), **outlet pressure P2T** and **turbine wheel rotational speed** are taken from laboratory measurement of representative gasoline engine at **2000 RPM**.



Graph 12 Behavior of P1T, T1T and P2T depending on engine RPM

Values shown in Graph 12 above for 2000 engine RPM are set as inlet and outlet boundary condition. These values are fixed for all calculations of current design and other designs at closed wastegate position and opened positions as well.

Turbine wheel rotational speed at 2000 engine RPM is 160,000 RPM. This is set for closed wastegate position only.

Rotational speed for opened wastegate valve positions is calculated proportionally to mass flow percentage through wastegate channel by technical estimation approach, as there is not appropriate laboratory measurement accessible at this time of design proposal. Turbine map and results from measurements done in similar conditions are used to determinate turbine wheel rotational speed decrease due to wastegate regulation.

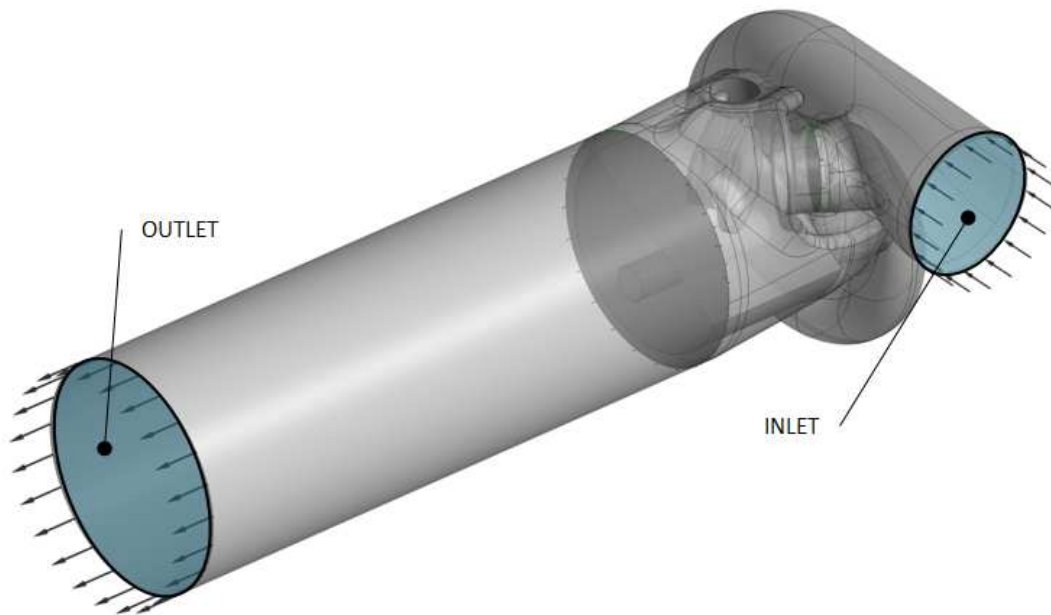


Figure 60 Inlet and outlet boundary condition location

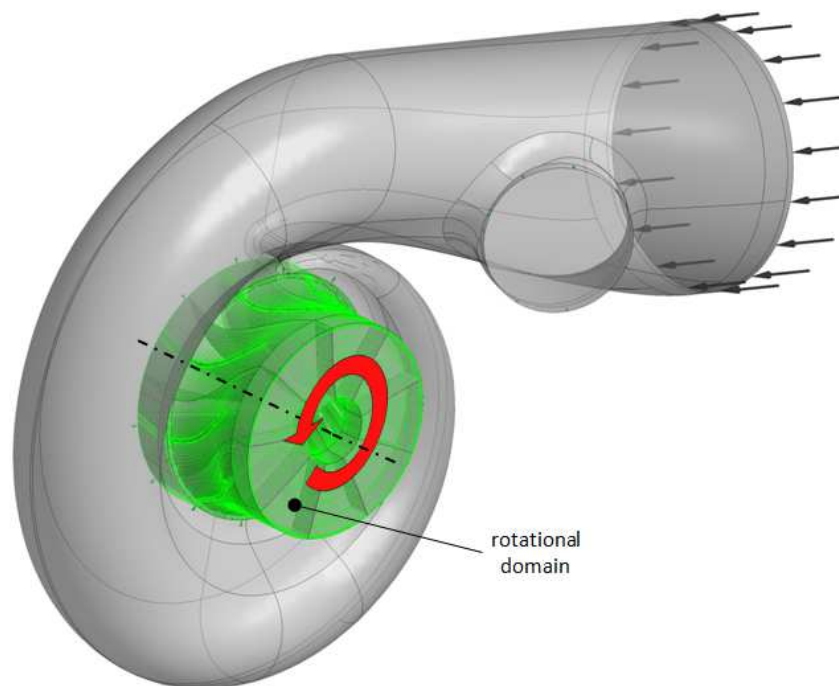


Figure 61 Rotational domain (the turbine wheel)

## 11.2.2 INTERFACES

The domains have to be connected together in pre-processor in order to define how the flow transits from one domain into another. For this reason, GGI (general grid interface) is used. Interface connecting stationary and rotational domain (the turbine wheel) has special frame change/mixing model defined as frozen rotor.

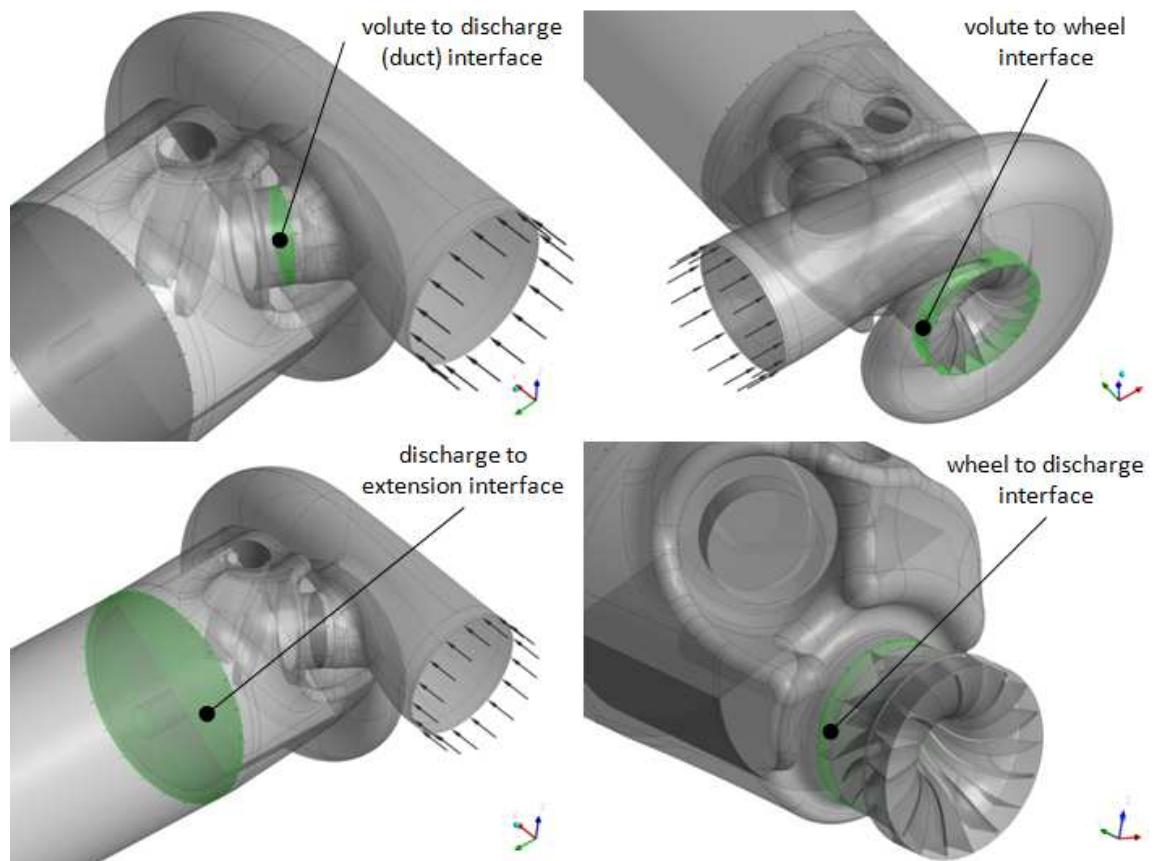


Figure 62 Interfaces locations

### 11.2.3 WALLS

Surfaces that are not defined as inlet, outlet or interface are set as no-slip walls. This means the velocity right on the wall surface is equal to the speed of wall (zero in a case of stationary domain). Wall roughness is set to **smooth wall** option and **adiabatic heat transfer**. Adiabatic walls do not allow the heat to transfer into turbine housing material and further to surroundings. This simplification results in slightly higher temperatures inside the turbine housing and subtly higher turbine wheel adiabatic efficiency.

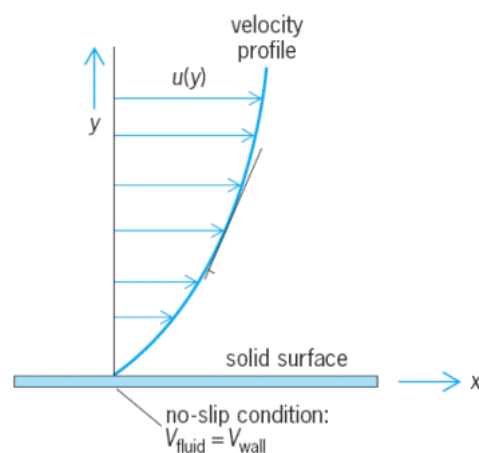


Figure 63 Velocity gradient close to wall [44]



### 11.2.4 POROUS DOMAIN

Extension is defined as porous domain using directional loss model. As mentioned previously, this allows to substitute honeycomb structure of catalytic converter with virtual porous domain without modeling detailed catalyst channel design.

Definition of porosity requires specification of quadratic resistance coefficient  $K_Q$  in streamwise direction (Formula 5 in Catalytic converter chapter). Values required to calculate  $K_Q$  can be taken from laboratory measurement, from which we know the pressure at turbine housing outlet P2T (pressure before catalytic converter). If we assume the pressure behind the catalytic converter is equal to atmospheric pressure, we get the pressure drop within the porous structure.

$\partial x$  represents the length of catalytic converter. This is 200mm. The diameter  $d$  is 75mm (see Turbine housing assembly chapter, Figure 48).

Average velocity  $U_x$  can be calculated from Formula 12 based on the mass flow through defined cross sectional area and the density calculated from equation of state for ideal gas.

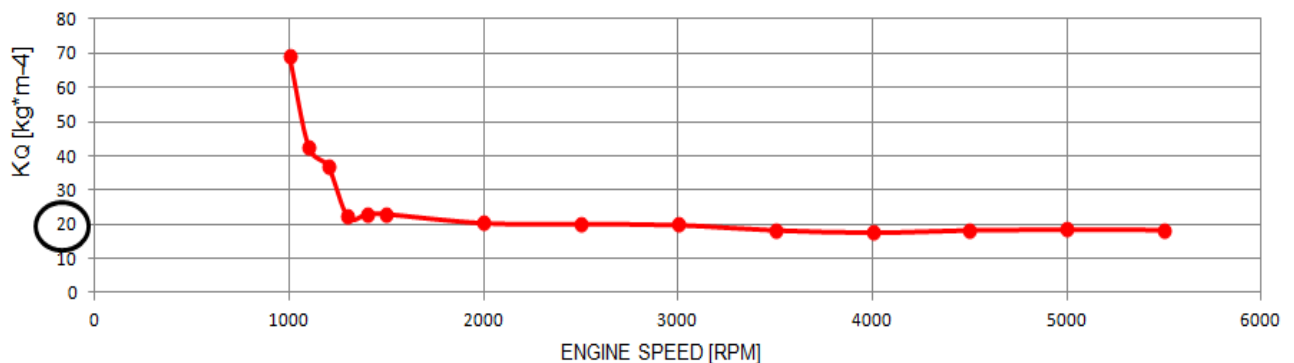
Velocity calculation:

$$U_x = \frac{\dot{m}}{\rho A} \quad (12)$$

where:

$\dot{m}$	[kg.s <sup>-1</sup> ]	- mass flow	
$\rho$	[kg.m <sup>-3</sup> ]	- fluid density	$\rho = P2T / r.T2T$
A	[m <sup>2</sup> ]	- cross sectional area	$A = \pi d^2 / 4$
P2T	[Pa]	- pressure at turbine housing outlet	
T2T	[K]	- temperature at turbine housing outlet	
r	[J.kg <sup>-1</sup> .K <sup>-1</sup> ]	- specific gas constant, for dry air $r = 287.058$ J.kg <sup>-1</sup> .K <sup>-1</sup>	
d	[m]	- catalytic converter diameter, $d=75$ mm	

The result for whole engine speed range is shown on a Graph 13. If we do not consider low engine speed operation, we can see the  $K_Q$  is nearly constant. Therefore quadratic resistance coefficient in streamwise direction  $K_Q$  is taken to be **20kg.m<sup>-4</sup>** for all calculations.



Graph 13 Quadratic resistance coefficient at different engine RPM



The transverse loss multiplier is taken to be 100 in order to inhibit gas flow in between the channels.

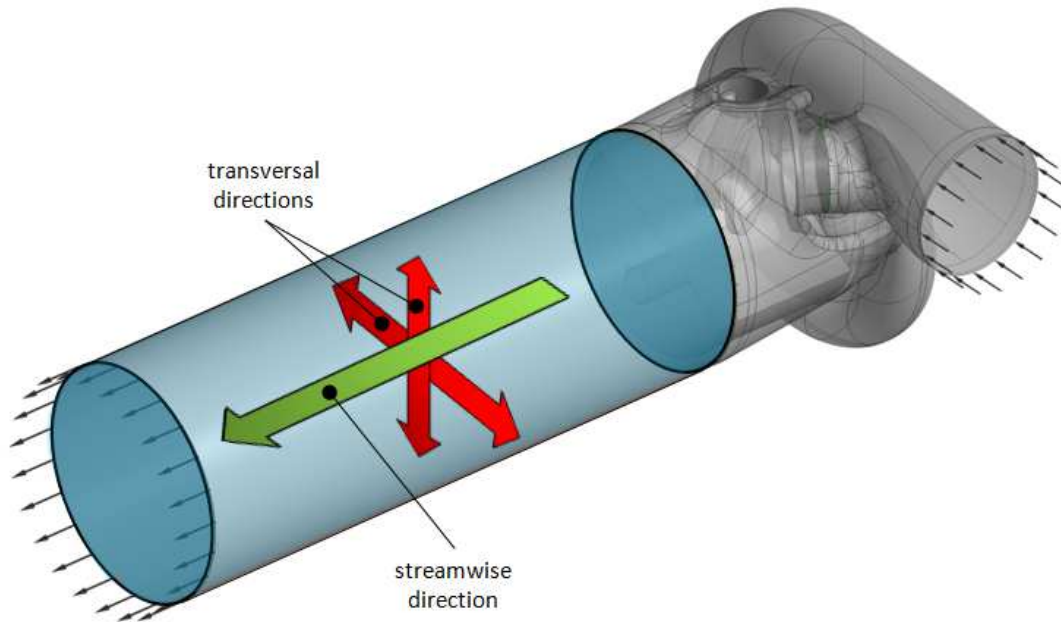
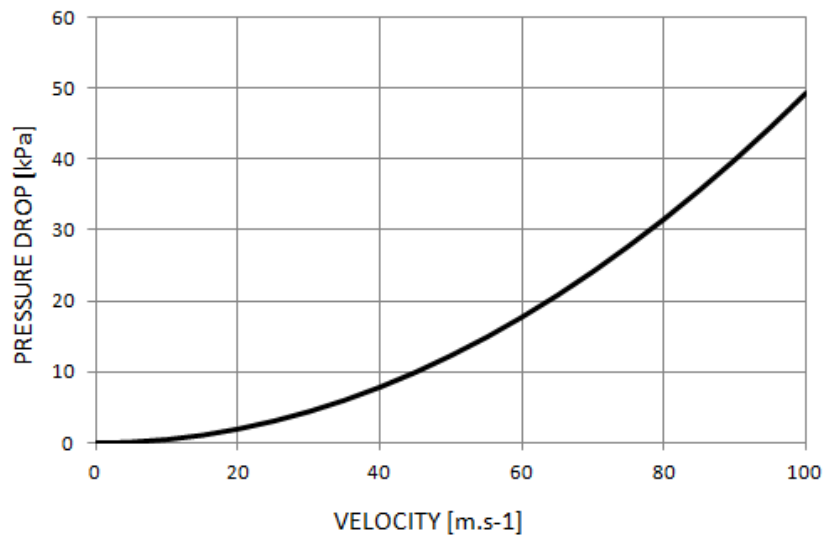


Figure 64 Streamwise and transversal directions in extension (catalytic converter) porous domain

Graph 14 shows flow characteristics in streamwise direction. We can see the quadratic dependency of pressure drop on velocity. Higher velocity causes higher pressure drop, therefore the mass flow right before catalytic converter is spread to larger area and the temperature distribution is more uniform compared to the case without catalytic converter (porous domain).



Graph 14 Streamwise pressure-drop characteristic of porous domain



### 11.2.5 OUTPUT CONTROL

In order to supervise the calculation in process, some of the important output values are monitored. Therefore, the output control has to be defined in pre-processor.

The monitored values are:

- area average pressure @ turbine housing outlet
- area average pressure @ turbine wheel exducer
- area average pressure @ extension outlet
- area average pressure @ turbine housing outlet
- mass flow @ inlet
- mass flow @ outlet
- mass flow @ duct interface (mass flow through the wastegate)
- mass flow @ turbine wheel exducer

Very important measure of correct calculation is the difference between inlet and outlet mass flow. These values have to be the same in ideal case. (+ represent inflow, - represents outflow)

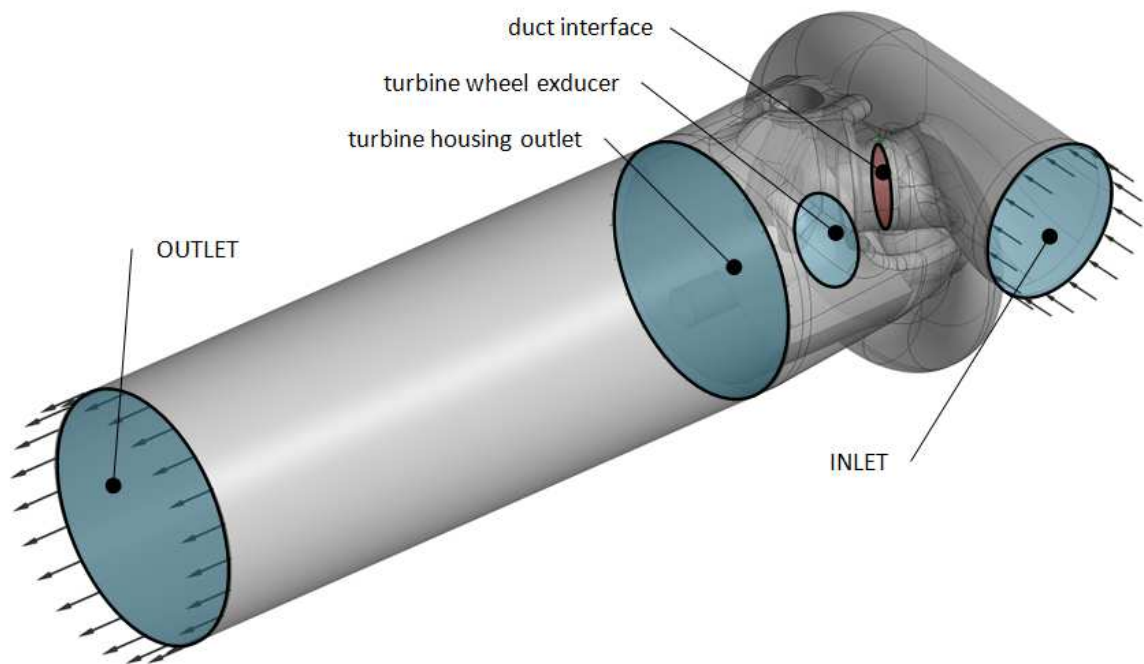


Figure 65 Output control monitored locations



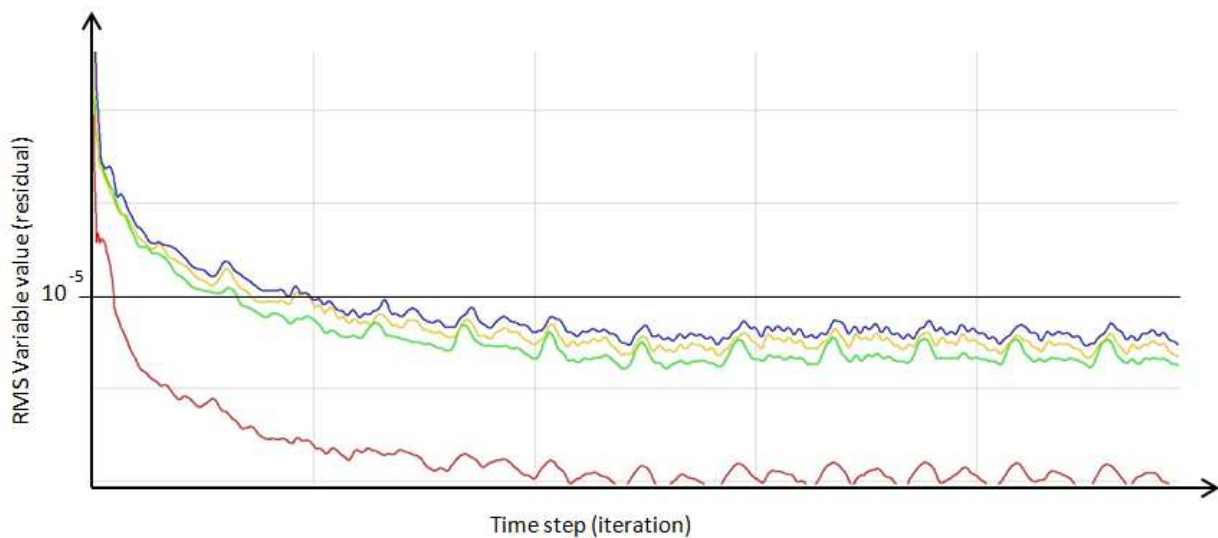
## 11.3 SOLVER

After all parameters and boundary conditions are defined, solution can be executed.

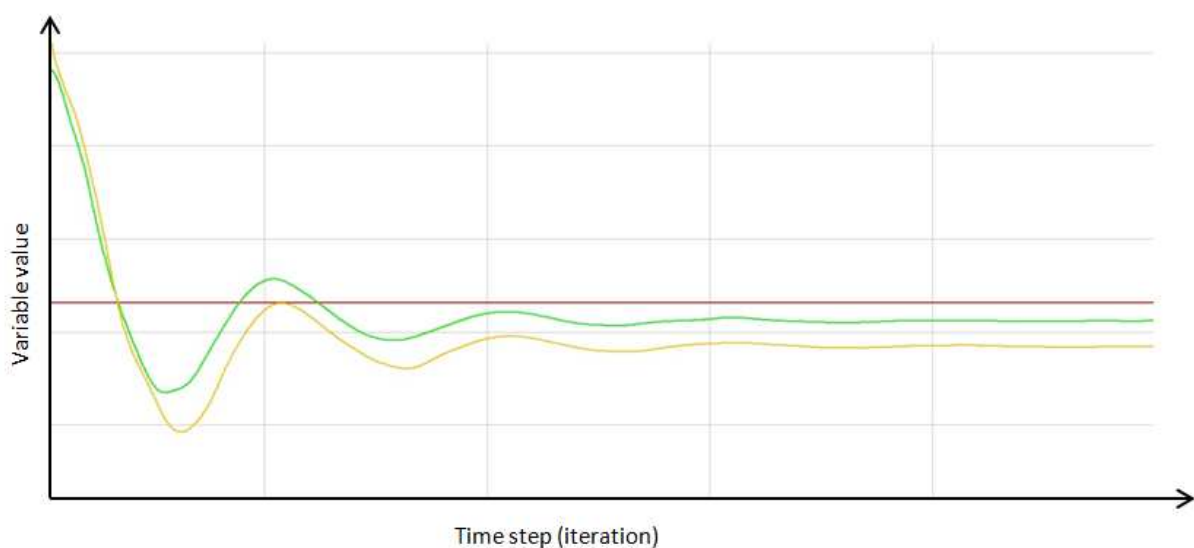
In average, the calculation time of one design at one wastegate position took around 10 hours and more than 700 iterations.

In order to judge the results accuracy, the convergence and values defined in output control have to be monitored.

We can say the results are sufficiently accurate when important output values stabilize and residual target is met.



*Graph 15 Convergence obtained by residuals drop*



*Graph 16 Monitored value stabilization*



## 11.4 POST-PROCESSING

The post-processing is done in ANSYS CFD-Post. Here all necessary information are graphically visualized and quantified.

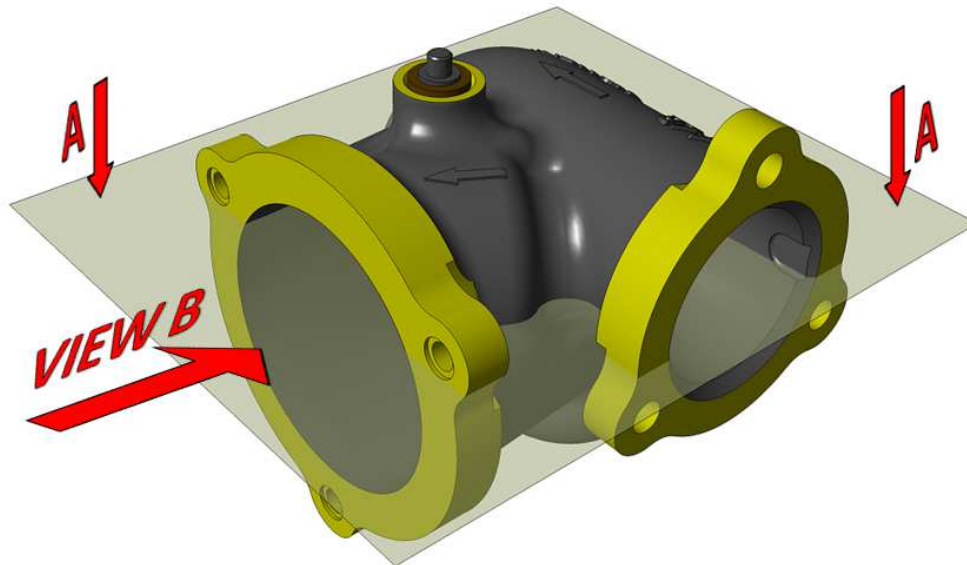


Figure 66 Section A-A and VIEW B orientation

The contours of total temperature are plotted at turbine housing outlet area (VIEW B) and in a cross sectional plane through wastegate valve (SECTION A-A) both shown on Figure 66.

Flow character is visualized by the vectors representing velocity by its size and total temperature by its color. Direction of flow is determined by pressure gradient, which describes in which direction and at what rate the pressure changes the most rapidly around a particular location.

Important values such as inlet/outlet total (static) pressure, inlet/outlet total temperature, total pressure at turbine wheel exducer, total mass flow at inlet, mass flow through wastegate channel are measured.

In order to quantify and numerically describe temperature distribution, the resulting values at turbine housing outlet area in every single facet are exported to EXCEL and processed in order to calculate **standard deviation** of temperatures. The smaller deviation of temperatures means better temperature distribution.

Standard deviation of temperature  $\sigma_T$  [43]:

$$\sigma_T = \sqrt{\frac{1}{N} \cdot \sum_{i=1}^N (T_i - \bar{T})^2} \quad (13)$$

where:

$N$	[-]	- number of facets on turbine housing outlet area
$T_i$	[°C]	- temperature in facet 'i'
$\bar{T}$	[°C]	- average temperature



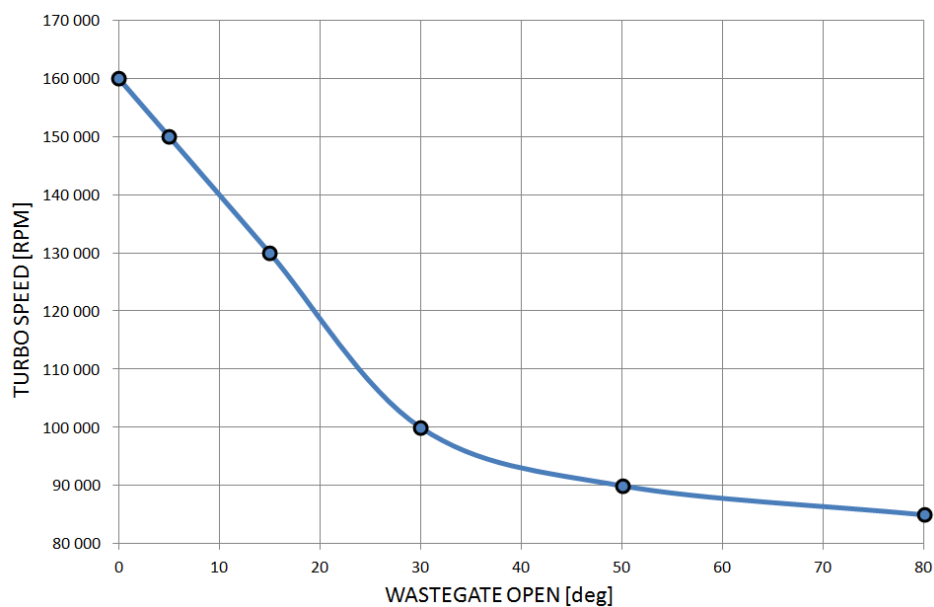
## 11.5 RESULTS

The current design 1 has been calculated in **closed** wastegate position and **5, 15, 30, 50** and **80** degrees wastegate open position with the boundary conditions and pre-processing described in previous chapter.

Input values are clearly shown in Table 4 below. As mentioned above the turbine wheel rotational speed has been estimated proportionally to expected and pre-calculated mass flow percentage through wastegate channel (Graph 17).

Table 4 Calculation input values

WASTEGATE OPEN	[deg]	0	5	15	30	50	80
INLET PRESSURE P1T	[bar]	1,82970					
INLET TEMPERATURE T1T (STATIC)	[°C]	875					
OUTLET PRESSURE (ATMOSPHERIC)	[bar]	1,01325					
QUADRATIC RESISTANCE COEFICIENT $K_q$	[kg.m-4]	20					
TURBO SPEED	[RPM]	160 000	150 000	130 000	100 000	90 000	85 000



Graph 17 Turbine wheel RPM at different wastegate positions



### 11.5.1 CLOSED WASTEGATE POSITION

In closed wastegate position, the gasses at turbine housing outlet are cooler than at inlet. This phenomenon is called adiabatic expansion, which is described in theory passages of this thesis. The energy is handed over to the turbine wheel, therefore the pressure and temperature decreases as a gas passes through wheel channels. We can see the temperature drop at a section view of turbine housing at Figure 67.

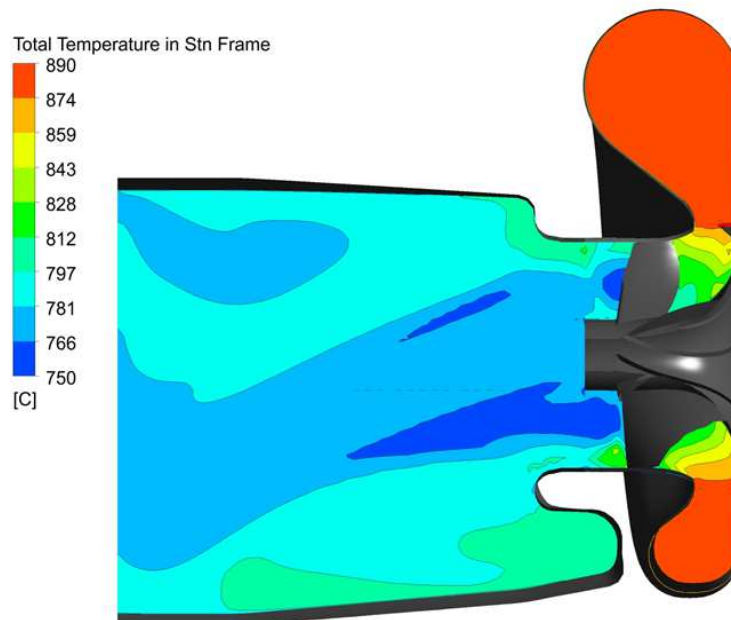


Figure 67 Section view through turbine wheel axis

Gasses do no flow straight forward to outlet as it is in a case of simulation without porous domain (catalytic converter). It deflects sideways a little bit into a space with lower resistance because of flow and pressure drop characteristic within porous domain.

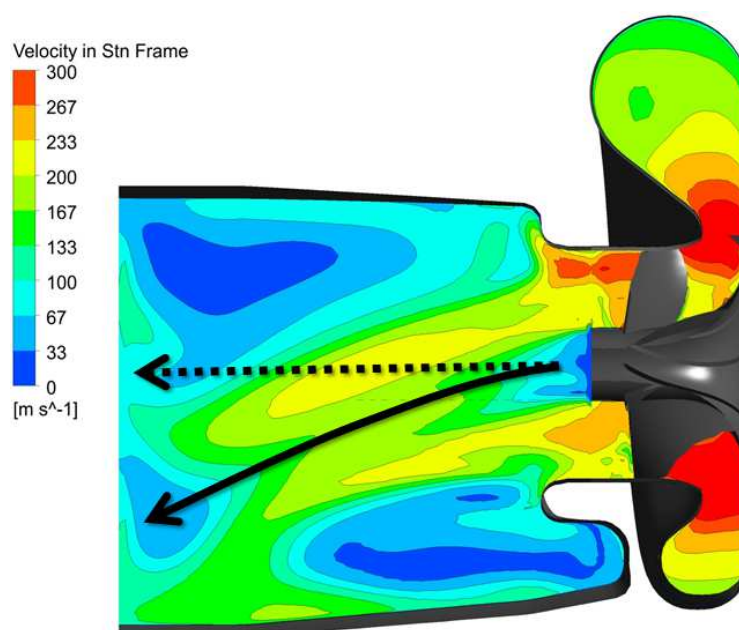


Figure 68 Flow deflection in turbine housing discharge due to porous domain



The exhaust gas does not flow through the wastegate channel. All of mass passes through the turbine wheel channels and enters the discharge with swirl movement. On Figure 69 we can see the how the wastegate channel influence the flow inside inlet section. Its position too close to T-T section would have negative impact on performance and pressure drop.

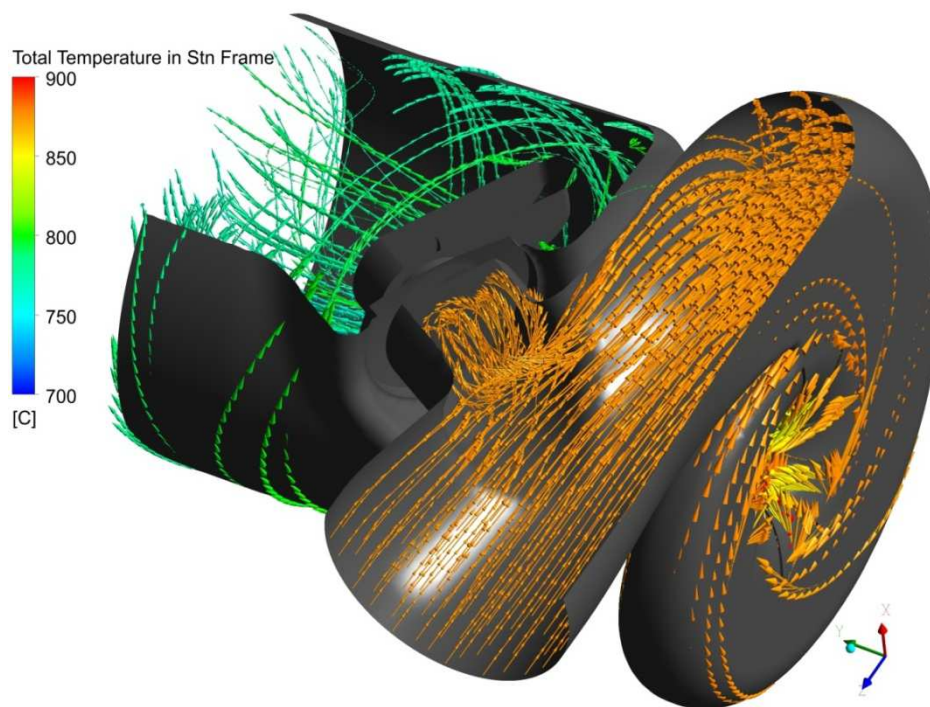


Figure 69 Flow in inlet section and around closed wastegate channel

The flow stabilizes when gas enters the catalytic converter. It flows through the narrow channels of honeycomb structure in one direction only as we can see on Figure 70.

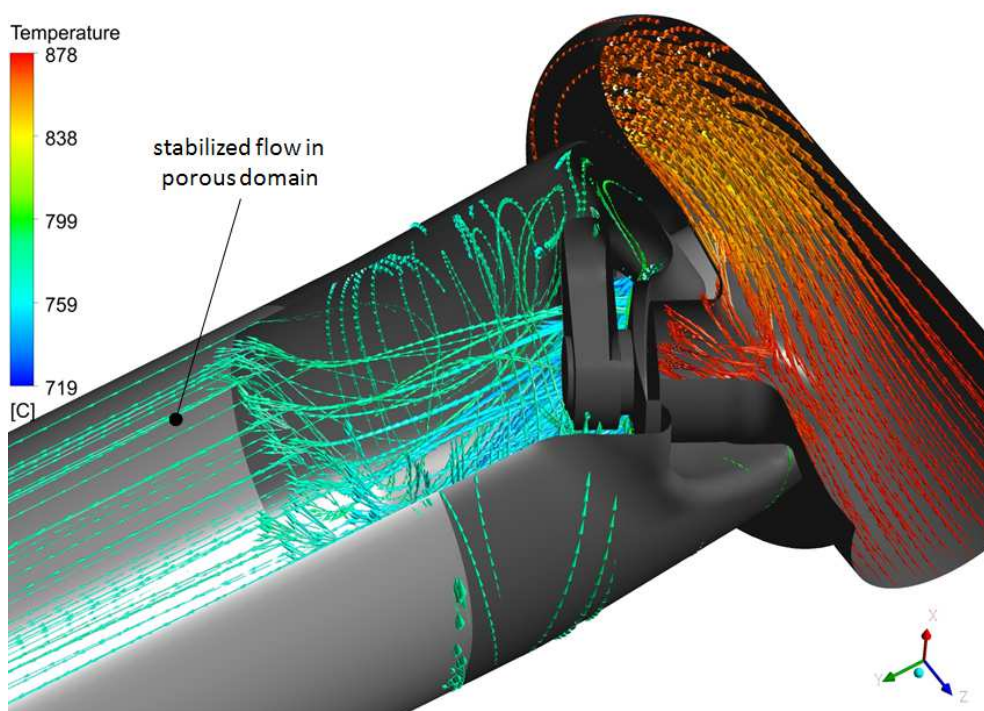


Figure 70 Flow in volute, discharge and porous domain



Section A-A through wastegate channel on Figure 71 shows the temperature proportions at inlet and discharge of turbine housing. We can see the temperature distribution at turbine housing outlet is nearly uniform when wastegate valve is closed.

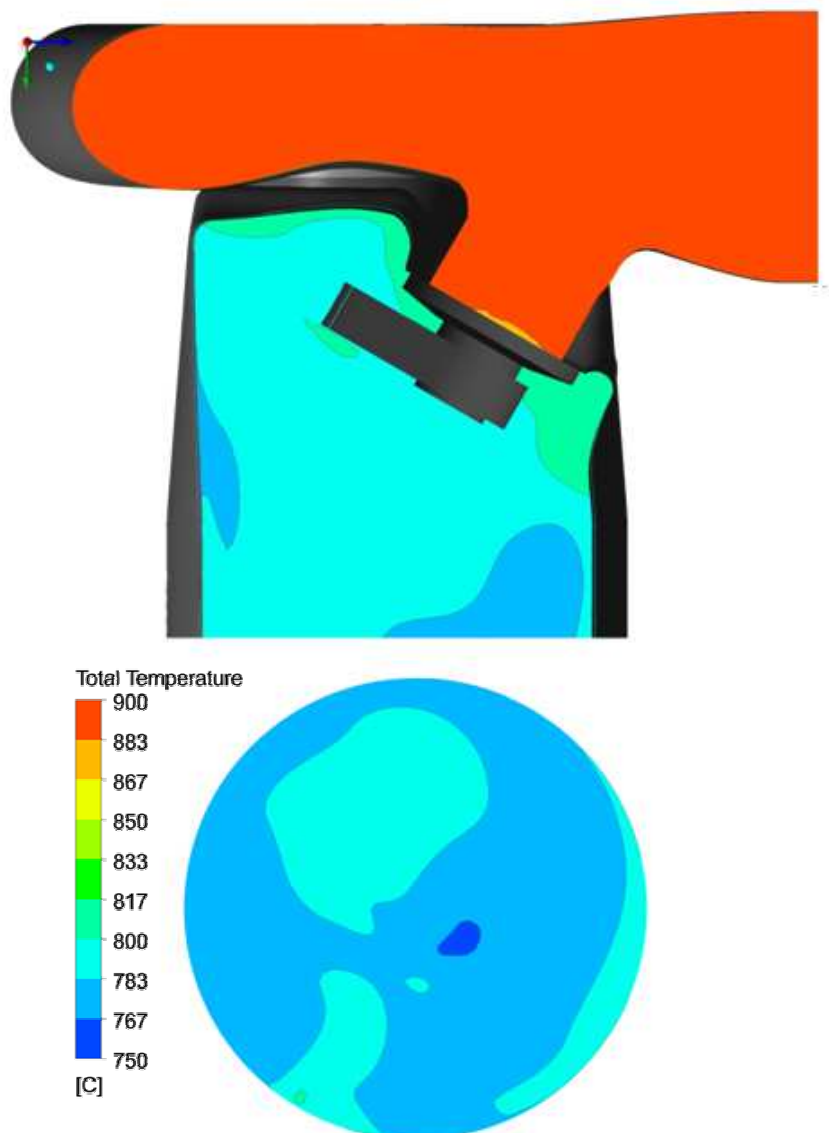


Figure 71 Contours of temperature at closed wastegate (section A-A (top) and view B(bottom))



11.5.2 5 DEG OPEN

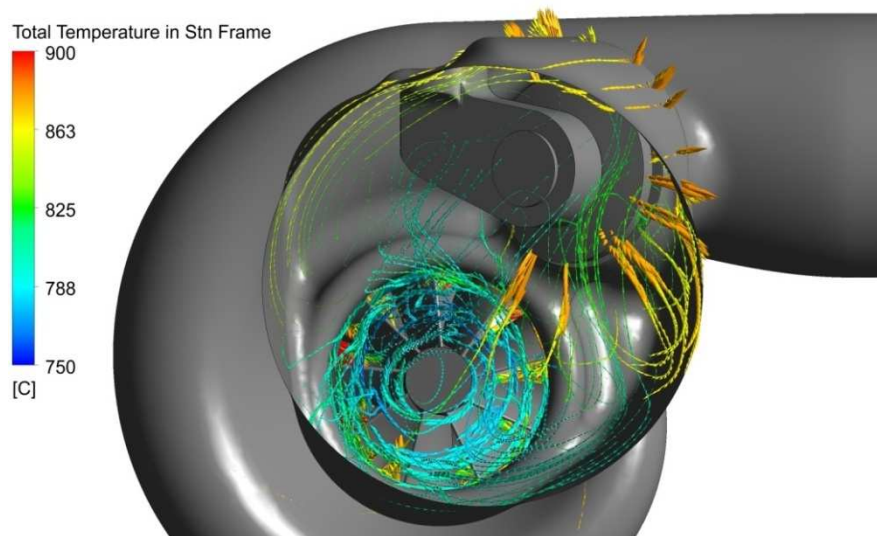


Figure 72 Flow vectors at 5degrees open position

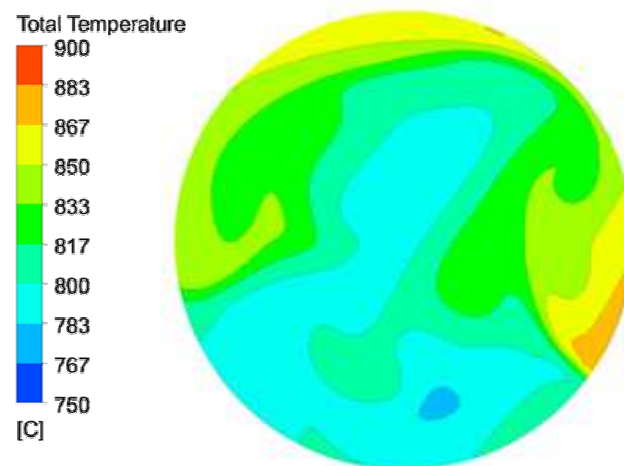
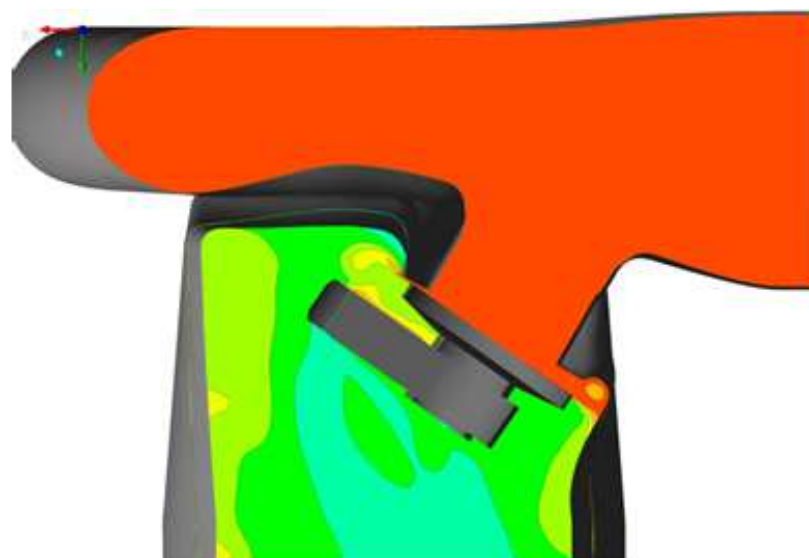


Figure 73 Temperature contours at 5degrees open position (section A-A and view B)



11.5.3 15 DEG OPEN

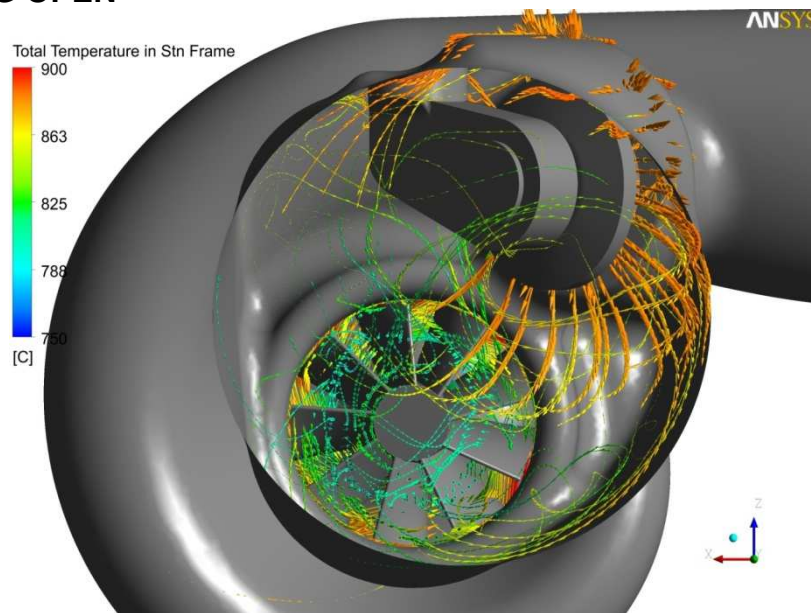


Figure 74 Flow vectors at 15deg open position

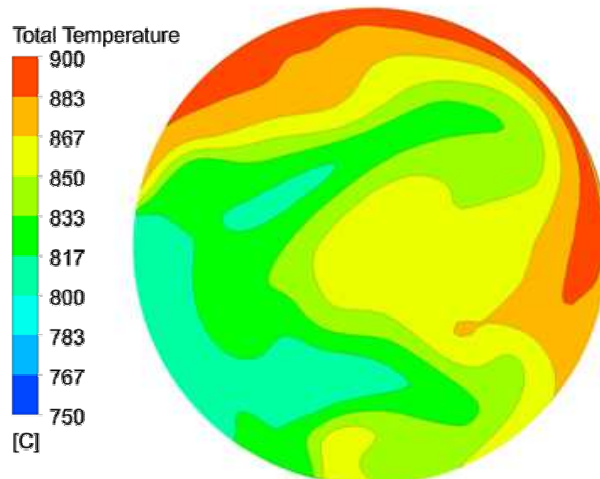


Figure 75 Temperature contours at 15deg open position (section A-A, view B)



11.5.4 30 DEG OPEN

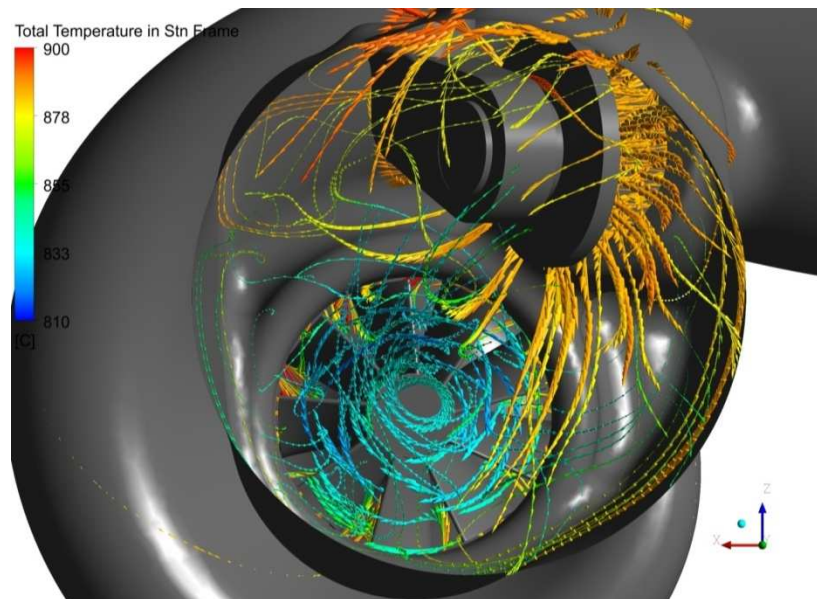


Figure 76 Flow vectors at 30deg open position

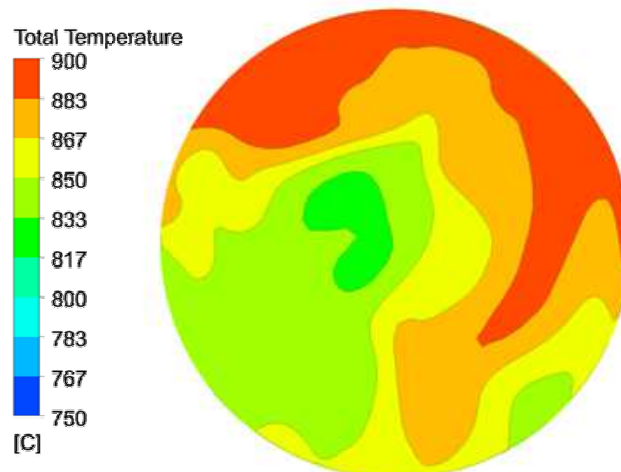


Figure 77 Temperature contours at 30deg open position (section A-A, view B)



### 11.5.5 50 DEG OPEN

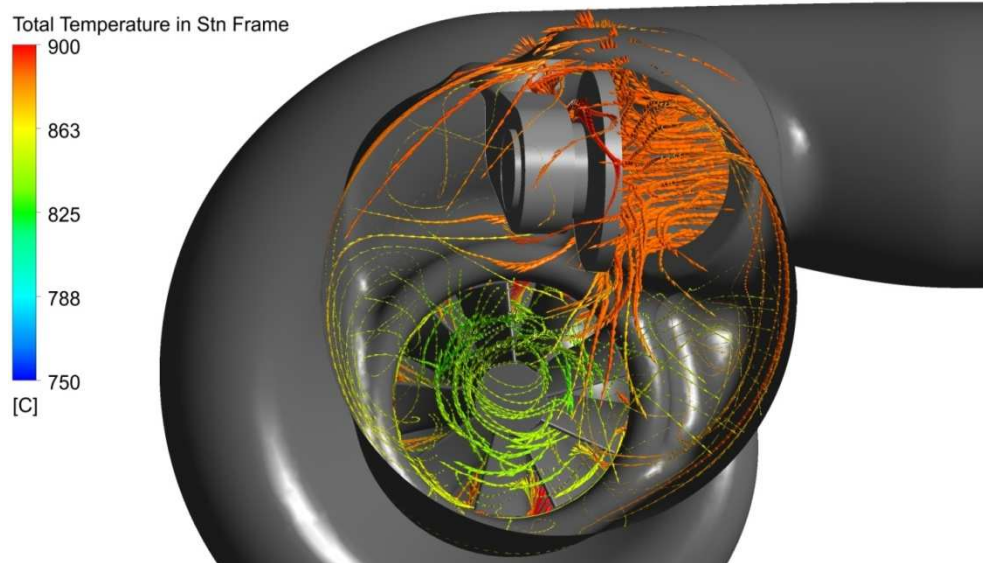


Figure 78 Flow vectors at 50deg open position

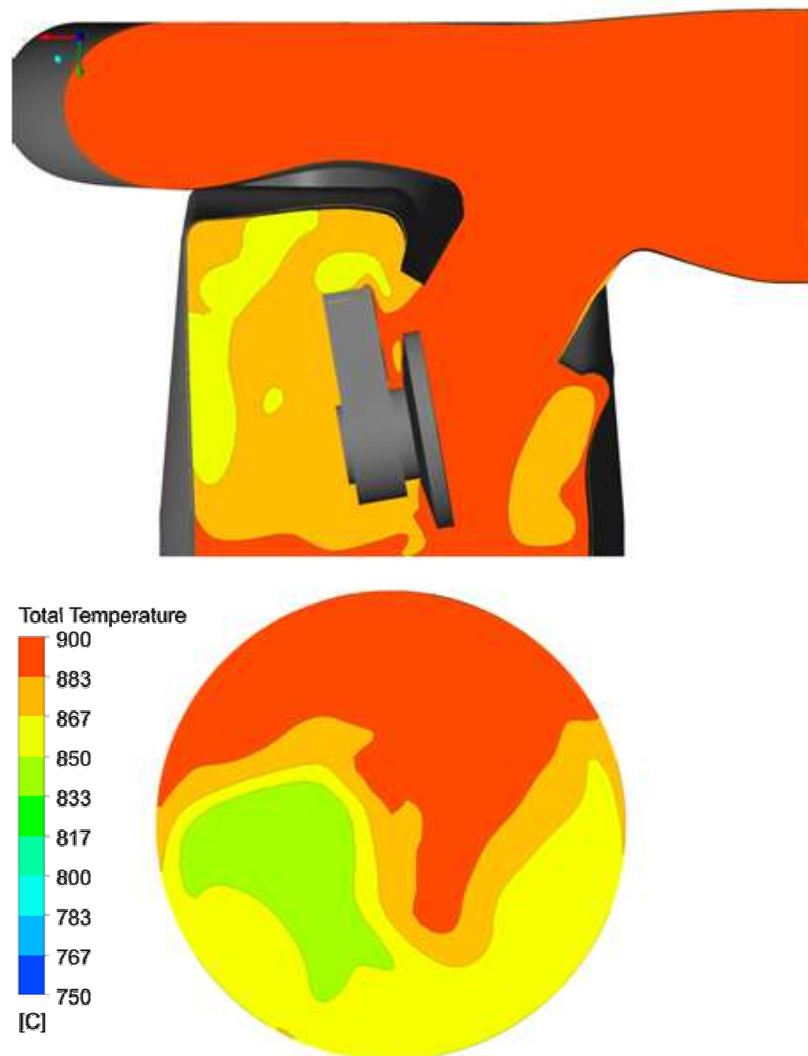


Figure 79 Temperature contours at 50deg open position (section A-A, view B)



11.5.6 80 DEG OPEN

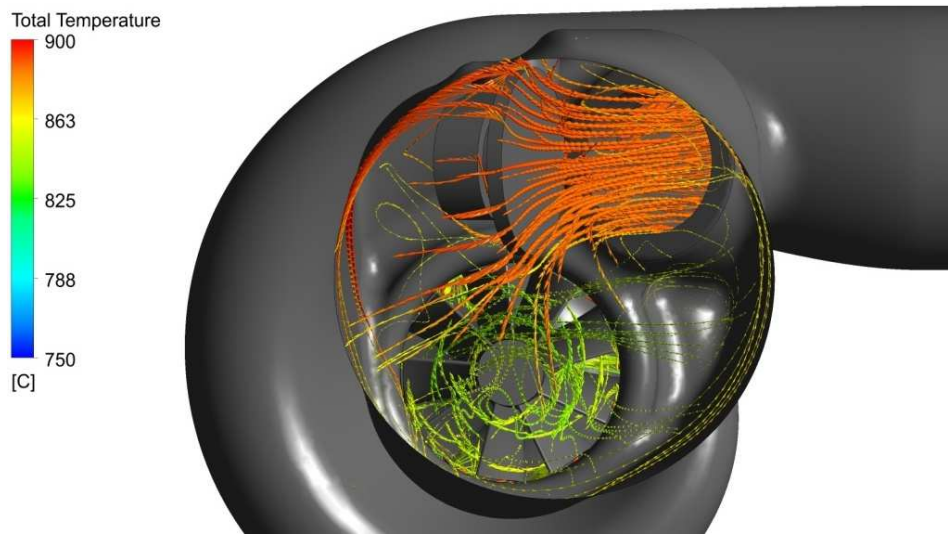


Figure 80 Flow vectors at 80deg open position

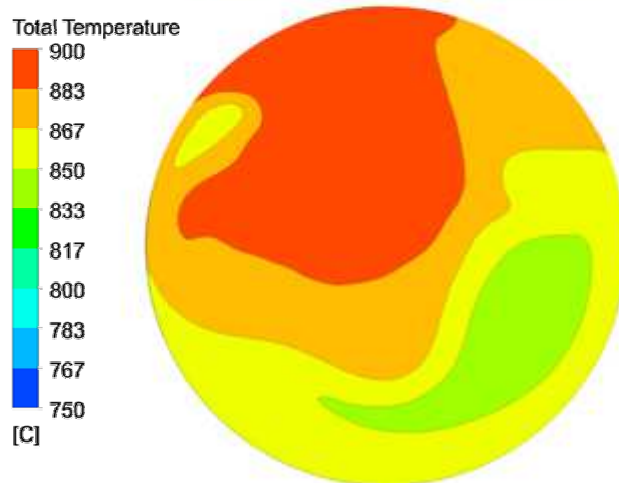


Figure 81 Temperature contours at 80deg open position (section A-A, view B)



### 11.5.7 SUMMARY OF CURRENT DESIGN CALCULATION

Average values of pressure, temperature, mass flow and others have been measured in the locations of interest. These are mainly the turbine housing inlet/outlet and turbine wheel exducer. Other important values have been calculated based on simulation results such as expansion ratio, efficiency, wastegate mass flow percentage and standard deviation of temperature at turbine housing outlet.

Total pressure at turbine wheel exducer is significant measure of wastegate opening and discharge design impact on turbine performance.

Standard deviation of temperatures at turbine housing outlet is a numerical expression of temperature distribution. The lower deviation means more uniform temperature distribution.

Table 5 below shows results at different wastegate position.

Table 5 Results summary of current design

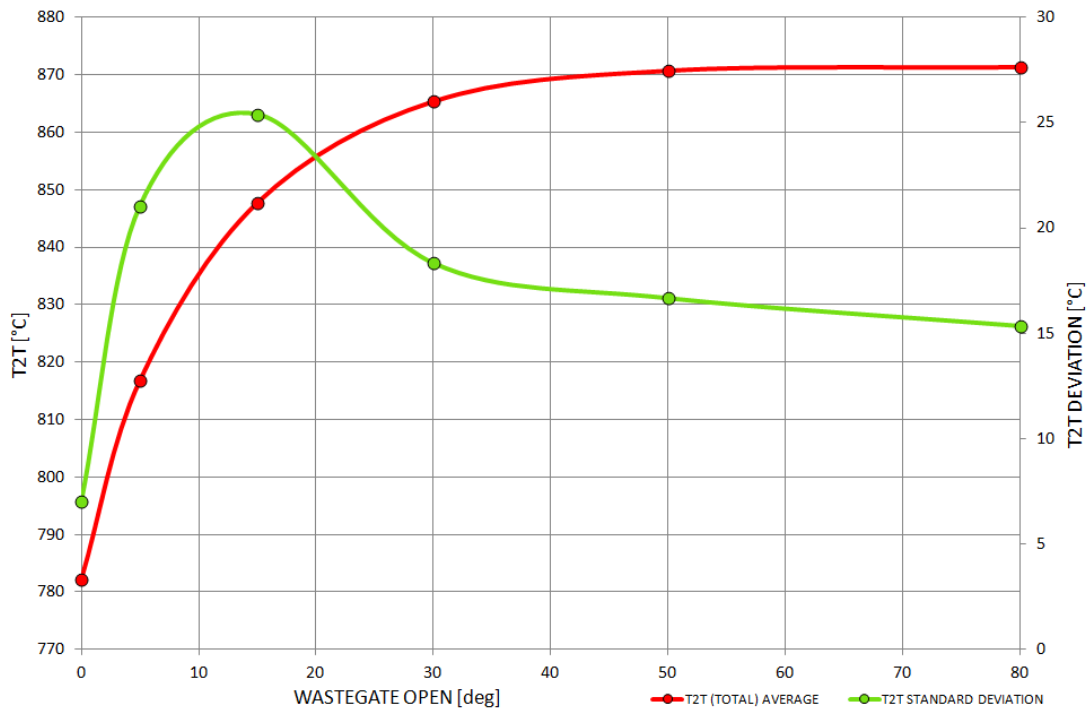
WASTEGATE OPEN	[deg]	0	5	15	30	50	80
TURBO SPEED	[RPM]	160 000	150 000	130 000	100 000	90 000	85 000
P1T (TOTAL) AVERAGE	[bar]	1,82969	1,82968	1,82967	1,82966	1,82965	1,82964
T1T (TOTAL) AVERAGE	[°C]	879,06	881,52	884,97	888,27	889,44	889,46
P2T (TOTAL) AVERAGE	[bar]	1,1845	1,2502	1,39956	1,49649	1,55129	1,5808
P2T (STATIC) AVERAGE	[bar]	1,16039	1,22858	1,35476	1,44839	1,49362	1,50993
T2T (TOTAL) AVERAGE	[°C]	782,21	816,85	847,75	865,37	870,7	871,33
T2T STANDARD DEVIATION	[°C]	7,04	21,05	25,38	18,33	16,67	15,35
TOTAL MASS FLOW	[g.s-1]	78,55	98,94	121,08	138,29	143,74	143,86
MASS FLOW THROUGH WASTEGATE	[g.s-1]	0,00	20,74	49,78	71,84	79,89	80,25
TOTAL PRESSURE @ TURBINE WHEEL EXDUCER	[bar]	1,22992	1,27979	1,39147	1,47265	1,50858	1,51036
% MASS FLOW THROUGHT WASTEGATE	[%]	0,00	20,96	41,11	51,95	55,58	55,78
EXPANSION RATIO (TOTAL TO STATIC) P1T/P2T	[-]	1,58	1,49	1,35	1,26	1,22	1,21
EFFICIENCY(TOTAL TO STATIC) $\eta_{T-S}$	[%]	73	55	42	33	31	31

On Graph 18 we can see that at closed wastegate position average outlet temperature is 782°C, which is lower almost by 100°C than inlet temperature due to adiabatic expansion and energy conversion. When a wastegate valve opens, outlet temperature rises sharply up to 870°C.

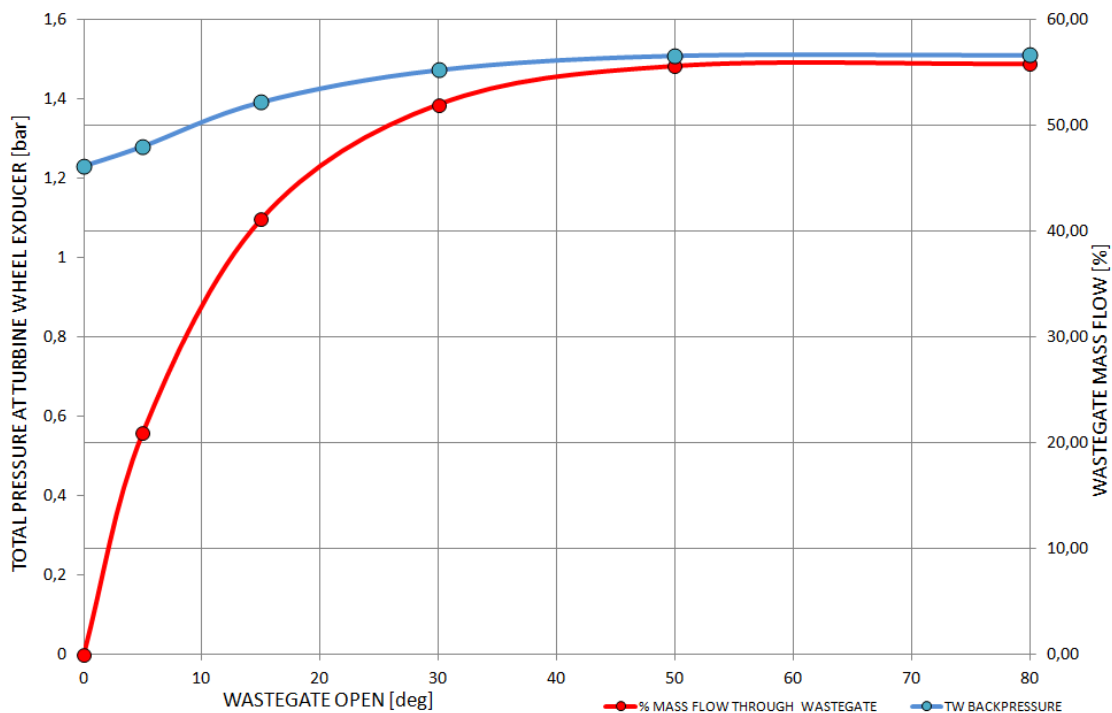
Temperature distribution at turbine housing outlet is uniform at closed wastegate. It rises up rapidly when a valve opens a little and then descend gradually with higher wastegate opening.

Graph 19 shows dependency of wastegate valve position and mass flow percentage through the wastegate channel. It rises up rapidly when a valve is opened a little. We can see the mass flow percentage stagnates at wastegate opening higher than 50 degrees.

Backpressure created at turbine wheel exducer is at its lowest point when a wastegate valve is closed. It increases as a wastegate valve opens and turbine housing discharge is clogged with the wastegated gasses.



Graph 18 Average temperature and temperature deviation at turbine housing outlet



Graph 19 Mass flow percentage through wastegate and backpressure at turbine wheel exducer

The result from the calculations of current design 1 shows that temperature distribution is very uneven when wastegate valve opens a little. The mechanism and actuator used today for control of wastegate allows opening up to 15 degrees. At this opening, temperature distribution is still non-uniform and gasses flowing out of wastegate channel are directed along discharge wall.

**Higher openings** of valve do not increase mass flow through wastegate channel radically but would lead to **better temperature distribution**. The development of appropriate control mechanism for higher openings should be considered.



## 12 DESIGN 2 (REVERSED BUSHING)

As we can see on the results of current design, the temperature distribution is non-uniform at wastegate openings covered by currently used actuator. For this reason, next designs are proposed to eliminate this flow character.

The volute, wheel and extension designs remain the same. The turbine housing inlet and outlet flanges stays in a position. Only the wastegate channel (duct) and discharge core are changed.

The first design change proposal is to use turbine housing with reversed bushing position. This way the valve opens reversely which could have positive effect on temperature distribution. The impact on performance needs to be verified.

The models of design 2 are created in a same manner in CATIA V5 as described on model of current design. The core model is shown on Figure 82. The bushing axis is positioned on the other side of duct.

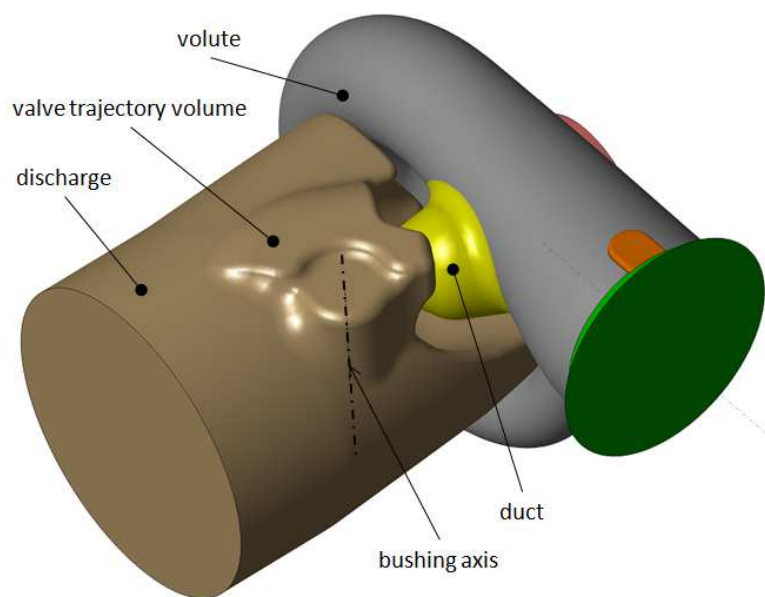


*Figure 82 Core model of design 2 with reversed bushing position*

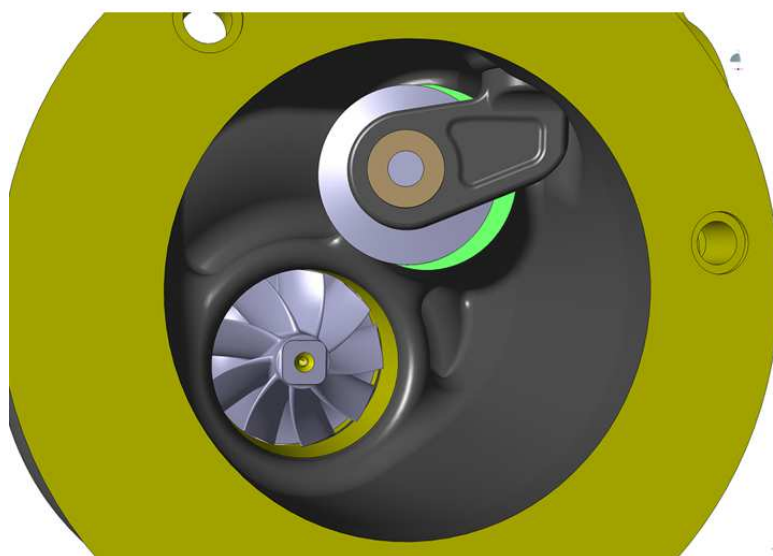


*Figure 83 Discharge design with reversed bushing position*

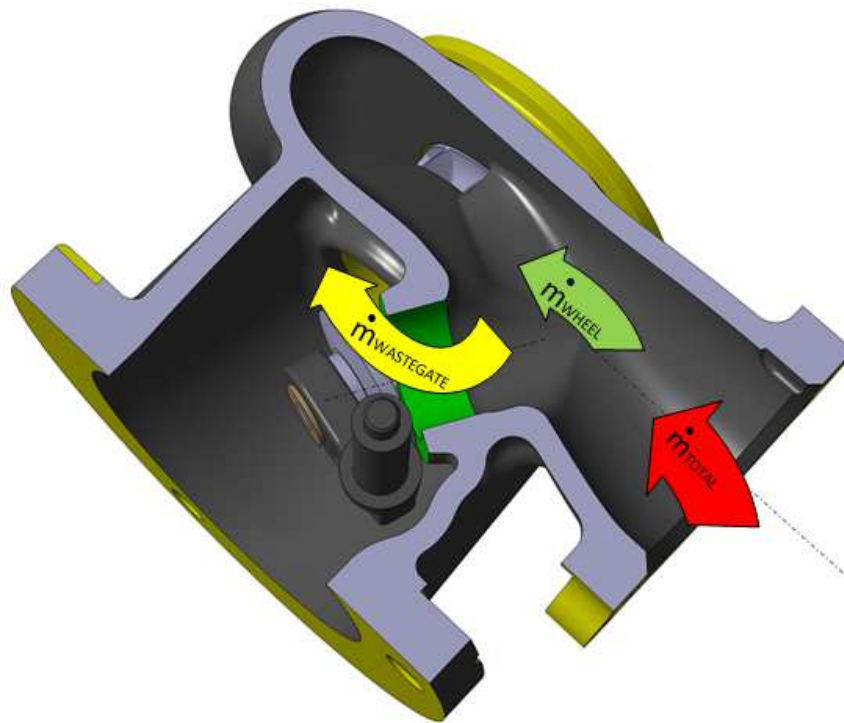


Figure 84 Section view through wastegate channel and awaited flow direction

## 12.1 RESULTS

The design 2 with reversed bushing position has been calculated in **closed** wastegate position and **15, 30 and 50** degrees wastegate open position with the boundary conditions and pre-processing described in previous chapter.

Geometry, mesh and pre-processing of calculation are done in a same manner as described on calculation of current design.

Calculation input values are the same as in current design so the results can be compared to current design 1.

Table 6 Input values for calculation of design 2

WASTEGATE OPEN	[deg]	0	15	30	50
INLET PRESSURE P1T	[bar]	1,82970			
INLET TEMPERATURE T1T (STATIC)	[°C]	875			
OUTLET PRESSURE (ATMOSPHERIC)	[bar]	1,01325			
QUADRATIC RESISTANCE COEFFICIENT Kq	[kg.m-4]	20			
TURBO SPEED	[RPM]	160 000	130 000	100 000	90 000

Contours of temperature are plotted on a same section (A-A) through wastegate channel and on the turbine housing outlet (view B) as current design 1 (see Figure 66)

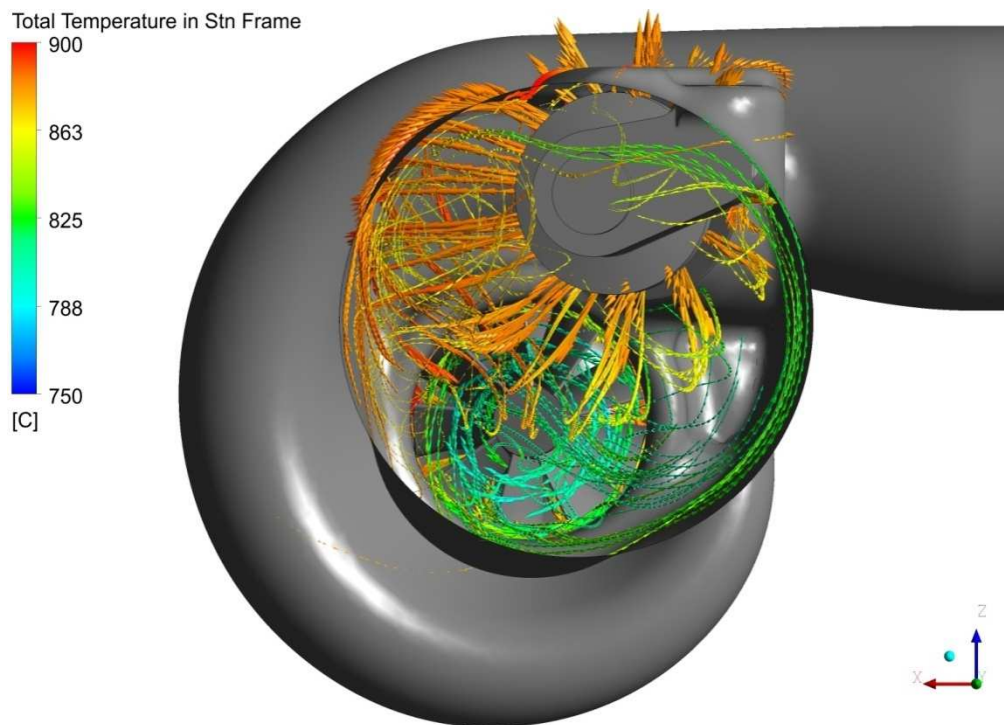


Figure 85 Flow vectors at 15 degrees open position of reversed bushing design

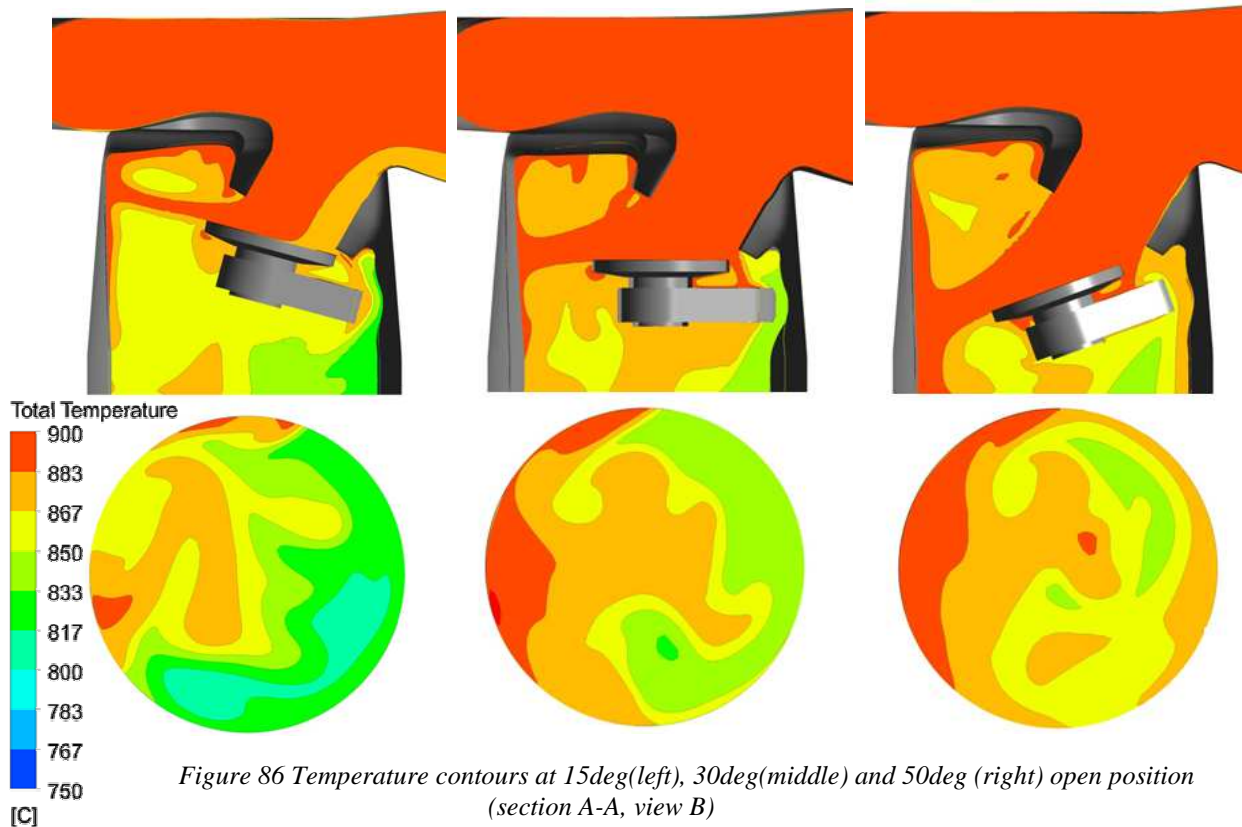


Figure 86 Temperature contours at 15deg(left), 30deg(middle) and 50deg (right) open position (section A-A, view B)



Closed wastegate position is not shown here as it has the same flow character as current design. The results in closed position differs slightly which is shown in Table 7.

Resulting values of temperature standard deviation and total pressure at turbine wheel exducer shown in Table 7 below are compared to current design and other designs at the end of this thesis.

Table 7 Results summary of design with reversed bushing

WASTEGATE OPEN	[deg]	0	15	30	50
TURBO SPEED	[RPM]	160 000	130 000	100 000	90 000
P1T (TOTAL) AVERAGE	[bar]	1,82968	1,82966	1,82965	1,82964
T1T (TOTAL) AVERAGE	[°C]	879,22	884,79	887,78	889,19
P2T (TOTAL) AVERAGE	[bar]	1,17867	1,35802	1,46326	1,50804
P2T (STATIC) AVERAGE	[bar]	1,15798	1,32602	1,41711	1,45171
T2T (TOTAL) AVERAGE	[°C]	783,26	846,06	863,62	870,36
T2T STANDARD DEVIATION	[°C]	5,94	23,43	18,77	12,49
TOTAL MASS FLOW	[g.s-1]	80,04	119,99	135,84	142,53
MASS FLOW THROUGH WASTEGATE	[g.s-1]	0,00	49,74	71,74	81,08
TOTAL PRESSURE @ TURBINE WHEEL EXDUCER	[bar]	1,22123	1,39566	1,48652	1,52374
% MASS FLOW THROUGH WASTEGATE	[%]	0,00	41,45	52,81	56,88
EXPANSION RATIO (TOTAL TO STATIC) P1T/P2T	[-]	1,58	1,38	1,29	1,26
EFFICIENCY(TOTAL TO STATIC) $\eta_{T-s}$	[%]	72	41	32	27



## 13 DESIGN 3 (HORIZONTAL BUSHING AXIS)

Behavior of fluid in hostile conditions of engine exhaust is very hard to predict. Therefore, every single design proposal has to be verified by CFD calculation in order to confirm or disprove the hypothesis of positive effect to temperature distribution. The performance influence of different design has to be clarified as well, especially at closed wastegate position.

The design 3 has a bushing axis in parallel plane to XY plane and is perpendicular to duct channel axis. The valve swings around bushing axis from the bottom closed position way up.

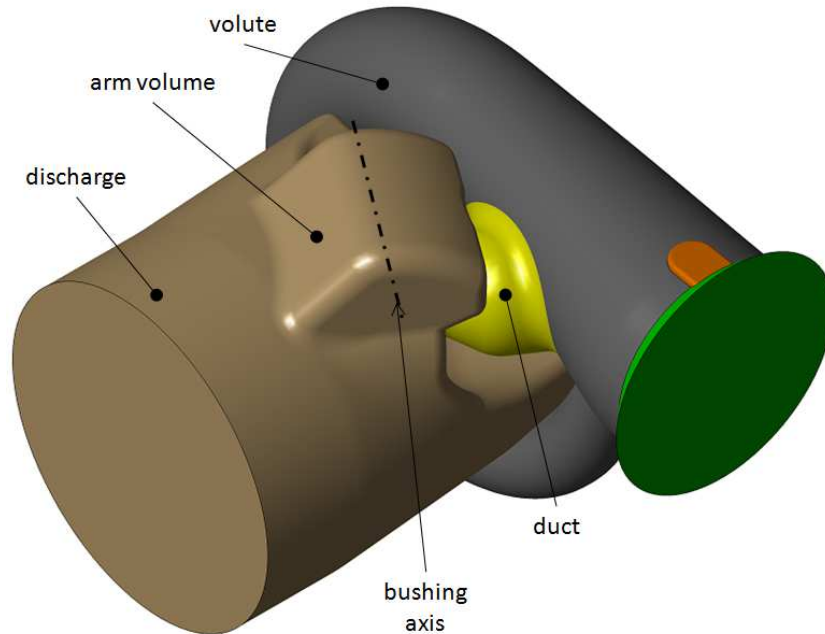


Figure 87 Core model of horizontal bushing design



Figure 88 Discharge design with horizontal bushing axis



Contours of temperature in following results chapter are plotted at turbine housing outlet (view C) and in a section view through wastegate channel (section D-D) both shown on Figure 89 below.

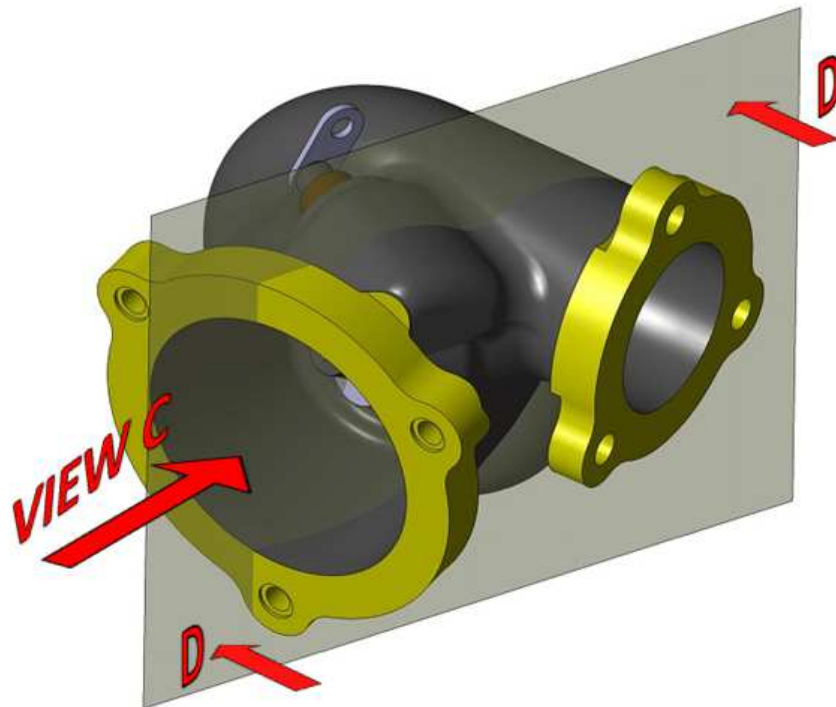


Figure 89 View C and section D-D orientation

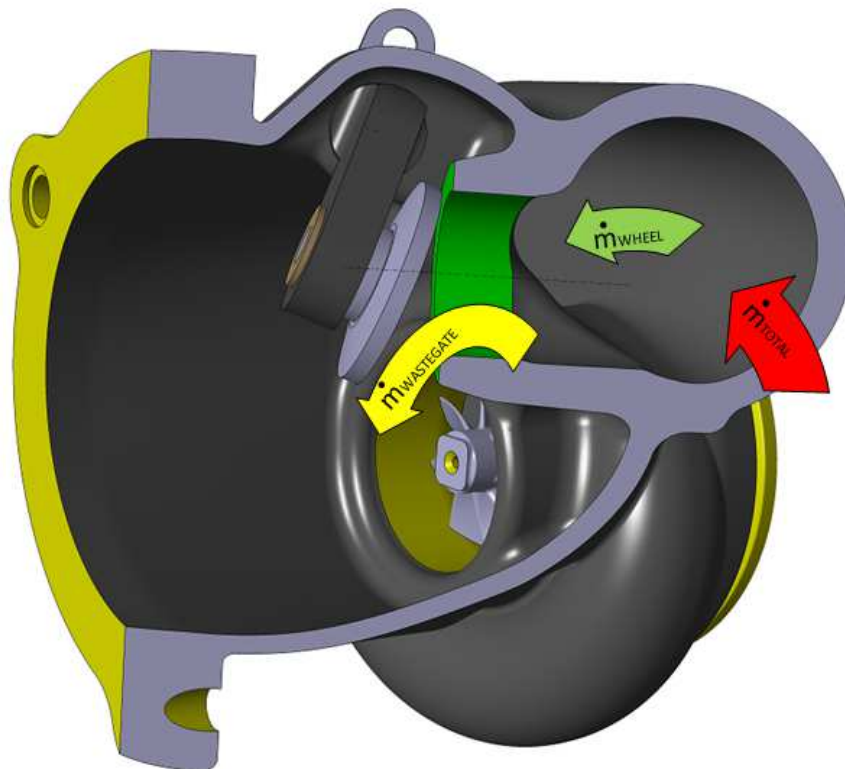


Figure 90 Section view D-D through turbine housing with horizontal bushing axis



### 13.1 RESULTS

Input values are shown in Table 6.

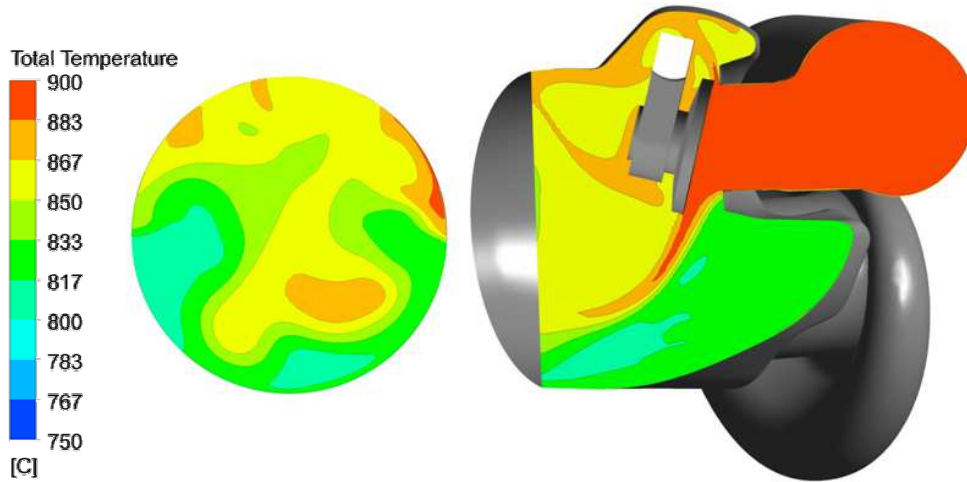


Figure 91 Temperature contours at 15 deg open position (view C and section D-D)

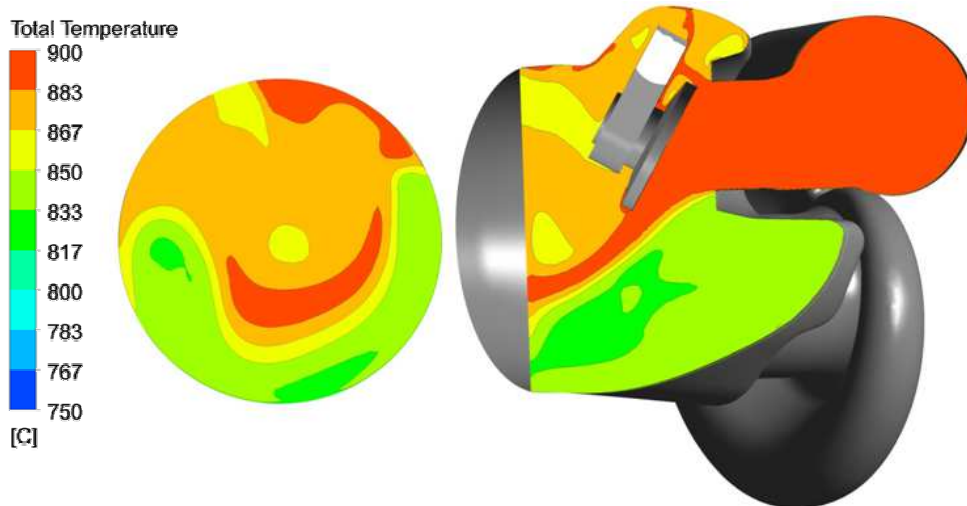


Figure 92 Temperature contours at 30 deg open position (view C and section D-D)

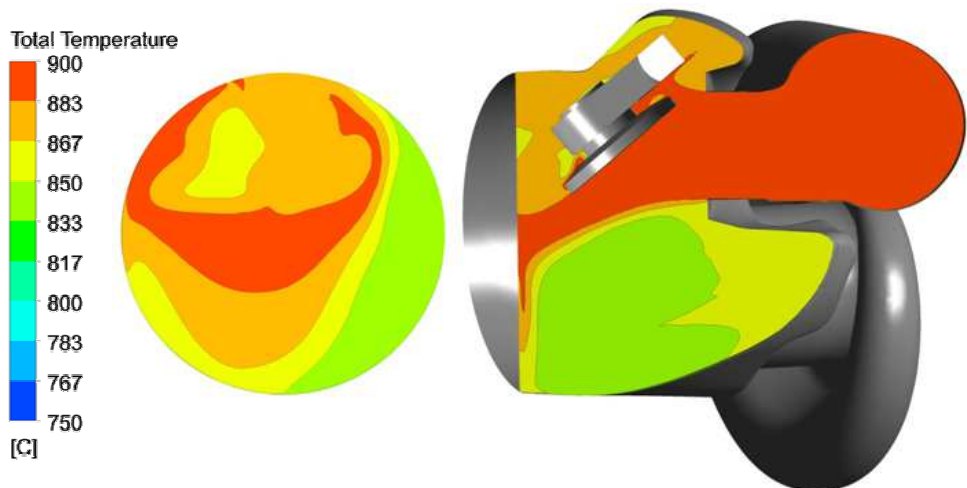


Figure 93 Temperature contours at 50 deg open position (view C and section D-D)

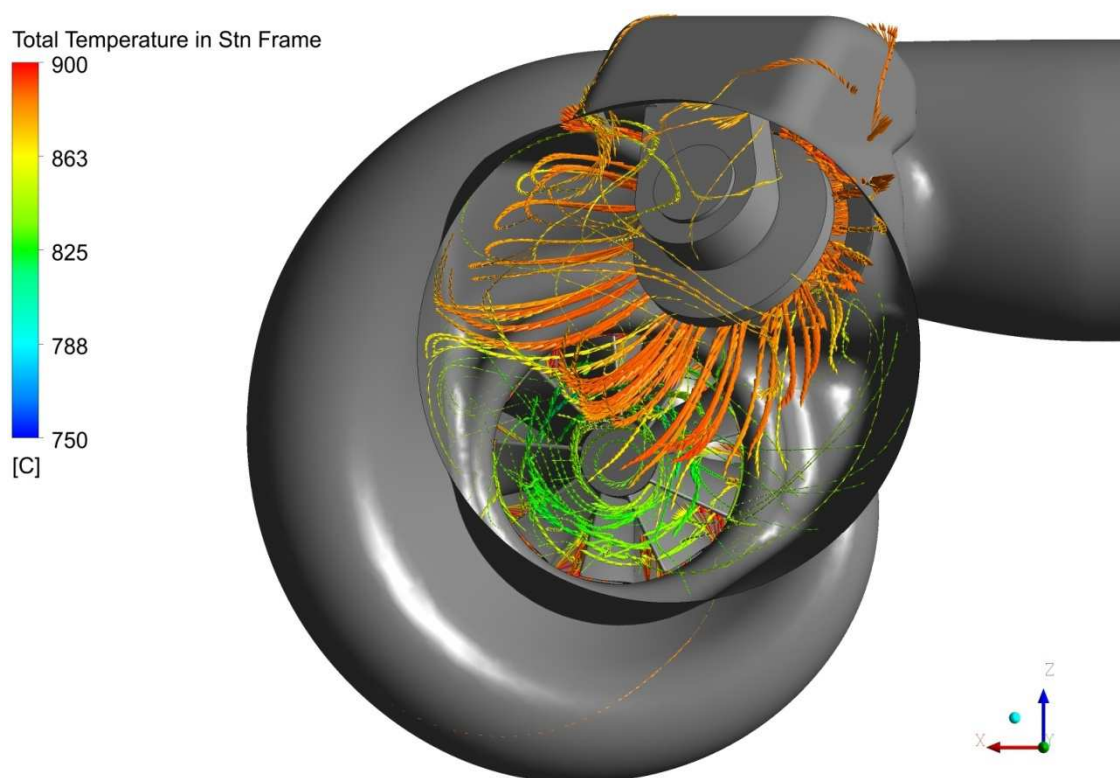


Figure 94 Flow vectors at 30deg open wastegate position

Important values measured in post-processor are shown in Table 8 below. Temperature deviation and performance impact comparison to current design and other designs is evaluated in the end of this thesis.

Table 8 Results summary of design with horizontal bushing axis

WASTEGATE OPEN	[deg]	0	15	30	50
TURBO SPEED	[RPM]	160 000	130 000	100 000	90 000
P1T (TOTAL) AVERAGE	[bar]	1,82968	1,82966	1,82965	1,82964
T1T (TOTAL) AVERAGE	[°C]	879,18	885,11	888,68	889,46
P2T (TOTAL) AVERAGE	[bar]	1,17722	1,3592	1,4545	1,53173
P2T (STATIC) AVERAGE	[bar]	1,15724	1,32669	1,41618	1,47799
T2T (TOTAL) AVERAGE	[°C]	782,49	844,8	862,47	868,31
T2T STANDARD DEVIATION	[°C]	6,11	20,72	19,52	15,41
TOTAL MASS FLOW	[g.s-1]	79,68	121,84	140,22	143,86
MASS FLOW THROUGH WASTEGATE	[g.s-1]	0,00	50,12	72,93	80,20
TOTAL PRESSURE @ TURBINE WHEEL EXDUCER	[bar]	1,21815	1,38654	1,46265	1,50744
% MASS FLOW THROUGHT WASTEGATE	[%]	0,00	41,14	52,01	55,75
EXPANSION RATIO (TOTAL TO STATIC) P1T/P2T	[-]	1,58	1,38	1,29	1,24
EFFICIENCY(TOTAL TO STATIC) $\eta_{T-S}$	[%]	73	42	34	33



## 14 DESIGN 4 (DUCT OUTLET LEANED OUT)

Design 4 has duct outlet leaned out by 50 degrees from its original position in design 1. This causes the gas to flow directly, almost perpendicularly and close to the center of turbine housing outlet when wastegate valve is opened.

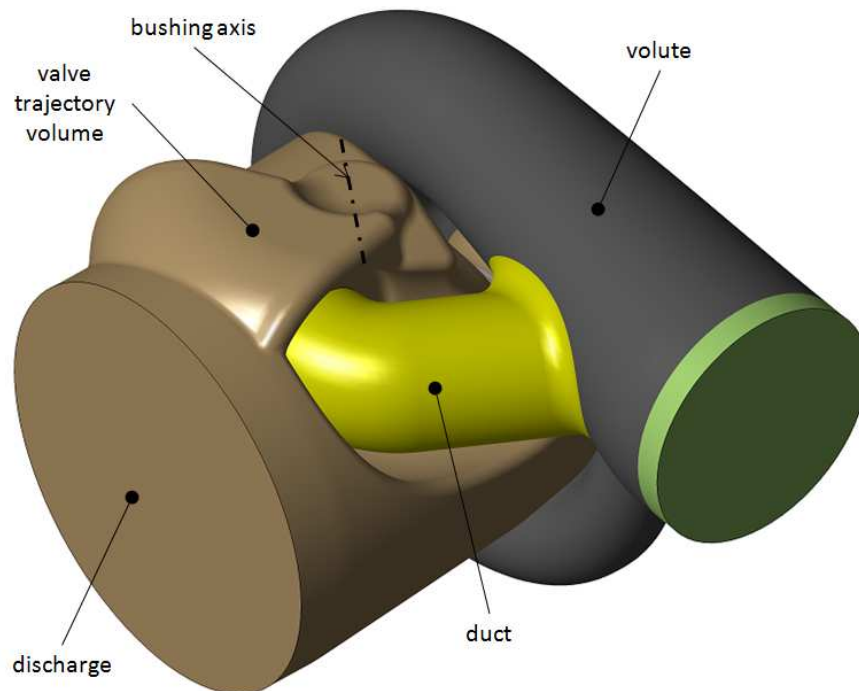


*Figure 95 Core model of design with duct outlet leaned out*

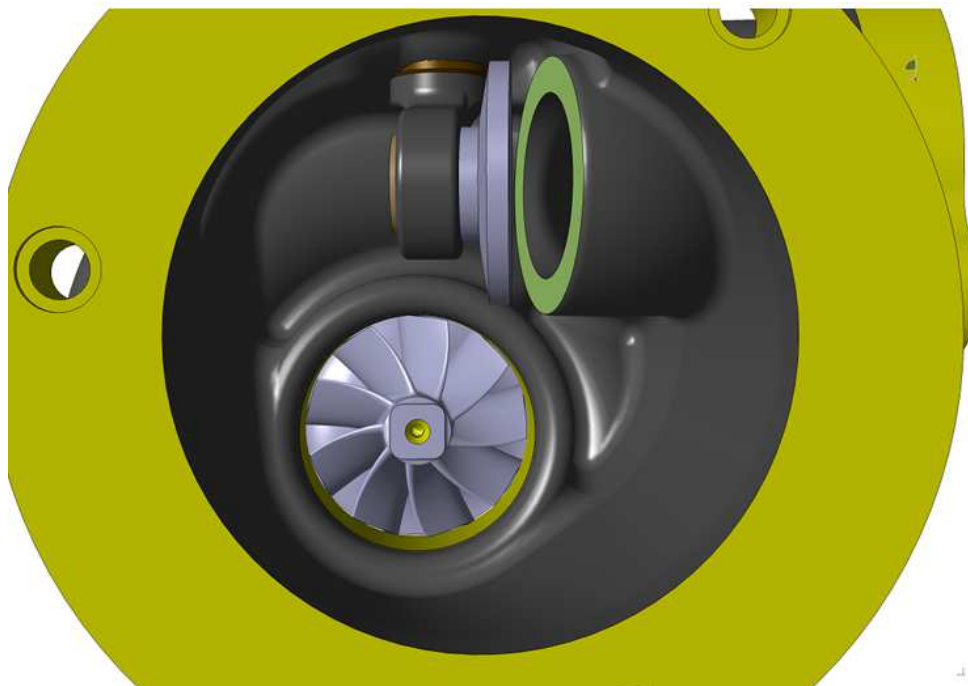


*Figure 96 Discharge design*



Contours of temperature in following results chapter are plotted at turbine housing outlet (view B) and in a section view through wastegate channel (section A-A). See Figure 66 for reference.



Figure 97 Section view (A-A) through wastegate channel

## 14.1 RESULTS

Design 4 has been calculated in four wastegate positions as well as all other previous designs. Input values are shown in Table 6.

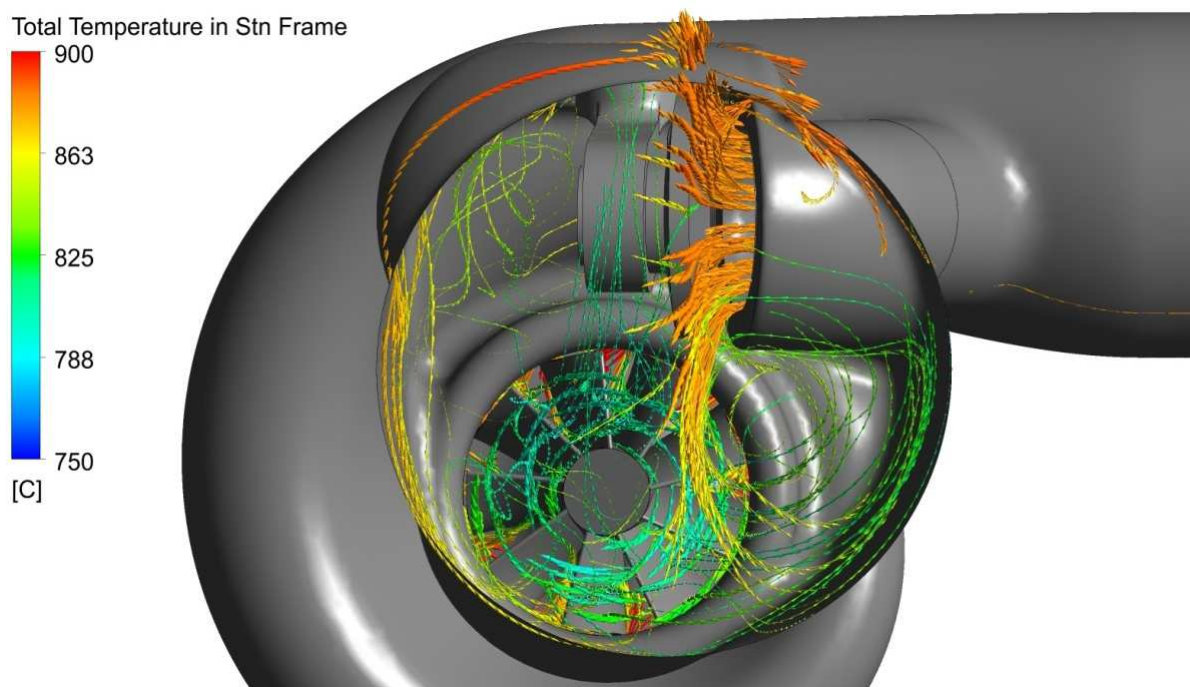


Figure 98 Flow vectors at 15 degrees open position

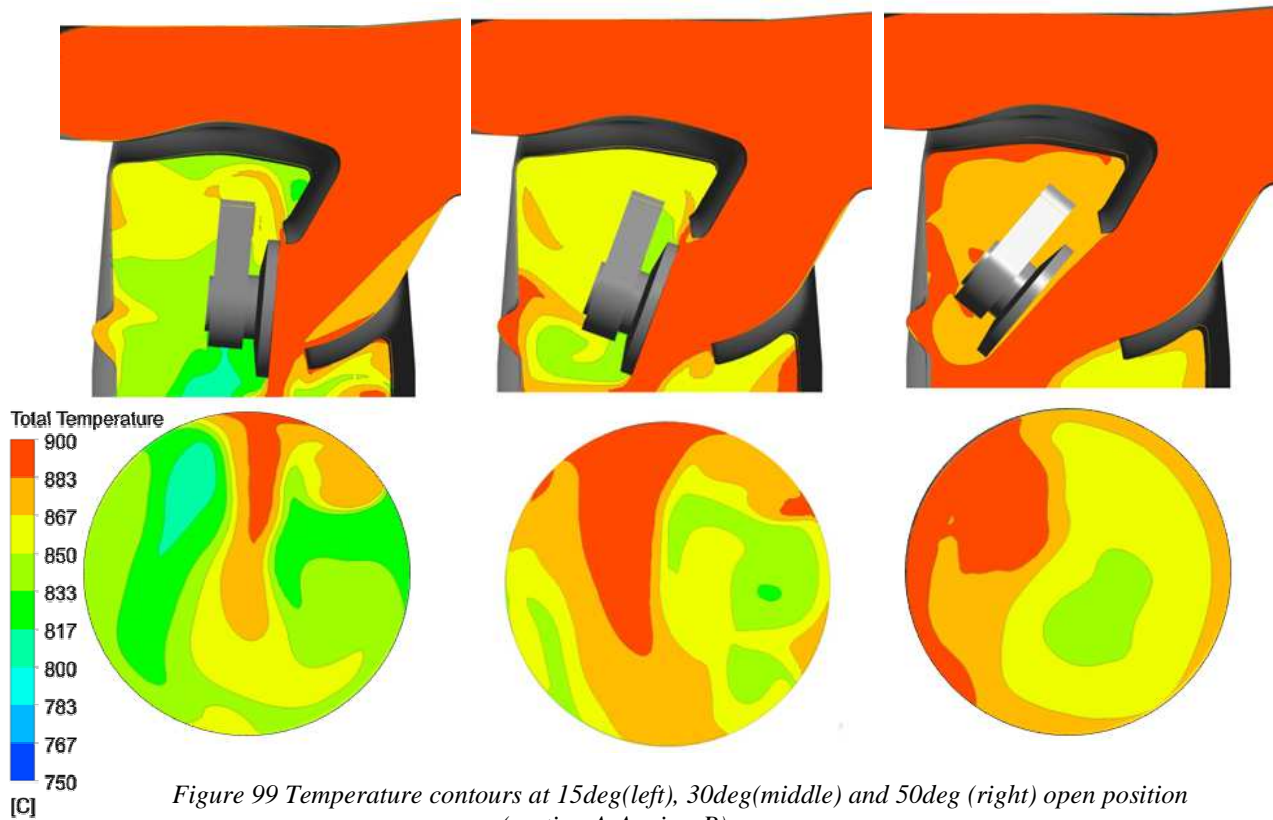


Figure 99 Temperature contours at 15deg(left), 30deg(middle) and 50deg (right) open position (section A-A, view B)

Table 9 Results summary of design with duct outlet leaned out

WASTEGATE OPEN	[deg]	0	15	30	50
TURBO SPEED	[RPM]	160 000	130 000	100 000	90 000
P1T (TOTAL) AVERAGE	[bar]	1,82968	1,82967	1,82965	1,82968
T1T (TOTAL) AVERAGE	[°C]	879,2	885,28	887,46	887,43
P2T (TOTAL) AVERAGE	[bar]	1,20054	1,39926	1,53788	1,55482
P2T (STATIC) AVERAGE	[bar]	1,17707	1,3525	1,46709	1,47295
T2T (TOTAL) AVERAGE	[°C]	781,8	846,71	867,75	869,5
T2T STANDARD DEVIATION	[°C]	6,12	19,43	16,08	14,04
TOTAL MASS FLOW	[g.s-1]	79,93	122,96	134,41	134,28
MASS FLOW THROUGH WASTEGATE	[g.s-1]	0,00	52,02	71,65	73,27
TOTAL PRESSURE @ TURBINE WHEEL EXDUCER	[bar]	1,23226	1,38883	1,51176	1,5344
% MASS FLOW THROUGH WASTEGATE	[%]	0,00	42,31	53,30	54,56
EXPANSION RATIO (TOTAL TO STATIC) P1T/P2T	[-]	1,55	1,35	1,25	1,24
EFFICIENCY(TOTAL TO STATIC) $\eta_{T-s}$	[%]	76	43	30	27



## 15 DESIGN 5 (BUTTERFLY VALVE)

Butterfly valve design uses almost the same turbine housing core as design 1. The only difference is in bushing position and wastegate channel. The axis of bushing intersects with the axis of wastegate channel. These two axes are perpendicular to each other. The butterfly valve is placed to the tail end of the channel. It rotates around bushing axis.

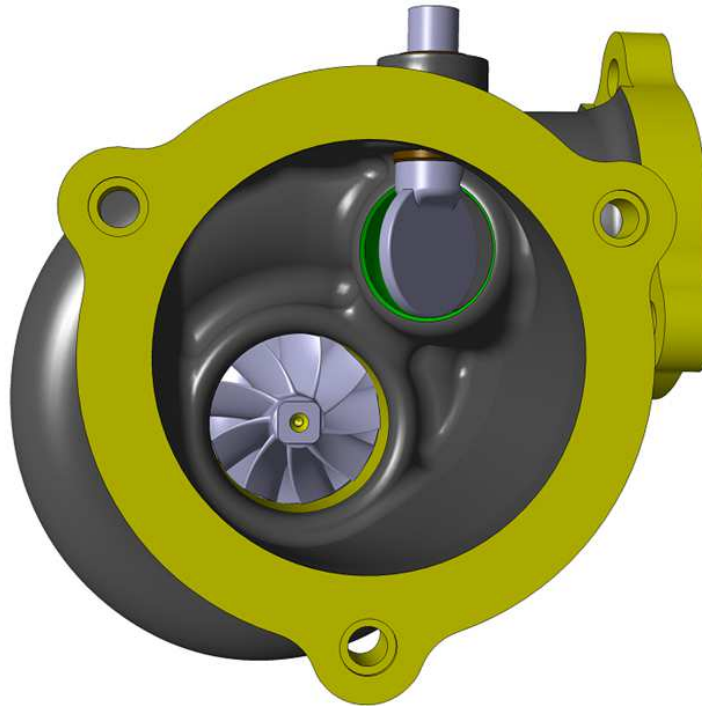


Figure 100 Discharge of butterfly valve design

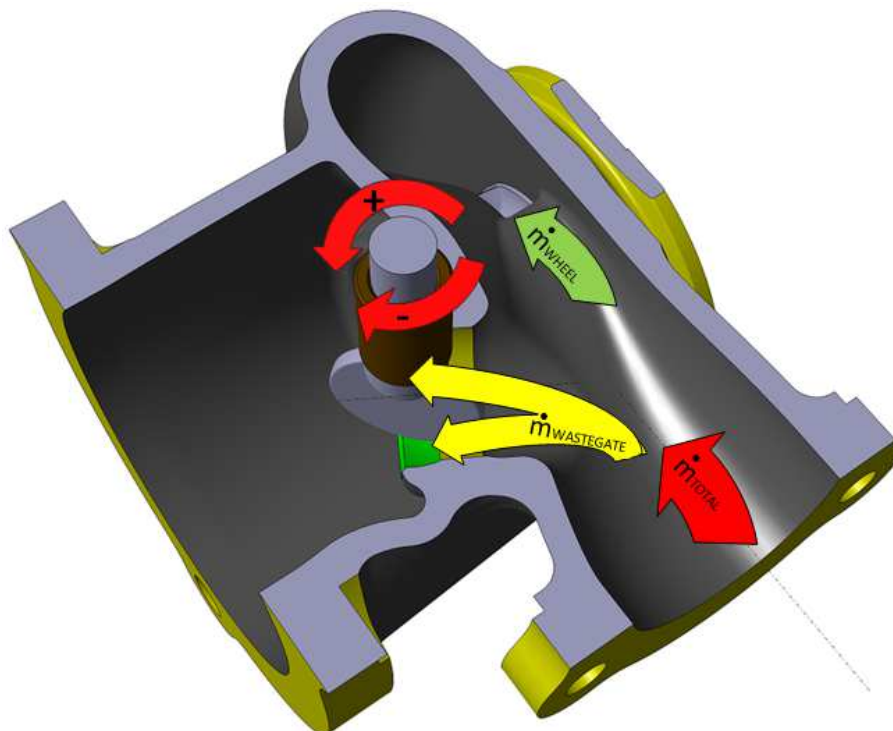


Figure 101 Section view through wastegate channel



### 15.1 RESULTS

Butterfly valve rotates around axis crossing the wastegate channel axis. Therefore, it is possible to open the butterfly valve in two directions (**clockwise** and **anticlockwise**).

**Closed position** has been calculated in order to determinate different discharge design impact on performance. Valve rotation around Z-axis by **45** and **65 degrees** in both positive and negative direction and **fully open** 90 deg position has been calculated as well.

Table 10 Input values for calculation of design 5

		← NEGATIVE ROTATION		CLOSED	POSITIVE ROTATION →		FULLY OPEN
BUTTERFLY OPEN	[deg]	-65	-45	0	45	65	90
INLET PRESSURE P1T	[bar]	1,82970					
INLET TEMPERATURE T1T (STATIC)	[°C]	875					
OUTLET PRESSURE (ATMOSFERIC)	[bar]	1,01325					
QUADRATIC RESISTANCE COEFICIENT Kq	[kg.m-4]	20					
TURBO SPEED	[RPM]	130 000	140 000	160 000	140 000	130 000	90 000

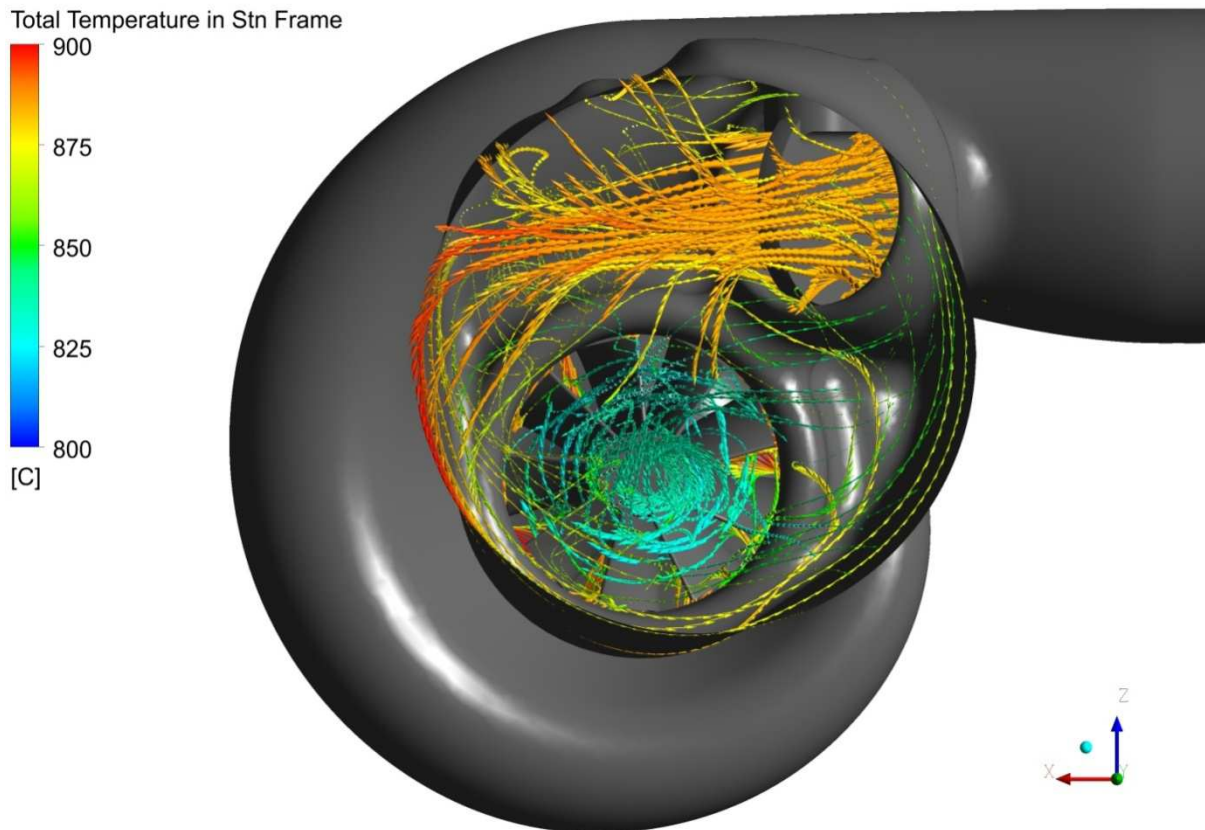
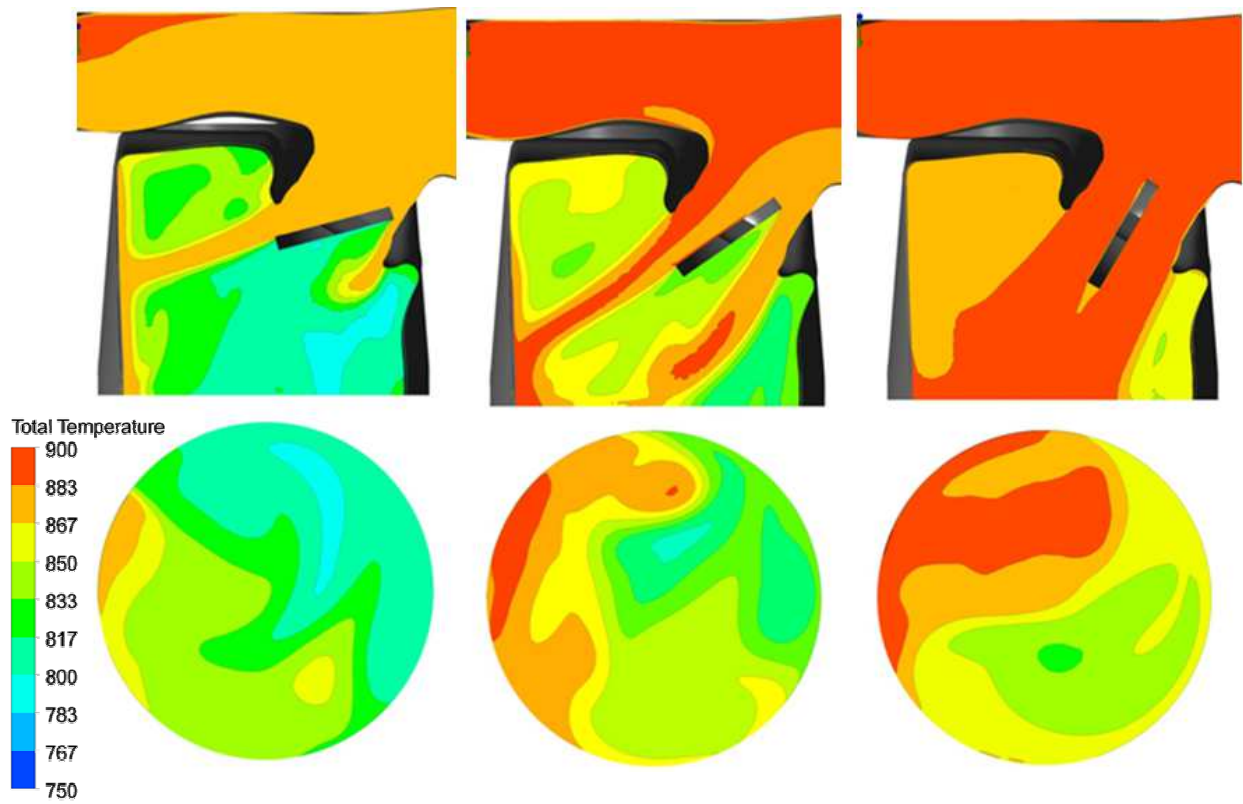
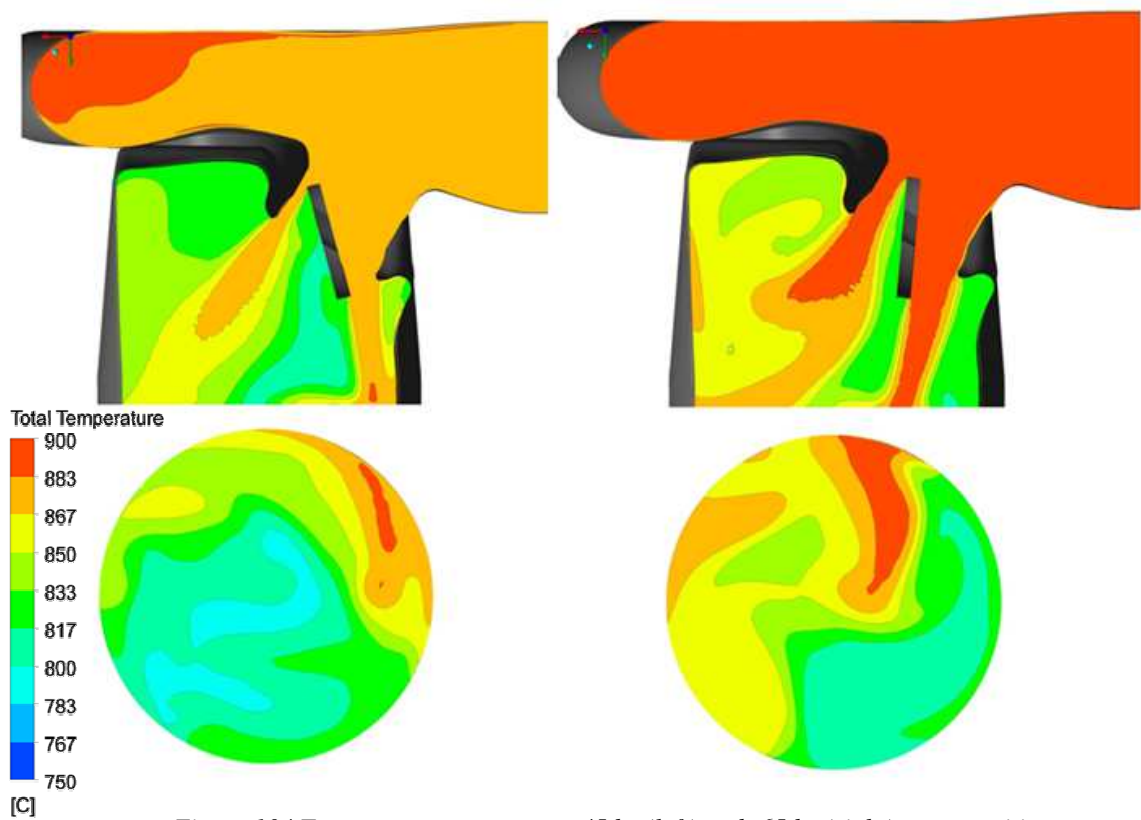


Figure 102 Flow vectors at fully open (90 degrees) position



[C] *Figure 103 Temperature contours at 45deg(left), 65deg(middle) and fully 90deg (right) open position (section A-A, view B)*

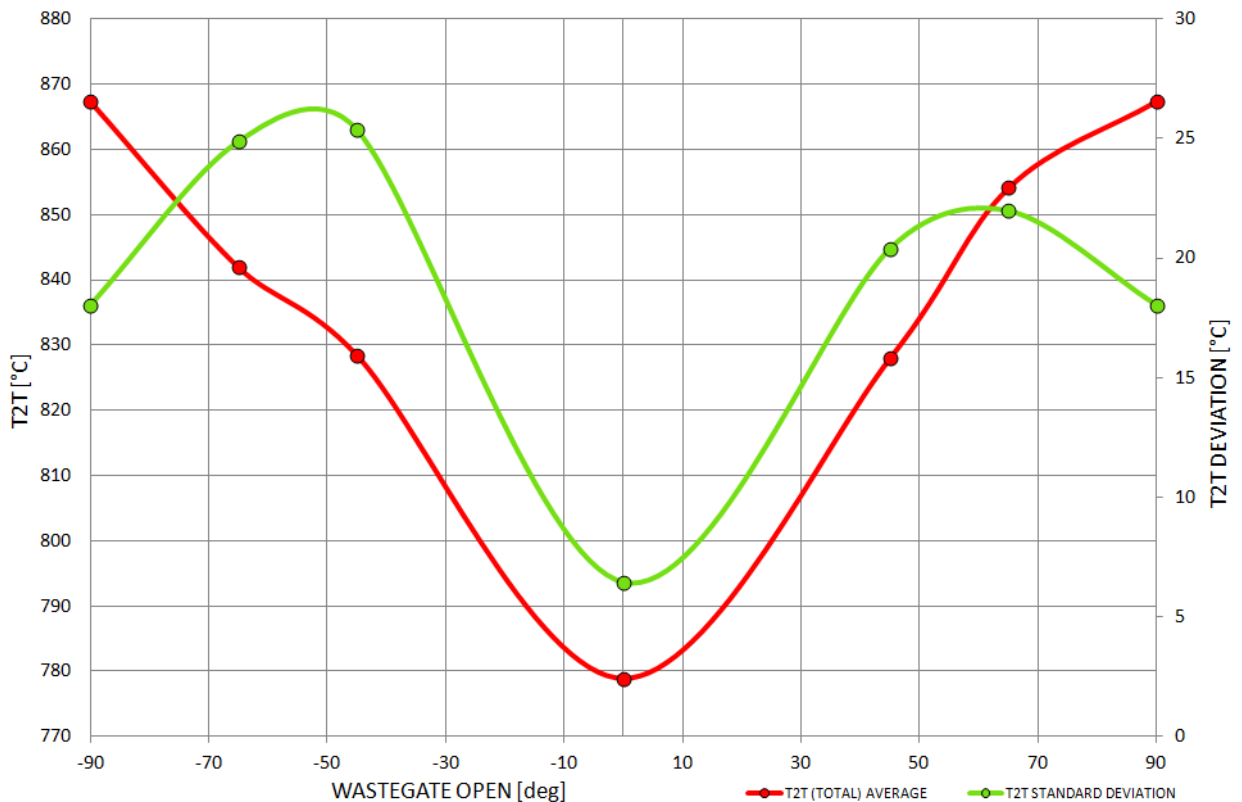


[C] *Figure 104 Temperature contours at -45deg(left) and -65deg(right) open position (section A-A, view B)*



Table 11 Results summary of butterfly valve design

WASTEGATE OPEN	[deg]	-65	-45	0	45	65	90
TURBO SPEED	[RPM]	130000	140000	160000	140000	130000	90000
P1T (TOTAL) AVERAGE	[bar]	1,82966	1,82968	1,82968	1,82967	1,82967	1,82967
T1T (TOTAL) AVERAGE	[°C]	885,94	882,76	879,18	882,49	885,21	887,65
P2T (TOTAL) AVERAGE	[bar]	1,38921	1,3296	1,1853	1,32638	1,43822	1,53974
P2T (STATIC) AVERAGE	[bar]	1,34891	1,29203	1,16593	1,291	1,38059	1,46912
T2T (TOTAL) AVERAGE	[°C]	841,93	828,43	778,81	827,96	854,11	867,39
T2T STANDARD DEVIATION	[°C]	24,87	25,37	6,44	20,4	21,97	18,02
TOTAL MASS FLOW	[g.s-1]	126,434	107,531	79,696	105,701	122,423	135,283
MASS FLOW THROUGH	[g.s-1]	54,1872	32,4853	0	32,5248	53,5792	68,4531
TOTAL PRESSURE @ TURBINE WHEEL EXDUCER	[bar]	1,37489	1,33527	1,2193	1,35014	1,41917	1,47666
% MASS FLOW THROUGH WASTEGATE	[%]	42,86	30,21	0,00	30,77	43,77	50,60
EXPANSION RATIO (TOTAL TO STATIC) P1T/P2T	[-]	1,36	1,42	1,57	1,42	1,33	1,25
EFFICIENCY(TOTAL TO STATIC) $\eta_{T-S}$	[%]	49	53	77	53	37	31



Graph 20 Average temperature and temperature deviation at turbine housing outlet



On Graph 20 we can see that negative opening angles cause very uneven temperature distribution with standard deviation of temperatures higher than 25°C, which is as high as in opened wastegate valve of current design 1. This is because exhaust gas flows along discharge wall. That means opening of butterfly valve in negative direction would not have positive effect to temperature distribution.

On the other hand, positive opening direction of butterfly valve has obviously better temperature distribution at turbine housing outlet. The best temperature distribution is achieved at fully open (90deg) butterfly valve position.

Negative direction of butterfly valve opening will not be included in the results comparison the end of this thesis, because it does not give positive results which would have chance to improve temperature distribution at turbine housing outlet.



## 16 RESULTS SUMMARY & CONCLUSION

Resulting values of every single design at different wastegate valve positions are clearly shown at Table 5, 7, 8, 9 and 11.

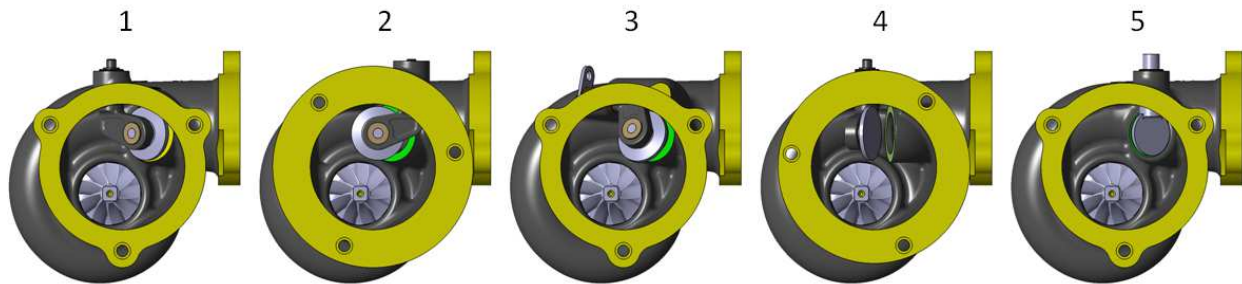
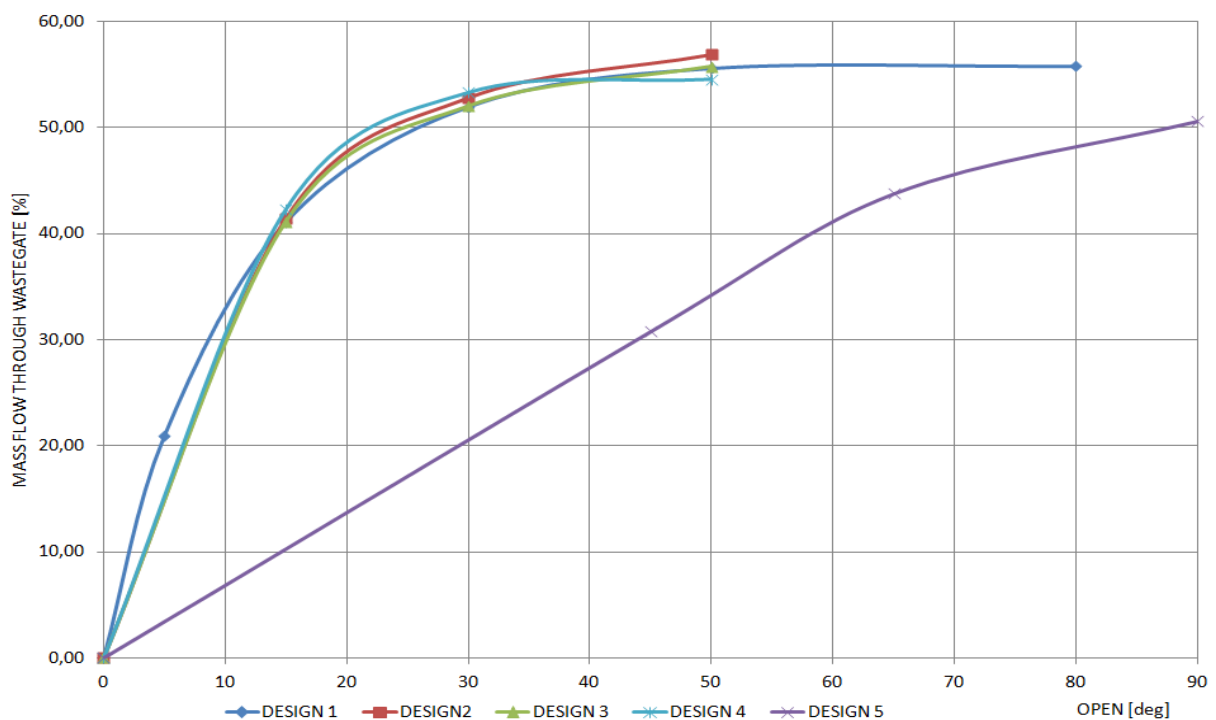


Figure 105 Five designs of turbine housing discharge and wastegate valve

On Graph 21 we can see the mass flow percentage at different wastegate openings in designs 1, 2, 3 and 4 has almost the same character. It rises up quickly and then stagnates with opening angles higher than 30degrees.

The **butterfly valve** (design 5) has different mass flow percentage characteristic. It climbs up gradually, which means the wastegate regulation is much smoother and allows very **precise control of flow** through wastegate channel.

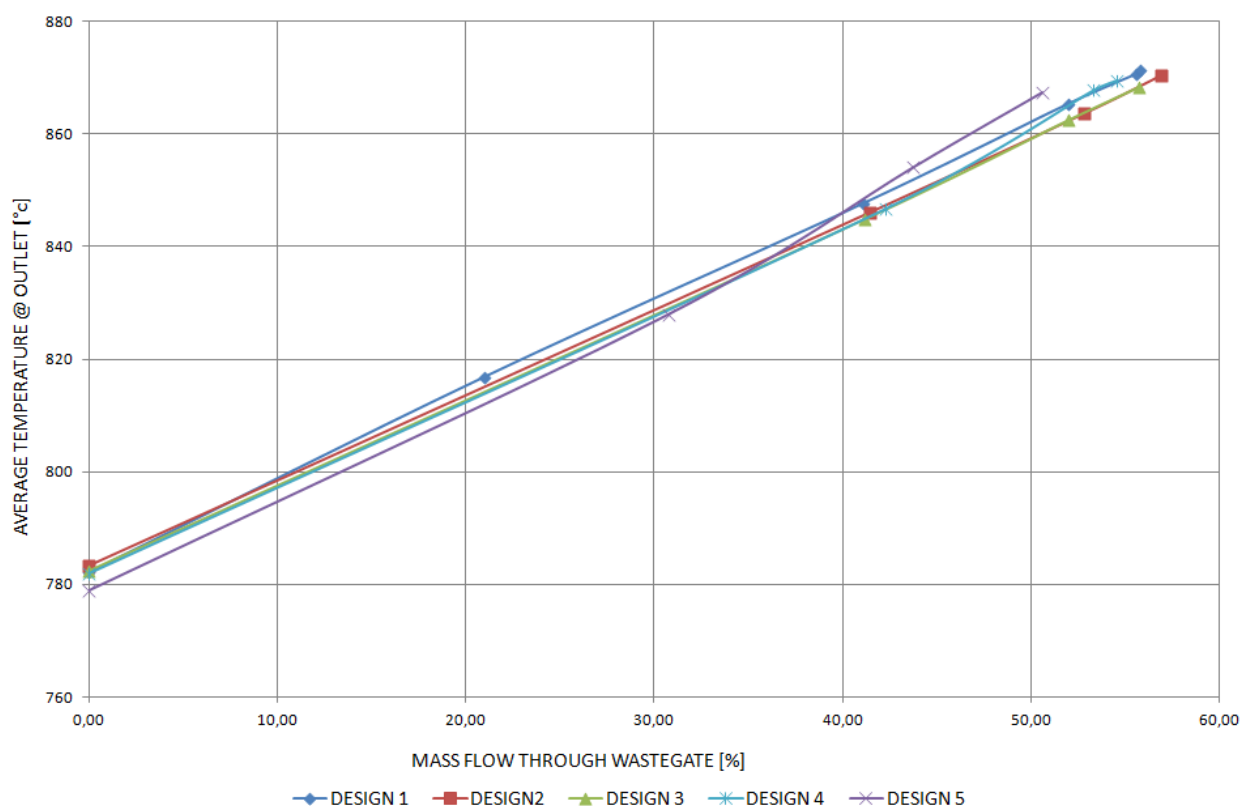
Torque created by aerodynamic forces applied to butterfly valve is expected to be lower than torque applied to classic swing type wastegate valve (designs 1, 2, 3 and 4). This would allow to shorten crank (lever), controlling the valve motion, and thus allows to obtain high rotation angles with currently used actuator. Rotary electric actuator (REA) may be used as well for control of butterfly valve. Further investigations of forces and torques applied to butterfly valve at different opening angles should be done in order to confirm this hypothesis.



Graph 21 Mass flow percentage at different opening angles



In order to evaluate results of all calculated designs and compare characteristic values of temperature field at turbine housing outlet the values in Graph 22, 23 and 24 are lined up by **mass flow percentage** (horizontal axis). Mass flow percentage through wastegate valve characterizes the operating point of turbine regulation.

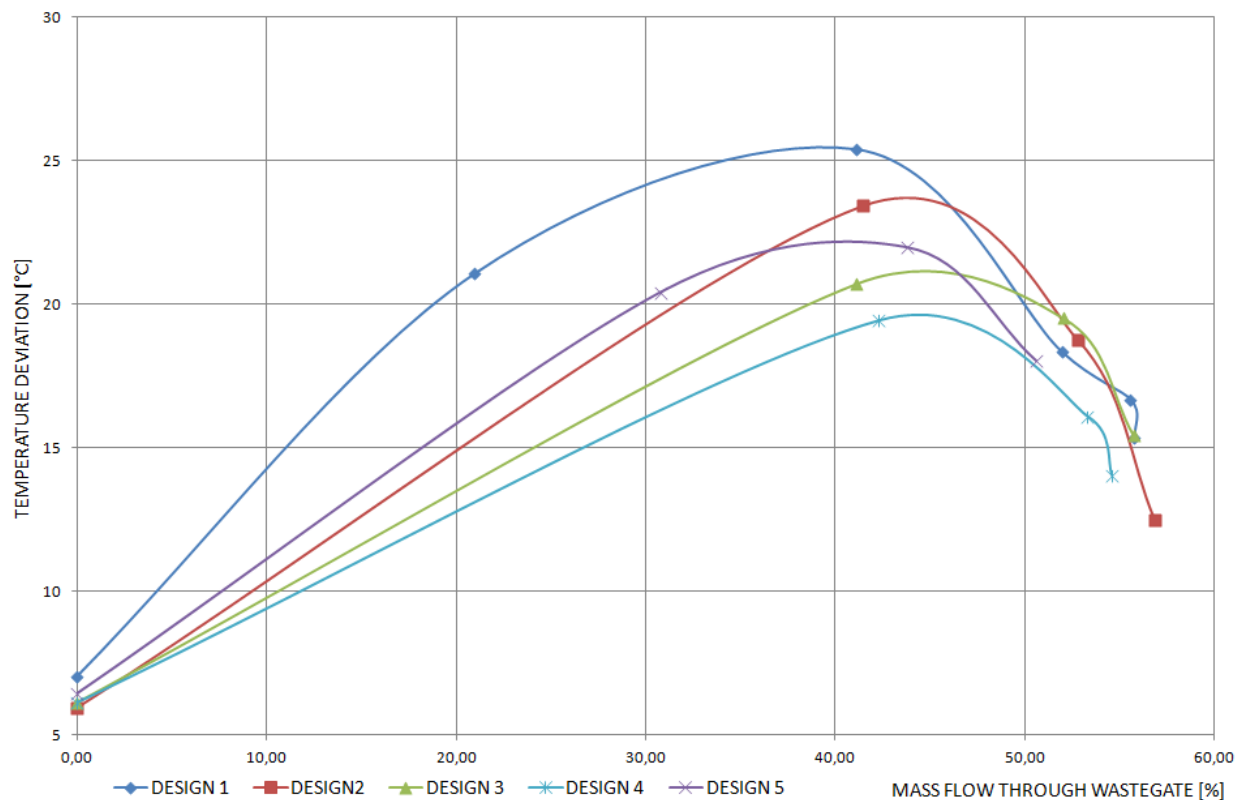


Graph 22 Average temperature T2T at turbine housing outlet

On Graph 22 above, we can see the average T2T temperature at turbine housing outlet is linearly dependent on mass flow percentage through wastegate valve. Higher mass flow through wastegate channel means higher outlet temperature. In other words, more mass through wastegate channel causes mass flow through turbine wheel to decrease and therefore less hot gasses expands and cools down.

We can see the values of average outlet temperature are almost the same in all designs. On the other hand, the **temperature distribution differs** which is noticeable at the temperature fields of calculated wastegate positions in different designs.

To judge on the scale of improvement the **standard deviation of temperature** at turbine housing outlet has been calculated. This value tells us how much the temperature at outlet differs. The lower deviation means better temperature distribution. Comparison of calculated designs at different wastegate positions is shown on Graph 23.



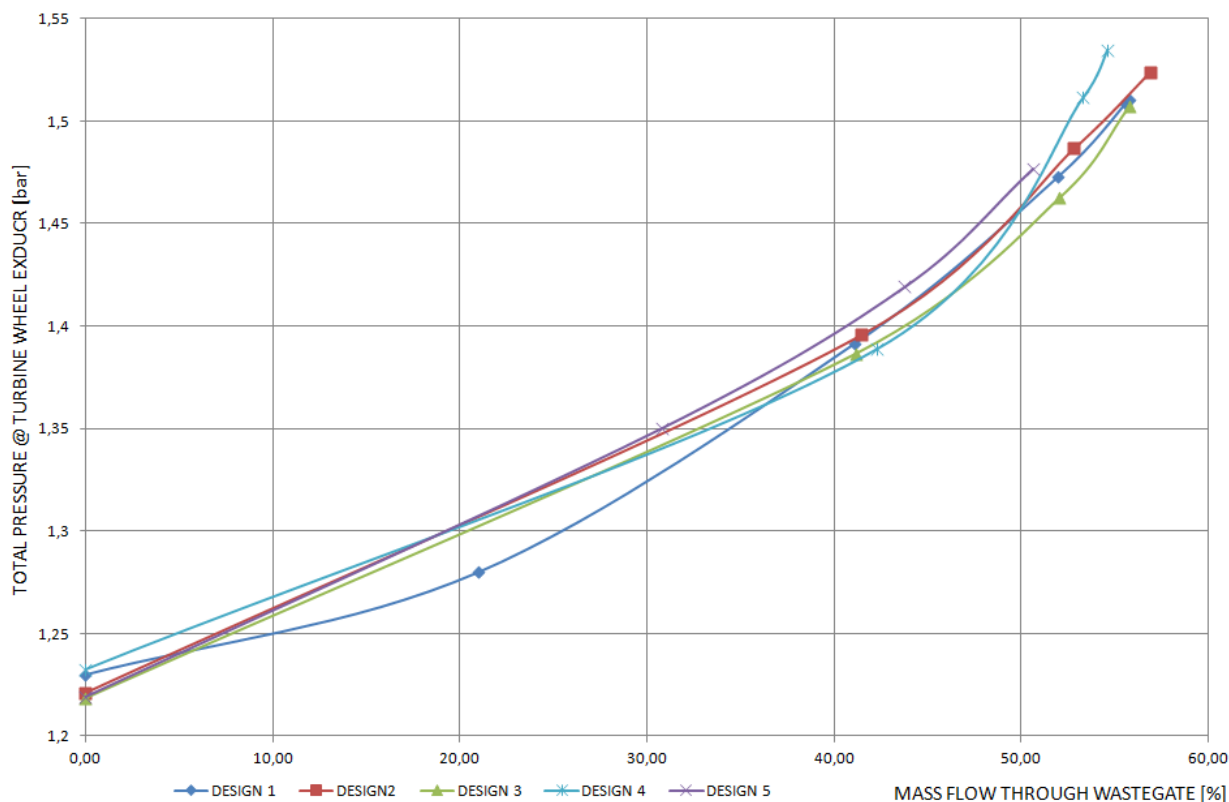
Graph 23 Standard deviation of temperatures at turbine housing outlet

We can see the deviation of temperatures at around 42% mass flow through wastegate is the highest in a case of current design 1. **All others calculated designs have more even temperature distribution at this point of regulation which is very significant result.** Currently used actuator is able to open the wastegate up to 15degrees openings in which around 40% of mass flows through wastegate channel. That means, with the use of classical actuator we can get more even temperature distribution at turbine outlet and thus **reduce close-coupled catalytic converter light off time and emissions at cold start conditions.** At higher opening angles, which could be obtained with high stroke actuator or special mechanism, the improvement is not very obvious.

The **design 4** with duct outlet leaned out looks like the **best solution** of the temperature distribution problem in a **whole range** of wastegate openings.

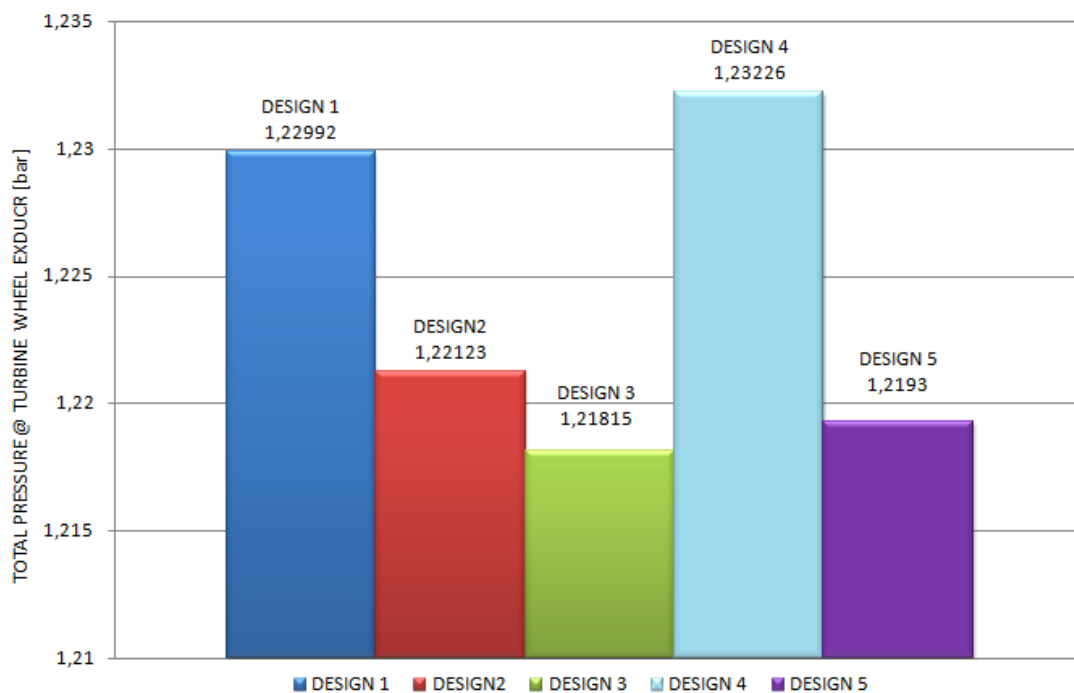
Another important impact of design changes is the **backpressure** crated to turbine wheel. Therefore, total pressure at turbine wheel exducer has been measured. The higher pressure at exducer means the pressure gradient (expansion ratio) within the wheel is lower and therefore output power goes down. This is very important especially in closed wastegate position, in which we require the best performance.

On Graph 24 we can see how the pressure at turbine wheel exducer rises up with opening of wastegate valve. It is around 1.23 bar when wastegate valve is closed and gradually rise up to pressures of 1.5 bars. This is caused by wastegate opening and the flow in discharge domain. The gasses flowing out of wastegate clog the discharge volume. That is the reason why pressure rise up with higher mass flow percentage through wastegate channel.



Graph 24 Backpressure created to turbine wheel

We can see the pressures in different designs have similar values in whole regulation range. However, only a small difference of pressure at turbine wheel exducer causes expansion ratio to change and therefore **influence the power output**. For this reason, we are concerned with the pressure impact especially at **closed wastegate**. Bar Graph 25 shows the total pressure at turbine wheel exducer at closed wastegate valve.



Graph 25 Backpressure at turbine wheel at closed wastegate position



We can see the design 4 with duct outlet leaned out creates the highest backpressure to the wheel. It is because the wastegate channel, arm and valve stand in a way of gasses flowing out of the wheel. This would have **negative impact to the performance**.

Designs 2, 3 and 5 creates lower backpressure compared to current design 1. This would lead to better performance at closed wastegate position.

Design 4 with duct outlet leaned out, which on the one hand has the best temperature distribution has on the other hand negative impact to the performance.

Good **compromise** seems to be the design 3 with horizontal bushing axis, which still has very good temperature distribution at openings covered by currently used actuator and has positive impact to the performance.

The design 5 with butterfly valve looks like a very good solution as well. It decreases the deviation of temperatures at outlet, has positive impact to the performance and moreover allows smooth regulation characteristics. The assembly process would need to be verified and impermeability at closed position could be a problem of very precise tolerances, materials and thermal expansivity.

This thesis has proved the temperature distribution at turbine housing outlet could be improved in a number of ways. The main reason why to do that is to lower exhaust gas emissions at cold start conditions in a close-coupled catalytic converter, which is mounted directly to turbine housing outlet flange in many gasoline applications nowadays. For this reason, interaction of turbine housing and catalyst in a way of exhaust gas flow is very important and plays vital role in light-off time and emission reduction. Better temperature distribution at catalytic converter inlet surface could improve the chemical reaction efficiency and help to meet EURO VI emissions standard awaited in 2014.

The results from this thesis had also shown the impact on turbocharger performance. Different discharge design, wastegate valve & arm position and wastegate channel design influence the pressure at turbine wheel exducer. This backpressure needs to be monitored especially at closed wastegate position, in which the best performance is vital.

Improvement to the temperature distribution does not necessarily mean the success. Performance impact has to be considered as well and certain compromises need to be kept in mind.

The thesis has revealed how does the flow in turbine housing looks like in different discharge designs and at different wastegate openings. The results also indicate the scale of improvement, which could be obtained with the design change. It has given a first overview to the solution of temperature distribution problem of current turbine housing design.

The aim of the thesis has not been to study problems connected with casting production, assembly process of wastegate components into the turbine housing, impact to the thermal and mechanical loads resistance and price of the production. All of these would need to be considered before next development steps, production and application to the gasoline engine. Further investigation of temperature fields and performance impact at different wastegate openings in more opening angles of wastegate should be done before next development steps as well.



## 17 BIBLIOGRAPHY

- [1] ACEA European Automobile Manufacturers' association, EU Economic report, July 2011, [online], [cit. 2011-12-10], URL: <[http://www.acea.be/images/uploads/files/20110927\\_ER\\_1105\\_2011\\_I\\_Q4.pdf](http://www.acea.be/images/uploads/files/20110927_ER_1105_2011_I_Q4.pdf)>
- [2] Richard J. Osborne, Ricardo, Future gasoline powertrain vision, Sep. 2007, [cit. 2011-12-10], Honeywell internal trainings
- [3] UKIP media events, International engine of the year awards, winners of the year 2011, [online], [cit. 2011-12-10], URL: <[http://www.ukipme.com/engineoftheyear/winners\\_11/14\\_18.html](http://www.ukipme.com/engineoftheyear/winners_11/14_18.html)>
- [4] Motortorque.com, Ford showcases new EcoBoost engines, Feb. 2010, [online], [cit. 2011-12-10], URL: <<http://www.motortorque.com/car-news/ford-showcases-new-ecoboost-engines-in-new-s-max-galaxy-11474.aspx>>
- [5] BMWblog.com, BMW confirms the new N20 four-cylinder engine will be used in 1 and 3 Series models, Feb.2011, [online], [cit. 2011-12-08], URL: <<http://www.bmwblog.com/2011/02/18/bmw-confirms-the-new-n20-four-cylinder-engine-will-be-used-in-1-and-3-series-models/>>
- [6] Honeywell Turbo Technologies, Turbo Fundamentals, Dec.2011, [online], [cit. 2011-12-10], URL: <<http://turbo.honeywell.com/turbo-basics/turbo-fundamentals/>>
- [7] Custom-car.us, Basic Engine Power, [online], [cit. 2011-12-10], URL: <<http://www.custom-car.us/basics/power-basics.aspx>>
- [8] HOFMANN, K. Turbodmychadla, vozidlové turbíny a ventilátory: Přepřňování spalovacích motorů. 2. vyd. VUT Brno : SNTL, 1985. 134 s.
- [9] Wikipedia, Turbocharger, [online], [cit. 2011-12-11], URL: <<http://en.wikipedia.org/wiki/Turbocharger>>
- [10] Brian Horner, Turbochargers overview, Feb.2005, [cit. 2011-11-25], Honeywell internal trainings
- [11] Honeywell, Ricardo, Diesel engine technology, [cit. 21011-11-25], Honeywell internal trainings
- [12] BARTONÍČEK, L. Přepřňování pístových spalovacích motorů. [online]. Studijní opory, Technická univerzita v Liberci, 2004, 76 s. [cit. 2011-01-12]. URL: <<http://www.ksd.tul.cz/studenti/texty/PZP-preplnovani-PSM.pdf>>.
- [13] Custom-car.us, Turbochargers, [online], [cit. 2011-12-10], URL: <<http://www.custom-car.us/turbo/default.aspx>>
- [14] Brian Horner, Turbochargers materials, Feb.2005, [cit. 2011-11-25], Honeywell internal trainings



- [15] Dipl.-Ing. V. Simon, Dipl.-Ing. G. Oberholz, Dr.-Ing. M. Mayer, Borg Warner Turbo Systems, Exhaust gas temperature, an engineering challenge, Sept.2000, [online], [cit. 2011-12-20], URL: <<http://www.3k-warner.de/tools/download.aspx?t=document&r=105&d=327>>
- [16] Trevor Cass, Honeywell, Basic turbocharging, Sept.2006, [cit. 2011-11-25], Honeywell internal trainings
- [17] Ondrej Kloupař, Honeywell, Casting training, April 2008, [cit. 2011-11-25], Honeywell internal trainings
- [18] Bill Connor, Fundamentals of turbocharger aerodynamics, Turbines, Honeywell, [cit. 2011-11-25], Honeywell internal trainings
- [19] Zvyšování výkonu, Turbodmyhadla. [online]. Studijní opory, VUT FSI Brno. [cit. 2011-12-20], URL: <[http://www.iae.fme.vutbr.cz/opory/prislusenstvi/prisl\\_prez\\_2007/zvys\\_vykonu\\_turbodmyhadla.ppt](http://www.iae.fme.vutbr.cz/opory/prislusenstvi/prisl_prez_2007/zvys_vykonu_turbodmyhadla.ppt)>
- [20] T.K. Garrett, K. Newton, W. Steeds, The Motor Vehicle, Thirteenth Edition, ISBN 07506 44494, 2001, 1188 pgs., Oxford
- [21] epi-eng.com, Turbochargers, [online], [cit. 2011-12-10], URL: <[http://www.epi-eng.com/piston\\_engine\\_technology/turbocharger\\_technology.htm](http://www.epi-eng.com/piston_engine_technology/turbocharger_technology.htm)>
- [22] Borg Warner Turbo Systems, Variable turbine geometry (VTG), [online], [cit. 2011-12-10], URL: <<http://www.3k-warner.de/products/vtg.aspx>>
- [23] Trevor Cass, Honeywell, Wastegates, Feb 2006, [cit. 2011-11-25], Honeywell internal trainings
- [24] autospeed.com, BMW's Twin Turbo Diesel, June 2005, [online], [cit. 2011-12-10], URL: <[http://autospeed.com/cms/title\\_BMWs-Twin-Turbo-Diesel/A\\_2544/article.html](http://autospeed.com/cms/title_BMWs-Twin-Turbo-Diesel/A_2544/article.html)>
- [25] Borg Warner Turbo Systems, Regulated 2-stage turbocharging, [online], [cit. 2011-12-10], URL: <<http://www.turbos.bwauto.com/products/r2s.aspx>>
- [26] aeristech.co.uk, Breakthrough Turbocharging Technology, [online], [cit. 2011-12-10], URL: <<http://www.aeristech.co.uk/technology---how-does-it-work>>
- [27] Brian Horner, Honeywell, July 2001, Turbocharger design and application, [cit. 2011-11-25], Honeywell internal trainings
- [28] wcengineering, com, Diesel vs. gasoline turbo design, [online], [cit. 2011-12-10], URL: <<http://www.wcengineering.com/articles/dieselturbo.html>>
- [29] Ing. Jaroslav Rauscher, CSc., SPALOVACÍ MOTORY, STUDIJNÍ OPORY, VUT Brno, [cit. 2011-12-19], URL: <<http://www.iae.fme.vutbr.cz/opory/Spalovaci.motory.2005.pdf>>
- [30] Richard. J. Osborne, Ricardo, Gasoline engine technology basics, Sept. 2007, [cit. 2011-12-10], Honeywell internal trainings



- [31] Úprava spalin, [online]. Studijní opory, VUT FSI Brno, [cit. 2011-12-20], URL: <[http://www.iae.fme.vutbr.cz/opory/prislusenstvi/prisl\\_prez\\_2007/uprava\\_spalin.ppt](http://www.iae.fme.vutbr.cz/opory/prislusenstvi/prisl_prez_2007/uprava_spalin.ppt)>
- [32] H. Santos, M. Costa, Evaluation of the conversion efficiency of ceramic and metallic three way catalytic converters, Oct 2006, Technical University of Lisbon, Lisbon, Portugal, [online], [cit. 2011-12-20], available at ScienceDirect.com, URL: <http://www.sciencedirect.com/science/article/pii/S0196890407001665>
- [33] Wikipedia.com, catalytic converter, [online], [cit. 2011-12-11], URL: <[http://en.wikipedia.org/wiki/Catalytic\\_converter](http://en.wikipedia.org/wiki/Catalytic_converter)>
- [34] Shahrin Hisham Amirnordin, Pressure Drop Prediction of Square-cell Honeycomb Monolith Structure, 2011 International Conference on Environment Science and Engineering, Automotive Research Group, Faculty of Mechanical and Manufacturing Engineering, Universiti Tun Hussein Onn Malaysia, [online], [cit. 2011-12-11], URL: <[http://eprints.uthm.edu.my/1657/1/Shahrin\\_Hisham\\_FKMP\\_\(ICESE2011\).pdf](http://eprints.uthm.edu.my/1657/1/Shahrin_Hisham_FKMP_(ICESE2011).pdf)>
- [35] ANSYS, CFX-5 Solver Modeling, ANSYS Canada Ltd., Waterloo, Ontario Canada, ANSYS help, URL: <<http://www.ansys.com/cfx>>
- [36] ANSYS, Flow through porous media, introduction to CFX, ANSYS tutorial, URL: <<http://www.ansys.com/cfx>>
- [37] Lester Berriman, Diverter for catalytic converter, Irvine, CA (US), Jun 2004, US patent, Patent no: US 6,745,562 B2, [online], [cit. 2011-12-11], URL: <<http://www.google.com/patents?id=Z2UQAAAAEBAJ&printsec=abstract&zoom=4#v=onepage&q&f=false>>
- [38] KOUSAL, Milan. Spalovací turbíny, 1980. 2. vydání, přepracované. Praha: Nakladatelství technické literatury
- [39] Wikipedia.com, Computational fluid dynamics, [online], [cit. 2011-12-11], URL: <[http://en.wikipedia.org/wiki/Computational\\_fluid\\_dynamics](http://en.wikipedia.org/wiki/Computational_fluid_dynamics)>
- [40] ANSYS, Fluid Dynamic Solutions, [online], [cit. 2011-12-11], URL: <<http://www.ansys.com/Products/Simulation+Technology/Fluid+Dynamics>>
- [41] prweb.com, Jaguar Land Rover Achieves Goal of Sophisticated Engineering with Exa PowerFLOW 4.1, [online], [cit. 2011-12-11], URL: <<http://www.prweb.com/releases/cfd/simulation/prweb1891174.htm>>
- [42] centaursoft.com, Mesh element types, [online], [cit. 2011-12-11], URL: <<https://www.centaursoft.com/mesh-element-types>>
- [43] wikipedia.com, Standard deviation, [online], [cit. 2011-12-11], URL: <[http://en.wikipedia.org/wiki/Standard\\_deviation](http://en.wikipedia.org/wiki/Standard_deviation)>
- [44] accessscience.com, boundary layer flow, [online], [cit. 2011-12-11], URL: <http://accessscience.com/content/Boundary-layer%20flow/092500>



## 18 NOMENCLATURE

BMEP	[Pa]	- brake mean effective pressure applied to piston
V	[m <sup>3</sup> ]	- volume of one cylinder
n	[s <sup>-1</sup> ]	- engine rotational speed
i	[-]	- number of cylinders
$\tau$	[-]	- cycle coefficient, $\tau = 2$ for four stroke; $\tau = 1$ for two stroke engine
P	[W]	-engine power output
H <sub>C</sub>	[J.kg <sup>-1</sup> ]	- heat of combustion
AFR <sub>stoich</sub>	[-]	- air - fuel ratio
$\lambda$	[-]	- lambda
$\rho$	[kg.m <sup>-3</sup> ]	- air density
$\eta_v$	[-]	- volumetric efficiency
$\eta_i$	[-]	- indicated efficiency
$\eta_m$	[-]	- mechanical efficiency
p	[Pa]	- boost intake air pressure
r	[J.kg <sup>-1</sup> .K <sup>-1</sup> ]	- specific gas constant, for dry air $r = 287.058 \text{ J.kg}^{-1}.\text{K}^{-1}$
T	[K]	- intake air temperature
m	[kg]	- mass of air-fuel mixture at the end of induction stroke
m <sub>t</sub>	[kg]	- theoretical air-fuel mixture mass at ideal induction state
$\frac{\partial p}{\partial x}$	[Pa.m <sup>-1</sup> ]	- pressure drop gradient in streamwise direction of porous domain
K <sub>Q</sub>	[m.kg <sup>-4</sup> ]	- quadratic resistance coefficient
U <sub>x</sub>	[m.s <sup>-1</sup> ]	- average velocity in streamwise direction
T <sub>1</sub>	[K]	- turbine housing inlet temperature
T <sub>2</sub>	[K]	- turbine housing outlet temperature
p <sub>1</sub>	[Pa]	- turbine housing inlet pressure
p <sub>2</sub>	[Pa]	- turbine housing outlet pressure
$\kappa$	[-]	-heat capacity ratio
c <sub>p</sub>	[-]	-isobaric specific heat capacity (constant pressure)
a <sub>t</sub>		-technical work



$\eta_{iz}^T$	[-]	-isentropic efficiency of energy conversion in turbine housing
$\eta_T^T$	[-]	- total efficiency
$\dot{m}$	[kg.s <sup>-1</sup> ]	- mass flow
A	[m <sup>2</sup> ]	- cross sectional area
r	[J.kg <sup>-1</sup> .K <sup>-1</sup> ]	- specific gas constant, for dry air r = 287.058 J.kg <sup>-1</sup> .K <sup>-1</sup>
d	[m]	- catalytic converter diameter
P2T	[Pa]	- pressure at turbine housing outlet
T2T	[K]	- temperature at turbine housing outlet
N	[-]	- number of facets on turbine housing outlet area
$T_i$	[°C]	- temperature in facet 'i'
$\bar{T}$	[°C]	- average temperature
$\sigma_T$	[°C]	- standard deviation of temperatures



## 19 SUPPLEMENT

Drawings of: DESIGN 1  
DESIGN 2  
DESIGN 3  
DESIGN 4  
DESIGN 5

Scientists study the world as it is,  
engineers create the world  
that never has been.

THEODORE VON KARMAN